

NATIONAL LIBRARY

BIBLIOTHÈQUE NATIONALE

OTTAWA



OTTAWA

NAME OF AUTHOR..... KAMAL NATH JHA .....  
 TITLE OF THESIS..... Kinetics of solvated electrons  
 Reactions during radiolysis of  
 Liquid Alcohols .....  
 UNIVERSITY..... of Alberta .....  
 DEGREE..... Ph. D. .... YEAR GRANTED..... Feb, 1969.

Permission is hereby granted to THE NATIONAL  
 LIBRARY OF CANADA to microfilm this thesis and to  
 lend or sell copies of the film.

The author reserves other publication rights,  
 and neither the thesis nor extensive extracts from  
 it may be printed or otherwise reproduced without  
 the author's written permission.

(Signed)..... Kamal Nath Jha.

PERMANENT ADDRESS:

Vill. - Uchhati,  
 P.O. → Biroul, Darbhanga  
 Bihar, INDIA.

DATED..... Feb 25, 1969.

THE UNIVERSITY OF ALBERTA

KINETICS OF SOLVATED ELECTRON REACTIONS DURING  
RADIOLYSIS OF LIQUID ALCOHOLS

by



KAMAL NATH JHA

A THESIS

SUBMITTED TO THE FACULTY OF GRADUATE STUDIES  
IN PARTIAL FULFILMENT OF THE REQUIREMENTS FOR THE DEGREE OF  
DOCTOR OF PHILOSOPHY

DEPARTMENT OF CHEMISTRY

EDMONTON, ALBERTA

Spring, 1969

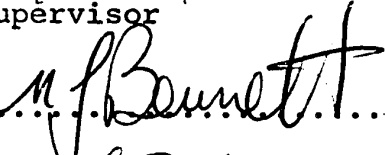
THE UNIVERSITY OF ALBERTA  
FACULTY OF GRADUATE STUDIES

The undersigned hereby certify that they have read, and recommend to the Faculty of Graduate Studies for acceptance, a thesis entitled

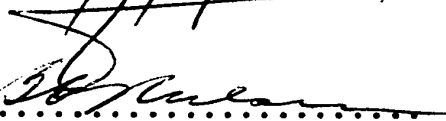
"KINETICS OF SOLVATED ELECTRON REACTIONS DURING  
RADIOLYSIS OF LIQUID ALCOHOLS"

submitted by KAMAL NATH JHA, M.Sc., in partial fulfilment of the requirements for the degree of Doctor of Philosophy.

  
.....  
Supervisor

  
.....

  
.....

  
.....

  
.....

  
.....  
External Examiner

February 24/69.....  
Date

A B S T R A C T

A study has been made of the effects of temperature, acid and nitrous oxide on the reactions of the hydrogen precursors in the gamma radiolysis of liquid methanol and n-propanol.

In pure methanol the value of  $G(H_2)$  varies from 4.9<sub>5</sub> at -98° to 5.4<sub>5</sub> at 25° and 8.0 at 240°. Scavenging studies with acid and nitrous oxide were carried out at -97°, 25° and 150°. The nitrogen and hydrogen yields were calculated as functions of the nitrous oxide concentration at each of the three temperatures. The calculations were based on a proposed mechanism. Homogeneous kinetics were used for the reactions of the free ions and nonhomogeneous kinetics were used for the ionic reactions in spurs. At -97°  $G(\text{total ionization}) = 4.6$ , and the value is assumed to be independent of temperature. The yield of free ions is  $G(e^-_{\text{solv}})_{\text{fi}} = 2.0 \pm 0.2$ , independent of temperature from -97° to 150°. The reaction  $e^-_{\text{solv}} + \text{CH}_3\text{O}^-_{\text{solv}} + \text{H}$  has a rate constant of  $4.6 \times 10^5 \text{ sec}^{-1}$  at 25° and an activation energy equal to that of dielectric relaxation (3.7 kcal/mole), which is 0.9 kcal/mole greater than that of self diffusion; the entropy of activation of the reaction is -21 cal/deg mole.

In pure n-propanol the value of  $G(H_2)$  changes from 4.3 at -120° to 4.9 at 25° and 6.0 at 140°. Acid and nitrous oxide were added as electron scavengers at -120°, 25° and 140°. The calculations of the nitrogen

and hydrogen yields at each of the three temperatures were similar to those for methanol. At  $-120^{\circ}$   $G(\text{total ionization}) = 4.3$  and the value is assumed to be independent of temperature. The yield of free ions was found to be  $G(e^-_{\text{solv}})_{\text{fi}} = 1.1$  at  $-120^{\circ}$ , 1.2 at  $25^{\circ}$  and 0.8 at  $140^{\circ}$ . There is a species X which reacts with acid to form hydrogen, but its identity is unknown. Secondary reactions involving nitrous oxide produce large yields of nitrogen at high temperatures and high nitrous oxide concentrations. The first order decomposition of solvated electrons to produce hydrogen atoms and alkoxide ions has a rate constant of  $4.9 \times 10^5 \text{ sec}^{-1}$  at  $25^{\circ}$  and an activation energy equal to that of self diffusion (4.3 kcal/mole), which is 1.8 kcal/mole smaller than that of dielectric relaxation; the entropy of activation of the reaction is  $-19 \text{ cal/deg mole}$ .

As in methanol and n-propanol, calculations of the nitrogen and hydrogen yields were performed on the data available for ethanol (24,132) and iso-propanol (25) systems. The value of  $G(\text{total ionization}) = 4.3$  was chosen for both alcohols and was assumed to be independent of temperature.

In ethanol the value of  $G(\text{H}_2)$  varies from 5.3 at  $-112^{\circ}$  to 6.9 at  $140^{\circ}$ . The yield of free ions at  $25^{\circ}$  is  $G(e^-_{\text{solv}})_{\text{fi}} = 1.5$ . The rate constant for the first order decay of the solvated electron is  $1.2 \times 10^5 \text{ sec}^{-1}$  at  $25^{\circ}$

and the activation energy is equal to that of dielectric relaxation and that of self diffusion ( $\approx 4.6$  kcal/mole). The entropy of activation of this decay is  $-21$  cal/deg mole.

In iso-propanol the value of  $G(H_2)$  changes from 4.0 at  $-85^\circ$  to 5.4 at  $140^\circ$ . The yield of free ions at  $25^\circ$  is  $G(e^-_{\text{solv}})_{\text{fi}} = 1.3$ . The rate constant for the unimolecular decomposition of solvated electrons is  $3.1 \times 10^5 \text{ sec}^{-1}$  at  $25^\circ$  and the activation energy equals that of self diffusion (5.3 kcal/mole) which is 1.6 kcal/mole smaller than that of dielectric relaxation; the entropy of activation of the reaction is  $-17$  cal/deg mole.

In all these alcohols, the ions that undergo geminate neutralization can participate in two types of reaction, only one of which produces hydrogen. The activation energy of the hydrogen forming reaction is roughly 1 kcal/mole greater than that which does not form hydrogen.

In each of these liquids, the decomposition of solvated electrons,  $e^-_{\text{solv}} \rightarrow RO^-_{\text{solv}} + H$ , has a large negative entropy of activation which indicates that the transition state has a relatively specific structure.

A C K N O W L E D G E M E N T S

I am deeply indebted to Professor G. R. Freeman, whose approach to the research problem made the work more rewarding and enjoyable.

It is a pleasure to express my gratitude to Dr. H. S. Sandhu for programming some of the calculations, to Mrs. Mary Waters for her preparation of the typescript and to the members of the Radiation Chemistry group for their helpful co-operation.

Special thanks are due to my wife, Prema, whose patience and understanding, during the course of the work, are greatly appreciated.

---

T A B L E O F C O N T E N T S

	Page
Abstract . . . . .	i
Acknowledgements . . . . .	iv
Table of Contents . . . . .	v
List of Tables . . . . .	ix
List of Figures . . . . .	ixx
I. <u>INTRODUCTION</u>	
(A) General . . . . .	1
(B) Reactive Species and Their Reactions . . . . .	2
1. Positive Ions . . . . .	3
2. Electrons and Negative Ions . . . . .	4
3. Free Radicals . . . . .	8
4. Excited Molecules . . . . .	9
(C) Gross Effects Observed in Radiation Chemistry	10
1. Effect of Phase . . . . .	10
2. Effect of Total Dose . . . . .	12
3. Effect of High Pressure . . . . .	12
4. Effect of Temperature. . . . .	13
(D) Electron and its Range . . . . .	14
(E) The Solvated Electron . . . . .	16
1. Production of Solvated Electrons . . . . .	17
2. Evidence for Solvated Electrons . . . . .	18
3. Reactions of the Solvated Electrons. . . . .	26
4. Structure of Solvated Electrons . . . . .	27
(F) Radiolysis of Alcohols . . . . .	29
(G) Present Study . . . . .	35

II. <u>EXPERIMENTAL</u>	Page
(A) Materials . . . . .	37
1. Radiolysed Compounds . . . . .	37
a. Methanol . . . . .	37
b. n-Propanol . . . . .	37
2. Compounds Used as Additives. . . . .	38
a. Hydrogen chloride . . . . .	38
b. Nitrous oxide. . . . .	38
c. Sulfuric acid . . . . .	39
3. Other Materials . . . . .	39
(B) Procedures and Techniques . . . . .	39
1. Sample Preparation . . . . .	39
2. Sample Irradiation . . . . .	41
3. Product Analysis . . . . .	44
III <u>RESULTS</u>	
<u>Part I</u> Radiolysis of Liquid METHANOL . . . . .	47
(A) Gaseous Products at 25° . . . . .	47
(B) Effect of Temperature on Gaseous Product Yields. . . . .	47
(C) Scavenger Studies in Liquid Methanol . . . . .	52
1. Calculation of the Scavenger Concentrations in Methanol . . . . .	53
2. Effects of Scavengers on the Gaseous Product Yields at -97°, 25° and 150° . . . . .	55
(D) Competition Between Nitrous Oxide and Acid at 25° . . . . .	67
<u>Part II</u> Radiolysis of Liquid n-Propanol	
(A) Effect of Dose on the Gaseous Product Yields at 25° . . . . .	69

	page
(B) Effect of Temperature on the Product Yields . . .	72
(C) Scavenging Studies in Liquid n-Propanol . . . .	72
1. Calculation of the Scavenger Concentrations in n-Propanol. . . . .	75
2. Effects of Scavengers on the Hydrogen Yields at $-120^{\circ}$ , $25^{\circ}$ and $140^{\circ}$ . . . . .	76
(D) Competition Between Nitrous Oxide and Acid at $25^{\circ}$ . . . . .	88
IV <u>DISCUSSION</u>	
(A) Methanol . . . . .	90
1. Pure Methanol . . . . .	90
2. Effects of Electron Scavengers . . . . .	94
3. Scavenging Kinetics, Nitrogen Yields . . . . .	95
a. One-Adjustable-Parameter Treatment . . . . .	95
b. Two-Adjustable-Parameters Treatment . . . . .	103
4. Competition Between Nitrous Oxide and Acid . . . . .	106
5. Hydrogen Yields . . . . .	108
6. Effect of Temperature on the Hydrogen Forming Reactions . . . . .	112
(B) n-Propanol. . . . .	116
1. Pure n-Propanol . . . . .	116
2. Effects of Electron Scavengers . . . . .	118
3. Scavenging Kinetics, Nitrogen Yields . . . . .	121
a. One-Adjustable-Parameter Treatment . . . . .	121
b. Two-Adjustable-Parameters Treatment . . . . .	126
4. Competition Between Nitrous Oxide and Acid . . . . .	129
5. Hydrogen Yields. . . . .	132

	<u>page</u>
6. Effect of Dose on the Hydrogen Yields . . .	.136
7. Effect of Temperature on the Hydrogen Forming Reactions . . . . .	.137
(C) Ethanol and iso-Propanol . . . . .	.140
1. Scavenging Kinetics, Nitrogen Yields . .	.141
a. One-Adjustable-Parameter Treatment .	.142
b. Two-Adjustable-Parameters Treatment .	.159
2. Hydrogen Yields . . . . .	.163
3. Effect of Temperature on the Hydrogen Forming Reactions . . . . .	.167
REFERENCES . . . . .	.173
APPENDIX	
(A) Relevant Equations for Nonhomogeneous Kinetics Calculations . . . . .	.183
(B) Estimation of Values of $g(H_2)_{min}$ , $G(H_2)_{53}$ and $k_{53}/k_{54}$ in Methanol . . . . .	.187

L I S T O F T A B L E S

<u>Table</u>		<u>Page</u>
I-1	Determination of charge on $e_{aq}$	22
I-2	Properties of the Solvated Electron at About 25°C	25
III-1	G Values of Products from $\gamma$ -Radiolysis of Methanol at 25°	45
III-2	Product Yields as a Function of Temperature in Methanol	49
III-3	Product Yields as a Function of Nitrous Oxide Concentration at -97° in Methanol	56
III-4	Product Yields as a Function of Acid Concentration at -97° in Methanol	57
III-5	Product Yields as a Function of Nitrous Oxide Concentration at 25° in Methanol	58
III-6	Product Yields as a Function of Acid Concentration at 25° in Methanol	59
III-7	Product Yields as a Function of Nitrous Oxide Concentration at 150° in Methanol	60
III-8	Product Yields as a Function of Acid Concentration at 150° in Methanol	61
III-9	Competition Between Nitrous Oxide and Acid at 25° in Methanol	68
III-10	Effect of Dose on the Hydrogen Yield at 25° in n-Propanol.	70
III-11	Gaseous Product Yields at 25° in n-Propanol	71
III-12	Effect of Temperature on the Gaseous Product Yields in n-Propanol	73
III-13	Product Yields as a Function of Nitrous Oxide Concentration at -120° in n-Propanol	77
III-14	Yield of Hydrogen as a Function of Acid Concentration at -120° in n-Propanol	78
III-15	Product Yields as a Function of Nitrous Oxide Concentration at 25° in n-Propanol	79

<u>Table</u>	<u>Page</u>
III-16 Yield of Hydrogen as a Function of Acid Concentration at 25° in n-Propanol	80
III-17 Product Yields as a Function of Nitrous Oxide Concentration at 140° in n-Propanol	81
III-18 Yield of Hydrogen as a Function of Acid Concentration at 140° in n-Propanol	82
III-19 Competition Between Nitrous Oxide and Acid at 25° in n-Propanol	89
IV-1 Quantities Relevant to the Reactions of Solvated Electrons in Methanol	96
IV-2 Some Relevant Data for Methanol	102
IV-3 N( $\gamma$ ) Spectra and Values of $\epsilon_{ave}$ in Methanol at Different Temperatures	105
IV-4 Competition Between Nitrous Oxide and Acid at 25° in Methanol	107
IV-5 Relevant Data for the Calculation of the Hydrogen Yields in Methanol	111
IV-6 Entropies of Activation of the First Order Decay of Solvated Electrons	115
IV-7 Quantities Relevant to the Reactions of Solvated Electrons in n-Propanol	123
IV-8 Some Relevant Data for n-Propanol	128
IV-9 N( $\gamma$ ) Spectra and Values of $\epsilon_{ave}$ in n-Propanol at Different TEMperatures	130
IV-10 Competition Between Nitrous Oxide and Acid at 25° in n-Propanol	131
IV-11 Relevant Data for the Calculation of the Hydrogen Yields in n-Propanol	135
IV-12 Quantities Relevant to the Reactions of Solvated Electrons in Ethanol	143
IV-13 Quantities Relevant to the Reactions of Solvated Electrons in iso-Propanol	144

<u>Table</u>		<u>Page</u>
IV-14	Some Relevant Data for Ethanol	157
IV-15	Some Relevant Data for iso-Propanol	158
IV-16	N(y) Spectra and Values of $\epsilon_{ave}$ in Ethanol at Different Temperatures	160
IV-17	N(y) Spectra and Values of $\epsilon_{ave}$ in iso-Propanol at Different Temperatures	161
IV-18	Relevant Data for the Calculation of the Hydrogen Yields in Ethanol	164
IV-19	Relevant Data for the Calculation of the Hydrogen Yields in iso-Propanol	165
A-1	Calculation of $g(N_2)$ in n-Propanol.	185

<u>Figure</u>	<u>L I S T O F F I G U R E S</u>	<u>Page</u>
I-1	Effect of Ionic Strength on Relative Rate Constants of $e^-_{\text{solv}}$ Reactions	21
I-2	Absorption Spectra of Solvated Electrons	24
II-1	Sample Preparation Manifold	40
II-2	Steel Pressure Cell Used for High-Temperature Irradiations	43
II-3	Sample Analysis System	45
III-1	The Yield of Hydrogen as a Function of Temperature in Methanol	50
III-2	Methane and Carbon Monoxide Yields as a Function of Temperature in Methanol	51
III-3	The Effect of Acid or Nitrous Oxide Concentration at $-97^\circ$ in Methanol	62
III-4	The Effect of Acid or Nitrous Oxide Concentration at $25^\circ$ in Methanol	63
III-5	The Effect of Acid or Nitrous Oxide Concentration at $150^\circ$ in Methanol	64
III-6	The Yield of Hydrogen as a Function of Nitrous Oxide Concentration in Methanol	65
III-7	The Yield of Hydrogen as a Function of Temperature in n-Propanol	74
III-8	The Effect of Acid or Nitrous Oxide Concentration at $-120^\circ$ in n-Propanol	83
III-9	The Effect of Acid or Nitrous Oxide Concentration at $25^\circ$ in n-Propanol	84
III-10	The Effect of Acid or Nitrous Oxide Concentration at $140^\circ$ in n-Propanol	85
III-11	The Yield of Hydrogen as a Function of Nitrous Oxide Concentration in n-Propanol	86

<u>Figure</u>		<u>Page</u>
IV-1	Plots of $1/g(N_2)$ Against $1/[N_2O]$ for Methanol	97
IV-2	A. Arrhenius Plot for Dielectric Relaxation in Methanol	101
	B. Arrhenius Plot of $[G(H_2)_{t^\circ} - G(H_2)_{-97^\circ}]$ in Methanol	
IV-3	Plots of $1/g(N_2)$ Against $1/[N_2O]$ for n-Propanol	124
IV-4	A. Arrhenius Plot for Dielectric Relaxation in n-Propanol	
	B. Arrhenius Plot of $[G(H_2)_{t^\circ} - G(H_2)_{-120^\circ}]$ in n-Propanol	127
IV-5	Plots of $1/g(N_2)$ Against $1/[N_2O]$ for Ethanol	145
IV-6	Plots of $1/g(N_2)$ Against $1/[N_2O]$ for iso-Propanol	146
IV-7	The Effect of Nitrous Oxide Concentration at $-112^\circ$ in Ethanol	148
IV-8	The Effect of Nitrous Oxide Concentration at $25^\circ$ in Ethanol	149
IV-9	The Effect of Nitrous Oxide Concentration at $90^\circ$ in Ethanol	150
IV-10	The Effect of Nitrous Oxide Concentration at $145^\circ$ in Ethanol	151
IV-11	The Effect of Acid or Nitrous Oxide Concentration at $-85^\circ$ in iso-Propanol	152
IV-12	The Effect of Acid or Nitrous Oxide Concentration at $25^\circ$ in iso-Propanol	153
IV-13	The Effect of Acid or Nitrous Oxide Concentration at $140^\circ$ in iso-Propanol	154
IV-14	A. Arrhenius Plots for Dielectric Relaxation in Ethanol and iso-Propanol	156

<u>Figure</u>		<u>Page</u>
	B. Arrhenius Plot of $[G(H_2)_{t^\circ} - G(H_2)_{-85^\circ}]$ in iso-Propanol	
IV-15	The Yield of Hydrogen as a Function of Temperature in Ethanol and iso-Propanol	166
IV-16	The Yield of Hydrogen as a Function of Nitrous Oxide Concentration in Ethanol	168
IV-17	The Yield of Hydrogen as a Function of Nitrous Oxide Concentration in iso-Propanol	169

---

I N T R O D U C T I O N

(A) General

Radiation chemistry is the study of the chemical effects produced in a system by the absorption of electromagnetic radiation or charged particles having energies of about 50 eV and above (e.g., X-rays,  $\gamma$ -rays, electrons, protons, helium ions, etc.).

The present study was carried out with  $^{60}\text{Co}$  gamma-rays. Energy from the gamma-rays is transferred to the system by several possible interactions, the most important of which is the Compton process. In this process a 1.3 MeV. gamma-ray from  $^{60}\text{Co}$  interacts with an electron which is bound to an atom or molecule, so that the electron is accelerated and the photon scattered. The energy and the momentum of the incident photon are shared between the recoil electron (primary electron) and the scattered photon. The energetic primary electrons (mean energy 0.6 MeV) thus produced cause further ionization and excitation of the medium. The electrons set in motion by the primary electrons are called secondary electrons. These secondary electrons, in turn, produce further ionizations and excitations. The ionization process in a medium forms large numbers of small regions with high concentrations of reactive species. These small regions are called "spurs".

The energy absorption process is essentially complete

I N T R O D U C T I O N

(A) General

Radiation chemistry is the study of the chemical effects produced in a system by the absorption of electromagnetic radiation or charged particles having energies of about 50 eV and above (e.g., X-rays,  $\gamma$ -rays, electrons, protons, helium ions, etc.).

The present study was carried out with  $^{60}\text{Co}$  gamma-rays. Energy from the gamma-rays is transferred to the system by several possible interactions, the most important of which is the Compton process. In this process a 1.3 MeV. gamma-ray from  $^{60}\text{Co}$  interacts with an electron which is bound to an atom or molecule, so that the electron is accelerated and the photon scattered. The energy and the momentum of the incident photon are shared between the recoil electron (primary electron) and the scattered photon. The energetic primary electrons (mean energy 0.6 MeV) thus produced cause further ionization and excitation of the medium. The electrons set in motion by the primary electrons are called secondary electrons. These secondary electrons, in turn, produce further ionizations and excitations. The ionization process in a medium forms large numbers of small regions with high concentrations of reactive species. These small regions are called "spurs".

The energy absorption process is essentially complete

in  $10^{-15}$  sec, before any chemical reactions have occurred. Between  $10^{-15}$  and  $10^{-12}$  seconds ion molecule reactions may take place within the spur and radicals are formed from the decomposition of ions and excited molecules. The spurs are dissipated by diffusion and reaction after about  $10^{-8}$  seconds and any intermediates that do not react in that time are available for reaction in the bulk medium. The reactions of these intermediates are discussed in the next section.

The yields of products formed in radiation chemical reactions are expressed as G values. The G value of a product is defined as the number of molecules of the product formed per hundred electron volts of energy absorbed by the system. The yield of primary ions is dependent on the energy required to form an ion pair (W value):

$$G(\text{Ion pair}) = \frac{100}{W(\text{eV/ion pair})} \approx 4$$

In the absence of a chain reaction, G values of products are usually less than ten.

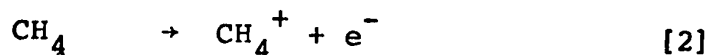
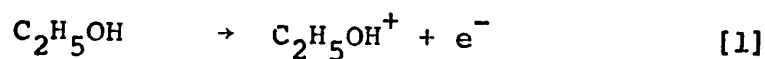
(B) Reactive Species and Their Reactions

The reactive species formed in radiolysis systems may be classified as positive ions, electrons, negative ions, free radicals and excited molecules. The reactions of these species have been discussed in detail in recent reviews (1,2). They will be summarized here briefly.

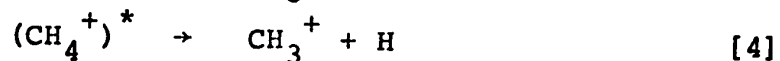
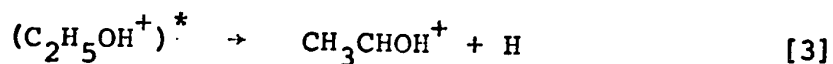
1. Positive Ions

Most of the information about positive ions has been obtained from gas phase studies in mass spectrometers (3). Positive ion reactions play an important role in many liquid systems, but the exact nature of these positive ions is still a matter of conjecture.

Primary ions are formed directly from the interactions of the radiation and the energetic electrons with the absorbing medium. For example,

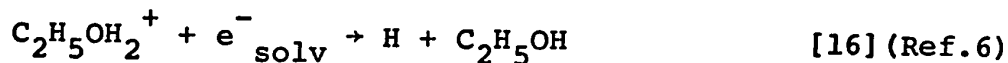
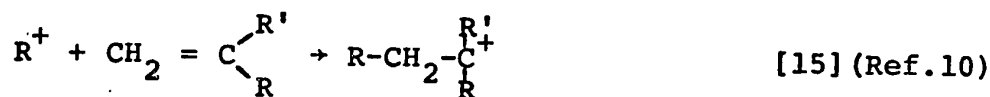
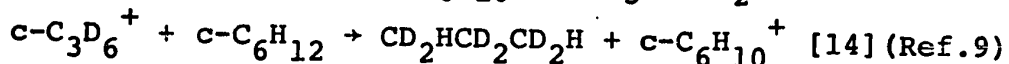
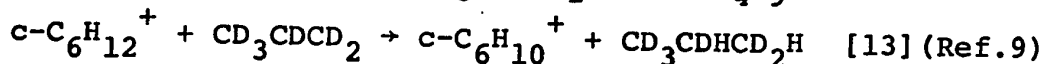
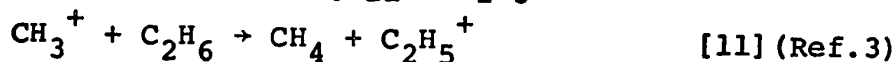
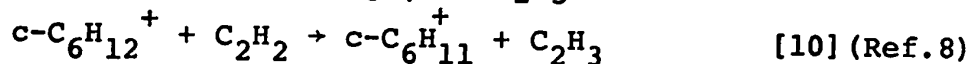
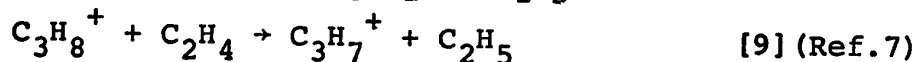
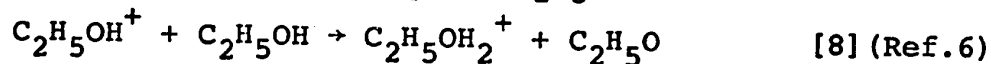
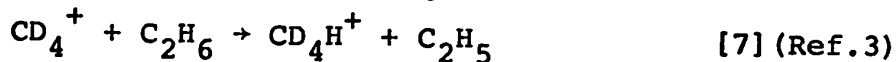
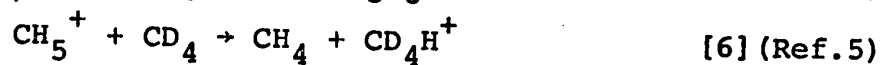
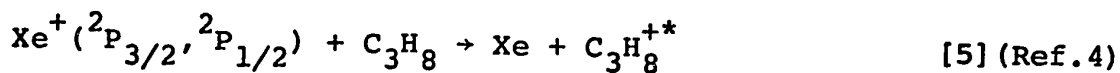


Some of the ions are formed in excited states which subsequently decompose. For example,

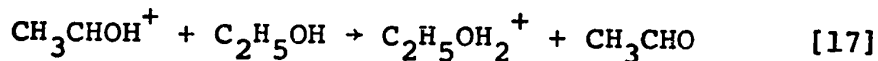


The positive ions undergo a number of transfer reactions. These reactions correspond to the abstraction or donation of the species  $\text{e}^-$ ,  $\text{H}^+$ ,  $\text{H}$ ,  $\text{H}^-$ ,  $\text{H}_2$  and  $\text{H}_2^-$ . For an ion to undergo an abstraction reaction it must possess an unsatisfied valence; to undergo a donation reaction it must have a reaction partner capable of accepting what the ion donates. The main types of reactions are illustrated by examples (i) charge transfer [5], (ii) proton transfer [6], (iii) hydrogen atom abstraction [7] and [8], (iv) hydrogen atom donation [9] and [10], (v) hydride ion abstraction [11]

and [12], (vi) hydrogen donation [13], (vii)  $H_2^-$  abstraction [14], (viii) condensation [15], (ix) neutralization [16]



It has been suggested (6,11-15) that in polar compounds ion molecule reactions such as the following (including reaction [8]),



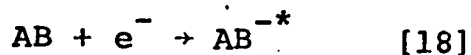
could precede the neutralization step in radiation chemistry.

## 2. Electrons and Negative Ions

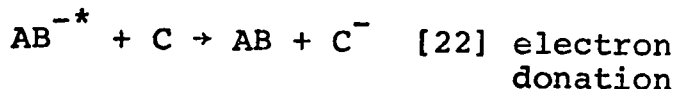
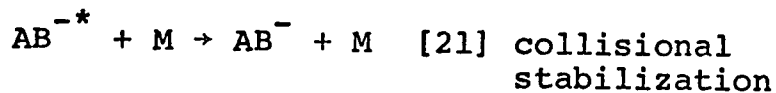
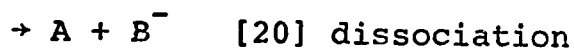
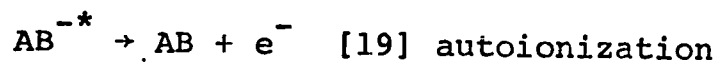
There are several states of the electron in which it is not bound to individual molecules. Two non-localized states are the free and quasi-free states, and two localized

states are the trapped and solvated states. The different states of electrons along with the properties of the solvated electron in different dielectric liquids are discussed in detail later (Part I Section E).

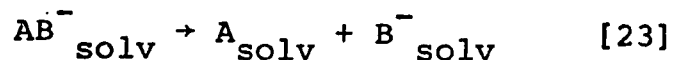
Electrons can be attached to neutral molecules which have positive electron affinities to form excited negative ions. For example,



The excited ion may then undergo one of four possible reactions:

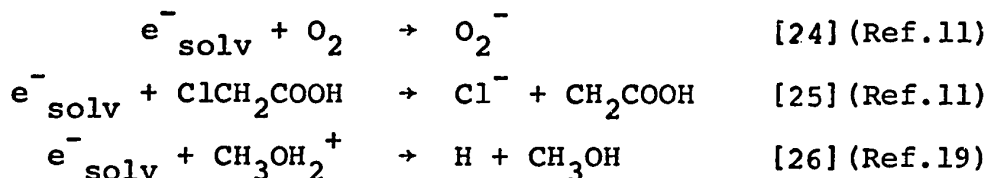


The reaction [21] would be greatly favoured over [20] in the liquid phase. However, solvation might aid the dissociation process in some, especially polar, solvents [23].



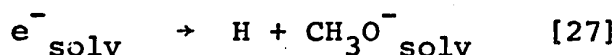
Reactions of electrons solvated in water have been much studied (16-18). The reactions of electrons solvated in organic liquids have so far received little attention (16). Few reactions of electrons solvated in alcohols have been

studied and they are very similar to the reactions observed in water. For example, if the solvent contains a sufficiently high concentration of a suitable solute, the electron attachment reaction [18] occurs;



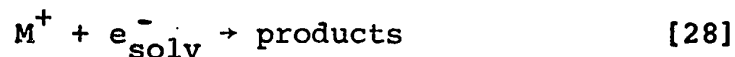
Presumably, if a solute is present at a high enough concentration, the electrons react before they become solvated - or even before being trapped.

In pure methanol, solvated electrons undergo a first-order reaction ( $\tau_{1/2} = 1.5 \mu\text{sec}$  at  $25^\circ$ ) to form hydrogen atoms (19,20). This reaction is possible because alcohols have labile protons.



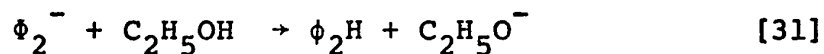
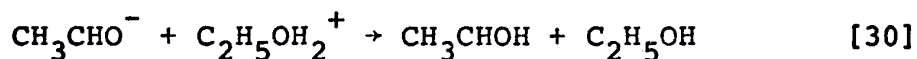
It has been suggested that in the radiolysis of liquids, a fraction of the electrons undergoes neutralization with the positive ions in the parent spurs (21,22). The size of this fraction of electrons which undergoes "geminate neutralization" is governed largely by the static dielectric constant of the liquid and by the range of the low energy secondary electrons in the liquid.

Recently it has been proposed that only a fraction of the total ion-neutralizations in alcohols leads to product formation, and that this fraction increases with the increase of temperature (23-25).



Reaction [29] might actually be a back reaction of the products of reaction [28].

Reactions of negative ions in liquid phase radiolysis have been little studied. The most common type of reaction is proton transfer (16,26):

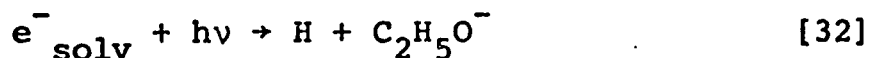


where  $\phi_2$  represents biphenyl.

The neutralization reaction has been discussed in the previous section (reactions of positive ions).

In the solid phase radiolysis of alcohols, both carbon tetrachloride and diphenyl have been used as electron scavengers (27). The electron trapped in solid alcohols has a blue colour which can be destroyed by bleaching with visible light.

In the case of ethanol, Hamill (27) suggested that the bleaching was due to reaction [32]

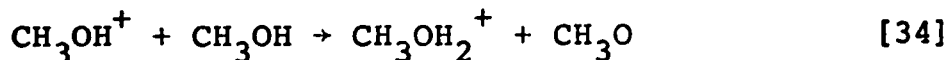
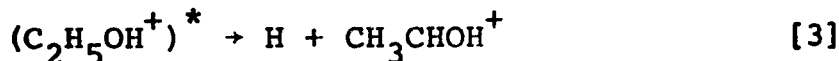
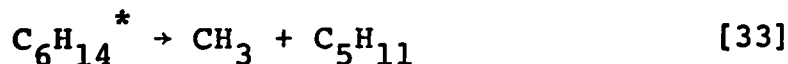


since on bleaching no photo electrons were observed.

Trapped and solvated electrons have been observed in solid hydrocarbons (28) but not directly in the liquid phase, although their presence has been postulated (21,22).

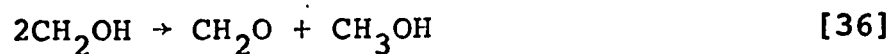
### 3. Free radicals

Radicals are formed by the decomposition of excited molecules and ions, by ion molecule reactions and by reactions of other free radicals with molecules. For example,

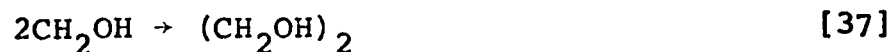


The presence of free radicals in irradiated solids (29-32) and liquids (33,34) has been confirmed by electron-spin resonance spectroscopy. For example, the presence of  $\alpha$ -hydroxyalkyl radicals has been detected during esr studies of irradiated solid primary alcohols (35-37). Optical absorption (38) and esr methods (34) have been used to observe radicals in the radiolysis of various liquids. For instance, the ultra violet absorption band in ethanol was attributed to the  $CH_3CHOH$  radicals (38).

The nature of the radicals present in a system during radiolysis can be deduced from product analysis after irradiation, assuming that radicals may undergo combination, disproportionation, abstraction, addition, dissociation or isomerization reactions. In methanol (19,39-41) formaldehyde is the major product formed by disproportionation.



The combination reaction product is glycol.



This indicates that the  $\text{CH}_2\text{OH}$  is the major radical present. The corresponding disproportionation and combination products are observed in other primary alcohols (11,26,42).

Hydrogen atoms can be observed and identified directly by their esr spectra. Hydrogen atoms produced by radiolysis of pure ice are stable at liquid helium temperature ( $-269^\circ$ ). As the sample is warmed they start to disappear, slowly at  $-253^\circ$ , and rapidly at  $-220^\circ$  (43).

#### 4. Excited molecules

In radiolysis systems, excited molecules are formed directly by energetic charged particles or photons, or indirectly by ion recombination or energy transfer from other molecules. A specific excited state may also be formed by

internal conversion or intersystem crossing (44) from another state in the same molecule.

Emission measurements in condensed phase radiolysis provide conclusive evidence for the presence of neutral electronically excited molecules (45-47). Luminescence of certain aromatic molecules has been used to study electronic energy transfer processes in several multicomponent systems (48,49).

It has been demonstrated by various workers that triplet excited states play an important role in the liquid phase radiolysis of carbonyl containing compounds (50-52) and aromatic hydrocarbons (53-55).

(C) Gross Effects Observed in Radiation Chemistry

1. Effect of Phase

In the gas phase when the mean free path of any species (few hundred Ångstroms) is very much larger than the molecular diameter (few Ångstroms), re-encounter of two fragments from the same molecule is extremely unlikely. Similarly, re-encounter of an electron with the parent molecular ion is of very low probability (1). As a consequence, collisions between neutral molecules and either the excited molecules, neutral fragments, ions, or electrons, are much more frequent than inter-radical, or inter-ion collisions. Ultimately the latter type of collisions must take place, otherwise there would be a

steady accumulation of radicals and ionic species during radiolysis. Thus the reactive species have a relatively homogeneous distribution.

Normally the condensed phase is roughly 1000 times more dense than the gas phase. The mean free path of a molecule in the condensed phase is less than a molecular diameter. Ions and excited molecules are formed close together resulting in a non-homogeneous distribution of reactive species (spurs). The higher concentration of reactive species in the spur leads to a greater likelihood of reaction between the primary products and thus shorter lifetimes than the corresponding gas phase species. The close packing of the molecules tends to keep radical pairs together long enough for recombination to occur (cage effect) (6,56). Consequently there is a decrease in the amount of C-C bond breaking in the condensed phase compared to the gas phase. Increased collisional deactivation of excited species and their low kinetic energy in the condensed phase tend to further decrease the total amount of decomposition.

Hydroxy compounds in the condensed phase have considerable amounts of hydrogen bonding, which affects the yield of the radiolysis products (6). In the gas phase, hydrogen bonding does not occur to an appreciable extent in alcohols but polar molecules can form clusters of various sizes about ions, depending upon the pressure and temperature (57-59).

The primary processes in the solid phase will be similar to those in the liquid phase. In the solid phase fragments of molecules are immobilized and these fragments may be radical or ionic in character, and may persist until the temperatures at which molecular motions enable the trapped species to undergo translational displacements. Electrons trapped in this way are designated  $e_t^-$ . Further, the limitation on molecular motion means that the probability of quenching of excited states is reduced with a corresponding increased probability of fluorescence, phosphorescence or in the case of crystals, of exciton transfer over considerable distances.

## 2. Effect of Total Dose

An increase in total dose will only affect the product yields if a radiolysis product acts as a scavenger of reactive species. For example, in the radiolysis of alcohols, the decrease in hydrogen yield with increasing dose was attributed to the scavenging of solvated electrons by carbonyl compounds which are radiolytic products (25,26,42). In the radiolysis of methanol there is no decrease in the hydrogen yield with increasing dose because formaldehyde, which is a product, is a poor electron scavenger (19,23).

## 3. Effect of High Pressure

At very high pressures, densities of gases approach

those of liquids. The reactions of gases at high density become more like liquid phase reactions. This may be due to the collisional deactivation of excited molecules and ions competing with their decomposition reactions and the increased probability of geminate recombination of radicals and ions.

When the molar volume of the transition state is greater than the sum of those of the reactants, the reaction is said to have a positive volume of activation. The rate constant of such a reaction may be decreased by isothermally increasing the pressure on, and thereby the density of, the system (60). If the volume of activation is negative an isothermal increase of pressure on the system increases the rate constant. The variation of the product yields with pressure up to several thousands of atmospheres has been studied for a limited number of systems (1).

#### 4. Effect of Temperature

The primary processes are independent of moderate changes of temperature, since the change in thermal energies would be small in comparison to the energies of the reactive species. Reactions of thermalized ions and radicals may show a temperature dependence, if effective competition reactions exist, with different activation energies.

Temperature effects have been found in liquid alcohols

(23-25) and attributed to excited molecules, resulting from electron-positive ion neutralization, which at low temperatures are deactivated and at high temperatures are hydrogen precursors.

(D) Electron and its Range

An extra electron in a molecular medium can attach to a single molecule, forming a negative ion, or it can be bound more or less equally by several molecules at the same time, becoming trapped or solvated. Alternatively it can be relatively uninfluenced by the medium, in which case it is considered as a quasifree electron. The mobilities of trapped and solvated electrons in the liquid phase are of the same order of magnitude as that of a negative ion, whereas that of quasifree electron is several orders of magnitude higher (22).

As an energetic electron moves along its path, it loses kinetic energy by interactions with the molecules until it encounters a potential barrier which it has insufficient energy to surmount. At this point the electron is trapped. The trapped electron becomes solvated as the dielectric medium relaxes about the region of the localized charge. Both solvated and quasifree electrons of thermal energy are called thermalized electrons.

Information as to the initial separation distances of

the positive ion and its corresponding thermalized electron has become increasingly important in some aspects of radiation chemistry (1,21,22). The range of electrons having energy greater than 20 keV can be fairly accurately estimated from the Bethe equation (61). Below this energy there is a serious discrepancy.

No satisfactory treatment of electron ranges for energies less than the average electronic excitation potential of the medium exists. Samuel and Magee (62) estimated the range of a 15 eV electron in water to be 12.5 to 18 Å, depending upon the fractional energy loss per collision that they assumed. These values were obtained by considering the electron to lose energy by collision and by interaction with the coulombic field of the parent positive ion. Platzman (63), on the other hand, has estimated the range of a 10 eV electron in water to be about 50 Å.

An alternative arbitrary procedure used by Freeman (21,22) consists of extrapolating the electron energy range plot to lower energies. Using the data of Lea (64) for the range of electrons in water with energies of 0.1 keV and greater, a range of 14 Å was estimated for a 15 eV electron by extrapolation using a parabolic function. Ranges in other liquids were calculated using the Bethe equation (61). This extrapolation is discussed in detail in the Appendix B of Ref. (22).

(E) The Solvated Electron

Several reviews of the properties of solvated electrons have appeared within the past few years (16,18, 65). Considerable attention has been paid to the formation, reactions, stability and structure of this species in various media. The main recent information comes from radiation chemistry.

Solvated electrons are characterised by paramagnetism and electrical conductivity. They absorb in the red or near infrared regions having bands invariably broad, intense and without fine structure. These properties characterise extra electrons stabilized in diverse media (27, 66,67) subjected to high energy radiations.

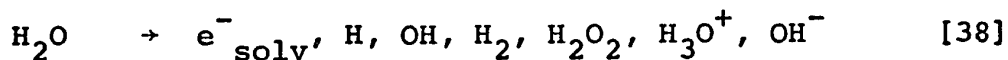
It was found that dilute solutions of alkali metals in liquid ammonia give rise to a species which has been identified as the solvated electron. Apart from other characteristics, the species is responsible for the single broad absorption band centered at  $15,000 \text{ \AA}$  (66). From density measurements and the e.s.r. line widths it is concluded that the electrons create and reside in large vacancies in this medium (66).

The participation of the solvated electron in aqueous radiation chemistry reactions was proposed by Stein (68) and Platzman (69). Platzman (69) most clearly discussed the thermalisation of the secondary electrons, their final hydration and some of their properties, including the blue

colour and the hydration energy of  $\approx 2$  eV. In spite of the early prediction of the solvated electron, its importance in radiation chemistry was not revealed and it continued to be mistaken for the hydrogen atom. Later it was demonstrated that the major reducing species in irradiated neutral water or alcohols has unit negative charge (70-72) and was responsible for the transient absorption spectrum in pulse radiolysis of aqueous or alcoholic solutions (16,73,74).

1. Production of Solvated Electrons

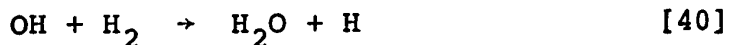
Radiolysis of water or alcohols is the most direct and convenient method for generating the solvated electron. For example,



In the flash photolysis of 0.001 N sodium hydroxide solution saturated with hydrogen, the solvated electron is formed by the following mechanism (75):



followed by



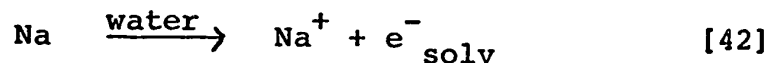
and



The rate constant for reaction [41] has been evaluated as  $2.2 \times 10^7 \text{ l mole}^{-1} \text{ sec}^{-1}$  (17).

The reaction of sodium with water also generates

the solvated electron (76).



## 2. Evidence for Solvated Electrons

Although the spectroscopic evidence for the solvated electron is the most convincing proof of its existence, it has also been demonstrated by kinetic methods that there are two different reducing species formed in irradiated water and alcohols.

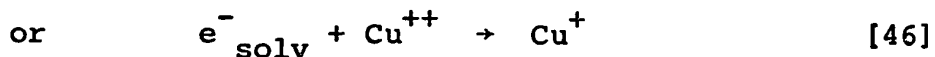
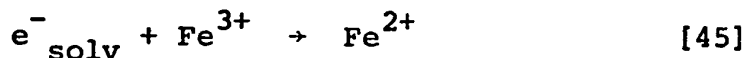
In 1958 Baxendale and Hughes (77) noted that the addition of high concentrations of  $\text{Fe}^{3+}$  and  $\text{Cu}^{2+}$  to acidified aqueous methanol solutions was more effective than predicted in reducing hydrogen yields from the reaction



This was understandable if  $e^-_{\text{solv}}$  was the precursor of hydrogen in acid solution



This reaction [44] is responsible for hydrogen atom formation in irradiated acid solution. At sufficiently high concentration of  $\text{Fe}^{3+}$  or  $\text{Cu}^{2+}$ , the reactions



intercept reaction [44], thereby preventing hydrogen formation by reaction [43].

The two-reducing-species concept was supported by the

results of other workers in the same year (78,79).

Confirmation and final identification of the solvated electron came from the determination of the magnitude and sign of its charge and the spectroscopic evidence.

For the determination of the magnitude and sign of the charge of the solvated electron, use was made of the Brönsted-Bjerrum theory of ionic reactions (80). This theory states that the rate constant  $k$  at ionic strength  $\mu$  will increase, decrease, or remain constant depending respectively on whether the charges of the reactants are of the same sign, opposite sign, or one is zero according to the equation:

$$\log_{10} \frac{k}{k_0} = 1.02(Ze^-_{\text{solv}})(Z_s) \{ \mu^{1/2} / [1 + \alpha(\mu^{1/2})] \}$$

where  $k_0$  is the rate constant at zero ionic strength,  $Ze^-_{\text{solv}}$  and  $Z_s$  are the charges on  $e^-_{\text{solv}}$  and the solute respectively and  $\alpha$  is a parameter numerically close to unity. If  $Z_s$  is known then a determination of the dependence of  $k$  on  $\mu$  will permit an evaluation of magnitude and sign of  $Ze^-_{\text{solv}}$ . Because many  $e^-_{\text{solv}}$  reactions are very fast and suitable techniques were not applied until 1962 for measuring their absolute rate constants, reliance had to be placed on relative rate constants. Czapski and Schwarz (70) established in this way that the principal reducing species in irradiated water has unit

negative charge. Figure I-1 and Table I-1 show their results along with those of other workers (71). In each of these curves the reaction rate of the indicated molecule or ion (A) of Table I-1 is compared with that of a neutral molecule (B) whose rate is unaffected by ionic strength. In the Figure I-1  $k$  represents the ratio  $k(e^-_{\text{solv}} + A)/k(e^-_{\text{solv}} + B)$  at ionic strength  $\mu$  and  $k_0$  is that ratio when  $\mu = 0$ .

The effect of ionic strength on the rate constant ratios has also been studied in the  $\gamma$ -radiolysis of methanol (72). The data presented are consistent with the reducing species in methanol having unit negative charge.

The discovery of the optical absorption spectrum of the solvated electron (63,64) not only confirmed its presence but this absorption band provided an unsurpassed method of studying its physical and chemical properties. The band has an absorption maximum at  $7200 \text{ \AA}$  which corresponds with an energy of 1.72 eV. The evidence that this spectrum is that of  $e^-_{\text{solv}}$  is rather convincing.

- (i) The energy of  $\lambda_{\text{max}}$  agrees reasonably closely with the early prediction (69), the current theoretical estimates (81) and the solvation energy determined from thermochemical data (82).
- (ii) The spectrum is suppressed by known electron scavengers, such as  $\text{H}_3\text{O}^+$ ,  $\text{N}_2\text{O}$ ,  $\text{O}_2$ ,  $\text{H}_2\text{O}_2$ ,  $\text{Cu}^{2+}$ , etc., (16)

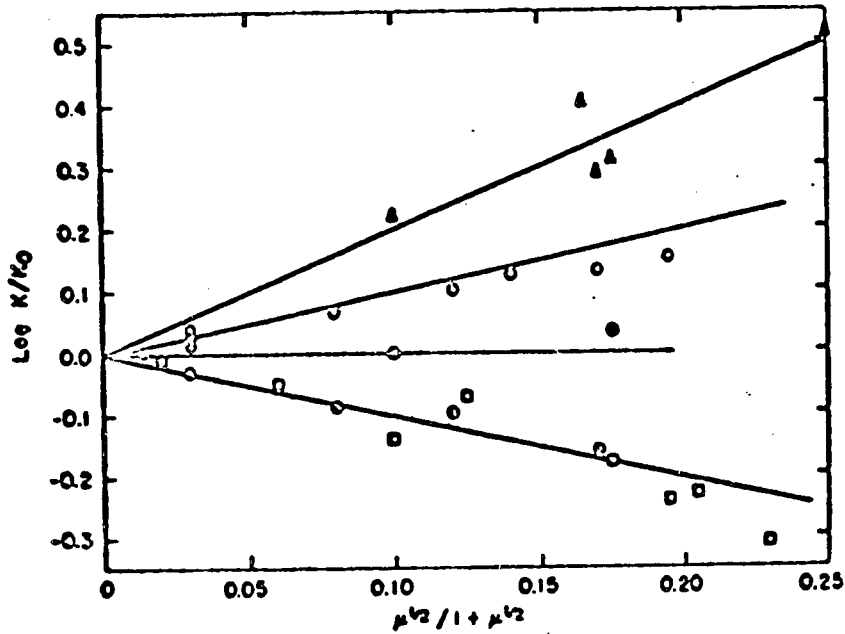


FIGURE I-1: Effect of ionic strength on relative rate constants of  $e_{aq}^-$  (70,71). Triangles,  $KFe(CN)_6^{4-}$  relative to  $N_2O$ ; circles with cross,  $O_2$  relative to  $H_2O_2$ ; circles, half solid,  $H^+$  relative to  $H_2O_2$ ; open circles  $NO_2^-$  relative to  $H_2O_2$ ; and squares,  $Ag^+$  relative to  $CH_2 = CHCONH_2$ .

TABLE I-1

Determination of Charge on  $e_{aq}$

<u>Solute</u>		$z_A$	Slope*	$z_{e_{aq}}^-$
A	B			
$NO_2^-$	$H_2O_2$	-1	+1.02	-1
$O_2$	$H_2O_2$	0	0.0	
$H^+$	$H_2O_2$	+1	-1.02	-1
$KFe(CN)_6^-$	$N_2O$	-2	+2.04	-1
$Ag^+$	$CH_2=CH\overset{O}{\parallel}CNH_2$	+1	-1.02	-1

\* From Fig. I-1 where  $\log k/k_0$  is plotted as a function of  $\mu^{1/2}/(1 + \mu^{1/2})$ .  $k$  is the rate constant for solute A, and  $k_0$  is the rate constant for the reference solute B.

- (iii) It resembles in form the absorption bands of the solvated electron in liquid ammonia and methylamine (83).
- (iv) The rate constants calculated from the decay of this absorption in the presence of scavengers give rate constant ratios which agree with those obtained by competitive studies with these scavengers in steady radiolysis (84).
- (v) The absorbing species responsible for the absorption has unit negative charge (70,71).

The solvated electron in alcohols exhibits a broad optical absorption extending from the ultraviolet to the near infra-red (85). The absorption spectra for ethylene glycol, methanol, ethanol, n-propanol and iso-propanol have been determined (85). In this series the static dielectric constant at 20°C ranges from 38.7 for ethylene glycol to 19 for iso-propanol. The absorption spectra are presented in Figure 1-2. The absorption maxima are respectively at 5800 (2.14 eV), 6300 (1.96 eV), 7000 (1.77 eV), 7400 (1.67 eV) and 8200 Å (1.51 eV). It is apparent that the maximum exhibits a red-shift with decrease in the static dielectric constant. This is consistent with the theory (16).

Table I-2 lists various properties of the solvated electron, including thermodynamic and electrical properties.

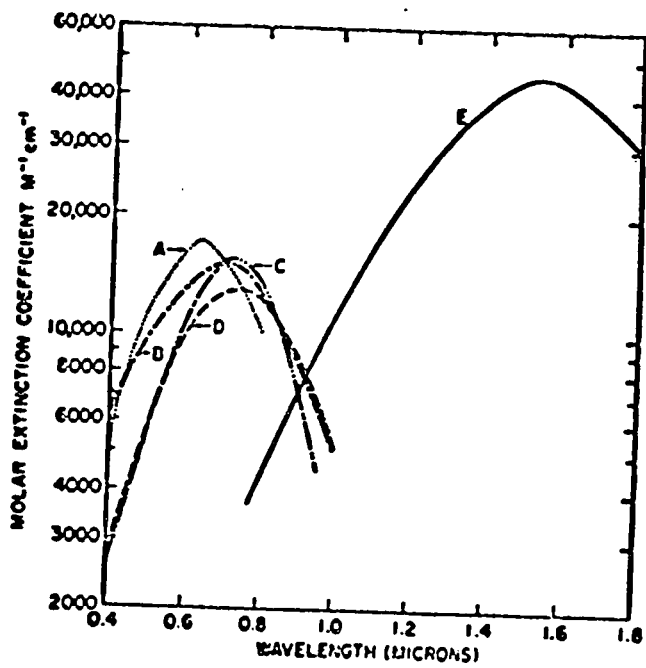


FIGURE I-2 Absorption spectra of solvated electrons  
A,-Methanol (16); B,-Ethanol (16); C,-Water (73,74);  
D,-n-Propanol (16); E,-Ammonia at  $-65^{\circ}C$  (83).

TABLE I-2

Properties of the Solvated Electron at about 25°C

Medium	Water	Methanol	Ethanol	n-Propanol	iso-Propanol	Ammonia	Ref.
Absorption	7200 Å	6300 Å	7000 Å	7400 Å	8200 Å	15,000 Å	16
maximum	1.72 eV	1.96 eV	1.77 eV	1.67 eV	1.51 eV	0.84 eV	
$\epsilon$ at $\lambda_{\text{max}}$	15,800 $\pm$ 10%	17,000	15,000	13,000	14,000	40,000	16
$M^{-1} \text{cm}^{-1}$							
Oscillator strength	0.7	0.8	0.9	0.6	0.7	0.7	16,83
$f_{\text{observed}}$							
Mobility							
$\text{cm}^2 \text{V}^{-1} \text{sec}^{-1}$	1.84x10 <sup>-3</sup>	---	---	---	---	8.4x10 <sup>-3</sup>	16,17
Equivalent conductivity	177 $\pm$ 10%	---	---	---	---	811	16,17
$\text{mhos cm}^2$							
$\tau_{1/2} (e_{\text{solv}}^- \rightarrow \text{H} + \text{RQ}^-)$	780	1.5	3	2	5	very long	16,23-26
$\mu\text{sec}$							
$S^\ddagger (e_{\text{solv}}^- \rightarrow \text{H} + \text{RO}^-)$	-23	-21	-21	-19	-17	---	---
cal/mole deg							
$E_a (e_{\text{solv}}^- \rightarrow \text{H} + \text{RO}^-)$	6.7	3.7	4.6	4.3	5.3	---	---
kcal/mole							
Dielectric Constant	78	33	25	20.3	19.4	22	16

3. Reactions of the Solvated Electron

The solvated electron is the most elementary chemical species and consequently its reaction with many reactants, both organic and inorganic has been studied in detail. Numerous reviews (16-18,65) have appeared during the last few years.

The rates of reactions of the solvated electron range from  $10^6 \text{ M}^{-1} \text{ sec}^{-1}$  to diffusion controlled processes. In all the direct kinetic measurements, the solvated electron is generated in minute concentrations of  $10^{-8} - 10^{-6} \text{ M}$ , while the other reactants are present in excess, so that a pseudo first-order decay of the solvated electron is observed. The rate constants for such reactions are thus obtained directly from the observed half-life of the solvated electron. The disappearance of the solvated electron by the reactions  $e^-_{\text{solv}} + e^-_{\text{solv}}$  or  $e^-_{\text{solv}} + \text{radicals}$  follows second order kinetics.

Since all reactions of the solvated electron are either electron attachment or dissociative electron transfer processes, it might be expected that the availability of a suitable low energy molecular orbital governs the reactivity of a solute. A number of reaction rates involving solvated electrons appear to be limited only by the diffusive encounter rate.

The reactivity of solvated electrons towards organic solutes varies considerably. Saturated hydrocarbons, alcohols,

ethers and amines, having no low-lying vacant orbitals, react slowly,  $k < 10^7 \text{ l mole}^{-1} \text{ sec}^{-1}$  (17). Compounds containing unsaturated groups or halogens have high reactivities. Many of them have rate constants greater than  $10^{10} \text{ l mole}^{-1} \text{ sec}^{-1}$ . It is unreactive towards benzene, phenol and toluene and in general behaves as an efficient and sharply discriminating nucleophilic reagent (86). Its reactivity towards aromatic compounds is related to the electron density of the  $\pi$  orbitals in the ring as expressed by Hammett's  $\sigma$  function (86).

#### 4. Structure of Solvated Electrons

Although the kinetic and thermodynamic properties of solvated electrons have been extensively studied, their nature and structure are still the subject of conjecture. This topic has been covered in several reviews (16-18,65) in detail. Here we will discuss it very briefly.

In metal-ammonia solutions both the diminution of density and hyperfine splitting of the e.s.r. absorption indicate that the electron is located in a vacancy of some  $3 \text{ \AA}$  radius. It has been proved that this species is responsible for the absorption band centered at  $15000 \text{ \AA}$ . In calculating the energy levels available to the electron within such a vacancy, it is considered to be essentially hydrogenic and its field decreasing coulombically from the central point (87). Using wave functions for a  $1s$

ground state and 2p excited state in the S.C.F. method, a value for the energy of the (2p+1s) transition of 0.93 eV is computed when a cavity radius of 3.2 Å is chosen. This agrees well with the experimental value of 0.80 eV for the energy of maximum absorption in ammonia (87).

In aqueous solutions the energy of the optical transition has been calculated in an analogous way to that in metal-ammonia solutions using hydrogenic-type wave functions for the ground and excited states (81). The energy of the transition is computed for various values of the cavity radius R. For example, when  $R = 3.3 \text{ \AA}$ ,  $E_{2p+1s} = 0.93 \text{ eV}$  and when  $R = 0$ ,  $E_{2p+1s} = 1.35 \text{ eV}$ . Since the experimental value for  $E_{2p+1s}$  is 1.72 eV, the cavity radius of the solvated electron in water appears to be vanishingly small.

The structure of the solvated electron in alcohols is expected to be similar to the one in water. However, from S.C.F. calculations it is predicted that the transition energies for solvated electrons in alcohols should lie intermediate between those in water and those in ammonia, but experimentally this is not true. The absorption maximum for methanol is at 1.96 eV (85). Thus refinement of the model is needed.

Recently, it has been suggested that solvated electrons are also formed in nonpolar liquids such as hydrocarbons (22).

The cavity model for the solvated electron is further

supported by the following experimental observations.

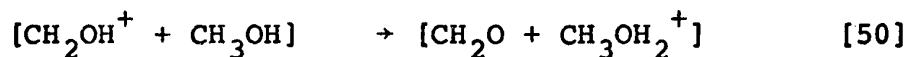
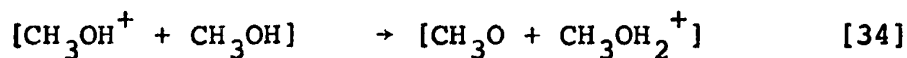
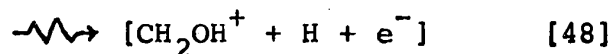
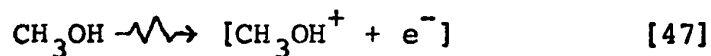
In highly concentrated aqueous solutions of potassium fluoride and lithium chloride a shift in the maximum of the solvated electron spectrum from 7200 Å to 6000 Å is observed (88). This blue shift is attributed to a shrinkage of the cavity radius. Similarly there is a blue shift in the absorption maximum with the increase of pressure on the system (89). This effect is also attributed to a shrinkage of the cavity radius. Further support comes from an increase in temperature shifting the absorption maximum to the red (90,91).

The solvation energy of the electron in aqueous solution has been estimated to be -39.7 kcal/mole (82,92). This is compared with the free energy of hydration of halide ions and is found that this is closest to that of iodide ion ( $\Delta G_s = 57$  kcal/mole) neglecting the contribution made by the entropy of hydration. Thus the enthalpy and free energy of hydration are equated so that  $\Delta H_s = -39.7$  kcal/mole or -1.72 eV. Since the hydration energy is a function of the ionic radius this small hydration energy implies a distribution of charge of the solvated electron certainly greater than the 2.2 Å radius of the iodide ion (93) a further support to the cavity model.

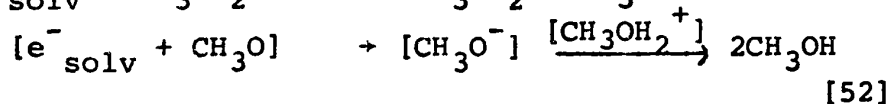
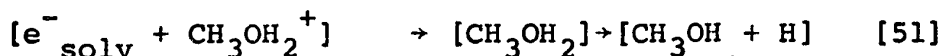
#### (F) Radiolysis of Alcohols

The reaction mechanisms for all alcohols are very similar to each other, with a few exceptions which will be mentioned

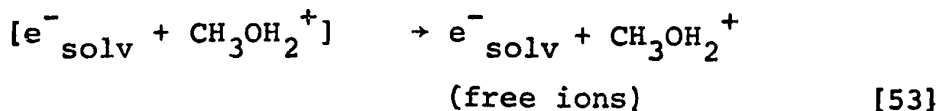
later (19,23-26,42,94,95). The following mechanism has been proposed for pure methanol (19,23) and is presented as a model for the alcohol family. Brackets around reactants or products in the following reactions denote that the species are inside a spur.



The solvated electrons in the spur appear to be involved in two types of reaction, only one of which results in hydrogen formation. The competition between these two types of reaction is slightly temperature dependent. This is exemplified by reactions [51] and [52]



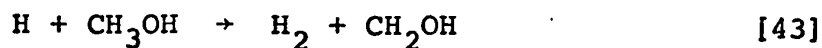
The ions that do not undergo reactions [51] or [52] escape the spur to become free ions



The free ion solvated electrons decompose, giving rise to hydrogen atoms.

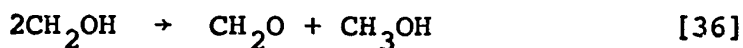


The hydrogen atoms attack the methanol.



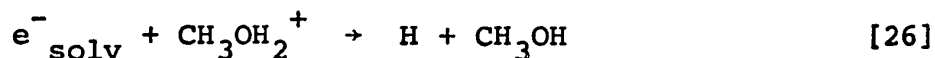
Hydrogen is the main gaseous radiolytic product. The yields of three kinetically distinguishable hydrogen precursors are found to be  $G(e_{\text{solv}}^-)_{\text{fi}} = 2.0$ ,  $G(\text{H}) = 1.7$  and  $G(\text{H}_2)_{\text{unscavengable}} = 1.8$  at  $25^\circ$ .

The main liquid products are formaldehyde and ethylene glycol which are formed largely by reactions [36], [37] and [50].



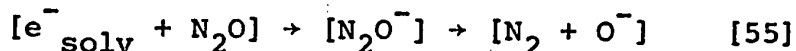
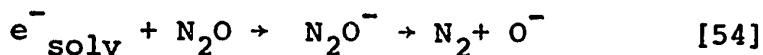
The mechanism does not involve excited molecules as such, however, reactions [48] is simply reaction [47] involving a more energetic precursor. Excited neutral molecule reactions cannot be excluded, but they appear to contribute less than do the ionic reactions to the present system.

It has been suggested that in the presence of acid, reaction [27] is replaced by reaction [26].



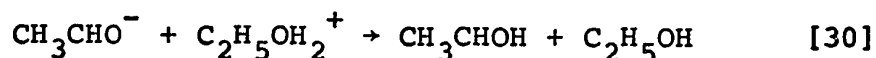
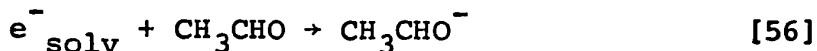
A sufficiently high concentration of acid causes reaction [52] to be replaced by reaction [51] and this explains the increase of hydrogen yield with increasing acid concentration (19,23-26, 94,95). In a similar way the addition of nitrous oxide causes the value of  $G(\text{H}_2+\text{N}_2)$  to increase

with increasing nitrous oxide concentration, by the occurrence of reactions [54] and [55],



The effect of a large number of other scavengers (e.g., acetone, benzene, naphthalene, methyl iodide, iodine,  $\text{Fe}^{3+}$ ,  $\text{NO}_3^-$ , etc.) on the product yields has been discussed in various papers (19,39-42,94-99).

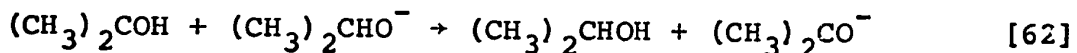
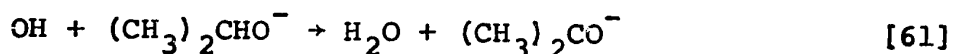
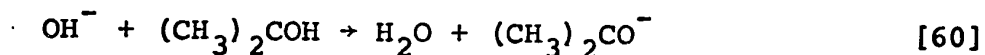
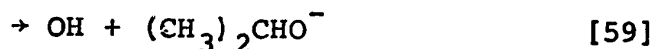
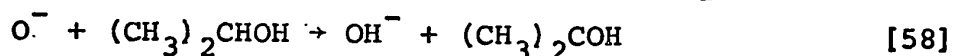
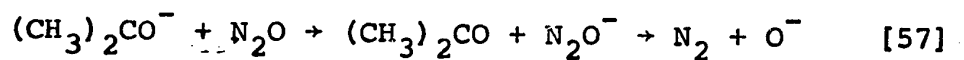
The above mechanism for neutral methanol holds good for other alcohols (e.g., ethanol, n-propanol and iso-propanol) as well. In these alcohols, the yield of hydrogen decreases with increasing dose. The decrease in hydrogen yield has been explained by the scavenging of solvated electrons by carbonyl compounds which are radiolytic products. For instance, in ethanol (26),



In methanol the hydrogen yield is independent of dose because formaldehyde, which is a radiolytic product, is a poor electron scavenger. In acidic ethanol the increase in hydrogen yield is attributed to two different processes, one of which is similar to reaction [51]. The other is due to a species "X" with a yield  $G(\text{X}) = 0.8$ , which reacts to form hydrogen, but its identity is unknown (24,100). The species "X" has not been found in earlier studies of acidic

ethanol (94).

In general the effect of nitrous oxide in the radiolysis of alcohols is to decrease the hydrogen yield and to produce nitrogen. In the case of iso-propanol, secondary reactions involving nitrous oxide are reported to produce large yields of nitrogen at high temperatures and high concentrations of nitrous oxide (25). Large yields of nitrogen have also been reported in the radiolysis of alkaline solutions of iso-propanol containing nitrous oxide (101). It has been proposed that the iso-propoxide radical anion is the chain carrier in such reactions (25,101).



It has been mentioned earlier that in the radiolysis of liquids, a fraction of the ions escape the parent spurs and becomes "free". The size of the fraction of ions that becomes free ions depends largely on the static dielectric constant of the medium and on the range of the low energy secondary electrons in the liquid (22). The range of the low energy secondary electrons in various alcohols is almost the same. Consequently, the free ion yields in different alcohols will be governed mainly by the static dielectric

constant of the liquid, i.e. the higher the dielectric constant of the medium, the higher the free ion yield. This free ion yield can be estimated by a recently developed statistical model (22). The validity of the model has been substantiated in the radiolysis of water, alcohols and hydrocarbons which differ widely in their polarity (23-25, 102-105). In the case of alcohols the measured values of the free ion yields are very much scattered (usually low) especially when they are estimated from the difference in hydrogen yields as functions of scavenger concentrations (19,26,94,99). This is not surprising because the radiolysis of alcohols is very sensitive to the presence of traces of impurities, some of which are very difficult to remove. These impurities scavenge the precursors of hydrogen and result in low values of the hydrogen yield. This explains the low yields of the free ions that have been estimated from the difference in hydrogen yields.

Some of the physical and chemical properties of the solvated electron in alcohols have been investigated by means of the pulse radiolysis technique. This has been discussed in the previous section. The yields of free ions measured in these irradiated alcohols are low (85). This might be due to the presence of impurities in alcohols.

The half-lives of the decomposition of solvated electrons in various alcohols have been measured both by pulse radiolysis and steady state studies (20,23-25) and

show good agreement. Absolute rate constants for a number of reactions of the solvated electrons in methanol and ethanol have been determined using pulse radiolysis (18).

(G) Present Study

A recently proposed model for the nonhomogeneous kinetics of reactions of radiolytic ions in dielectric liquids (22) is being tested under a wide variety of conditions. It has been applied to the gamma radiolysis of hydrocarbons (22, 103-105) and water (102) at 25° and of ethanol (24) and iso-propanol (25) over a range of temperatures. It has been proposed that the use of the complex dielectric constant may be required in the calculations in the case of alcohols because they have unusually long dielectric relaxation times (106).

The present investigation was undertaken to apply the model to the radiolysis of methanol and n-propanol in the liquid phase. The methanol system was studied over a 247° range of temperature, in which the dielectric constant changes from 73 to 15 and the dielectric relaxation time varies from  $3.3 \times 10^{-9}$  to  $7.6 \times 10^{-12}$  sec. The radiolysis of n-propanol was carried over a 260° range of temperature, in which the dielectric constant changes from 45.7 to 8.1 and the dielectric relaxation time varies from  $6.5 \times 10^{-6}$  to  $2.8 \times 10^{-11}$  sec. To study the reactions of electrons in these alcohols, nitrous oxide and acids (sulfuric and

hydrochloric) were used as electron scavengers.

The other purpose of this work was to obtain a more accurate measure of the yields of the hydrogen precursors in view of the considerable lack of agreement among the published values.

E X P E R I M E N T A L

(A) Materials

1. Radiolysed Compounds

- a. Methanol: Reagent Grade methanol from Shawinigan Chemicals was used. Traces of aldehyde were removed by refluxing 2 l. of methanol for 12 hours in an oxygen free nitrogen atmosphere, after the addition of 3 g of 2,4-dinitrophenylhydrazine and 2 ml of conc. sulfuric acid. It was then distilled through a column packed with glass helices into a reservoir attached to a vacuum line under dry nitrogen atmosphere. The purified methanol was degassed and stored under vacuum in a Pyrex vessel and will be referred to hereafter as sample A. This treatment greatly reduced the optical absorbance (from 0.65 to 0.01) of the methanol in the region of 270  $\mu$  (carbonyl compounds) which was measured in a 10 cm quartz cell. Some of sample A was treated, under vacuum with potassium hydroxide pellets, to reduce the trace amounts of carbon dioxide (sample B).
- b. n-Propanol: 'Baker Analysed' Reagent Grade n-propanol from J. T. Baker Chemical Co., and Certified n-propanol from Fisher Scientific Company were used. They were purified as follows. Two liters of n-propanol to which 30 g of silver oxide had been added was refluxed for 24 hrs. It was then distilled through a column packed with glass helices

into a reservoir. The middle fraction of this distillate was refluxed for 2 hrs with 1.5 g of 2,4-dinitrophenylhydrazine and 1 ml of conc. sulfuric acid. It was then distilled into a reservoir attached to the vacuum line, as in case of methanol. During the refluxing and distillation, the alcohol was protected from atmospheric oxygen and moisture by passing a gentle stream of dry nitrogen through the system. The purified n-propanol was degassed and stored under vacuum in a Pyrex vessel. This treatment drastically reduced the optical absorbance (from 2.0 to 0.05) of the n-propanol in the region of 270  $\mu$  (carbonyl compounds) which was measured in a 10 cm quartz cell. Some of purified n-propanol was further treated with potassium hydroxide pellets, to reduce the trace amounts of carbon dioxide.

## 2. Compounds Used as Additives

- a. Hydrogen chloride: Hydrogen chloride (anhydrous) from Matheson of Canada Ltd., was purified by trap-to-trap sublimation in a vacuum apparatus, discarding the first and last portions. It was stored in a Pyrex reservoir.
  
- b. Nitrous oxide: Nitrous oxide from Matheson of Canada Ltd. was purified by trap-to-trap sublimation under vacuum, discarding the first and last portions. It was stored in a Pyrex reservoir.

c. Sulfuric acid: Reagent Grade sulfuric acid from C.I.L. was used as received.

3. Other Materials:

Nitrogen: Pure Grade nitrogen from Linde, Canada was used after passing through liquid nitrogen trap.

Other materials were used as received; for example; carbon monoxide and methane.

B. Procedures and Techniques

1. Sample Preparation (Fig. II-1): Five milliliter samples were irradiated in Pyrex glass cells with a bulbous, easily cleaned break-seal (Figure II-3). They were filled through a side arm which was sealed off after filling. The total volume of each cell was approximately 10 ml. The cells were cleaned with ethanol and conc. nitric acid, and were rinsed repeatedly with triply distilled water. They were dried in an oven for two hours at 150° and then evacuated, heated with a flame, and pumped under vacuum for 1 hr before filling.

Samples were prepared by vacuum distilling the alcohol from the reservoir into a measuring tube and then redistilling it into the sample cell through the side arm. Nitrous oxide and/or hydrogen chloride were added by condensation onto the frozen sample, and the cell was sealed off with the sample maintained at -196°C. The pressure, volume and temperature of the additive gases were measured before



transferring onto the frozen sample. The cells that were to contain sulfuric acid were filled with dry nitrogen after degassing, then removed from the vacuum line. The known volume of acid was added with a long needle syringe. Then, the cell was put onto the sample filling line (Figure II-1). The acid was frozen with liquid nitrogen, then degassed by successive pump-thaw-freeze-pump cycles. The alcohol was distilled into the measuring tube and then redistilled into the sample cell. The sample was degassed again and then sealed off.

2. Sample Irradiation: The irradiation source was a 12,000 curie Gammacell-220 (Atomic Energy of Canada Ltd.) containing  $^{60}\text{Co}$ .

The samples were irradiated at various temperatures. A glass Dewar vessel fixed with epoxy resin to a metal positioning plate was used to hold the samples, which were fixed in a metal jig, up to 140°C. Suitable slushes were used to obtain constant temperatures below 0°; water was used for temperatures between 0° and 90°; glycerol was used for temperatures between 100° and 140°. Above 140°, the vapor pressures of the alcohols used rapidly exceeded that which could be contained by the glass cells used. The samples irradiated above 140° were placed in the usual glass cells in a steel pressure vessel partially filled with the same alcohol as that to be irradiated.

The alcohol which partially filled the pressure vessel exerted its vapour pressure on the glass sample cell, equalizing the interior and exterior pressures. Thus, a glass cell could be used at very high pressures.

The pressure vessel was placed in a small, electrically heated oven and warmed to the desired temperature, allowed to equilibrate, and then irradiated. The temperature was measured with an iron-constantan thermocouple and was controlled to  $\pm 1^\circ\text{C}$ .

The design of the pressure vessel is shown in Figure II-2. The walls were made as thin as practicable to minimize attenuation of the  $\gamma$ -radiation. The vessel was machined from a bar of SPS-245 steel and heat treated to Rockwell C-30. The estimated bursting pressure of the vessel was 650 atm before heat treatment and 1350 atm after heat treatment. The vessel was pressure tested on a hydraulic pressure system to 300 atm before use. Lead was found to be the most suitable gasket material, as a good seal was formed without the application of a high force through the screws in the head, and lead was not affected by temperature or radiation under the experimental conditions.

It was found to be necessary to flush the pressure vessel with nitrogen gas before closing it. At high temperatures and pressures, oxygen in the entrapped air oxidizes the alcohol, and the resulting acid rapidly attacks the

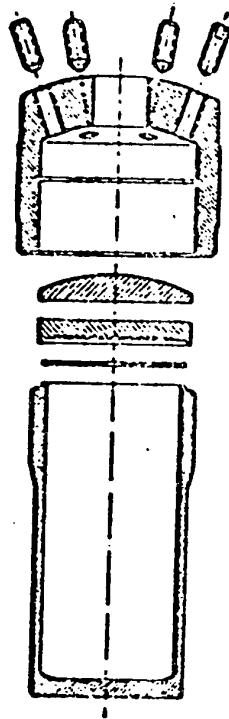


FIGURE II-2: Steel pressure cell used for high temperature irradiations. The diagram is drawn to scale and the inside diameter of the steel pressure cell is 5.1 cm.

steel. The vessel could be constructed from stainless steel, but this would require a greater wall thickness for the same strength.

Fricke dosimetry was used. The dosimetry solution was 1 mM  $\text{Fe}(\text{NH}_4)_2(\text{SO}_4)_2$  and 1 mM NaCl in 0.8 N  $\text{H}_2\text{SO}_4$ . Dosimetry calculations were based on the value  $G(\text{Fe}^{3+}) = 15.5$ ,  $\epsilon(\text{Fe}^{3+})$  at  $304 \text{ m}\mu = 2225 \text{ l mole}^{-1} \text{ cm}^{-1}$  at  $25^\circ\text{C}$  and a temperature coefficient of  $\epsilon(\text{Fe}^{3+})$  of  $0.7\%/^\circ\text{C}$ .

Various liquids were used as temperature bath as mentioned above. The absorption of gamma rays was different for different liquids due to their different electron densities. The dose rate (D.R.) of alcohol samples in a liquid bath was calculated from the dose rate in air, adjusted for absorption by the bath. The adjustment was made as follows:

$$\begin{aligned} (\text{D.R.})_{\text{liq. bath}} &= (\text{D.R.})_{\text{air}} - (\text{D.R.})_{\text{absorbed by liquid bath}} \\ &= (\text{D.R.})_{\text{air}} - [(\text{D.R.})_{\text{H}_2\text{O}} - (\text{D.R.})_{\text{air}}] \rho_{\text{liq. bath}} / \rho_{\text{H}_2\text{O}} \end{aligned}$$

where  $\rho_{\text{liq. bath}} / \rho_{\text{H}_2\text{O}}$  is the ratio of the electron densities of liquid bath and water.

The dose rate was approximately  $4 \times 10^{17} \text{ eV ml}^{-1} \text{ min}^{-1}$  in the alcohol. The dose rates were continuously corrected for the radioactive decay of  $^{60}\text{Co}$  ( $t_{1/2} = 5.27 \text{ years}$ ).

3. Product analysis: The gas analysis system is shown in

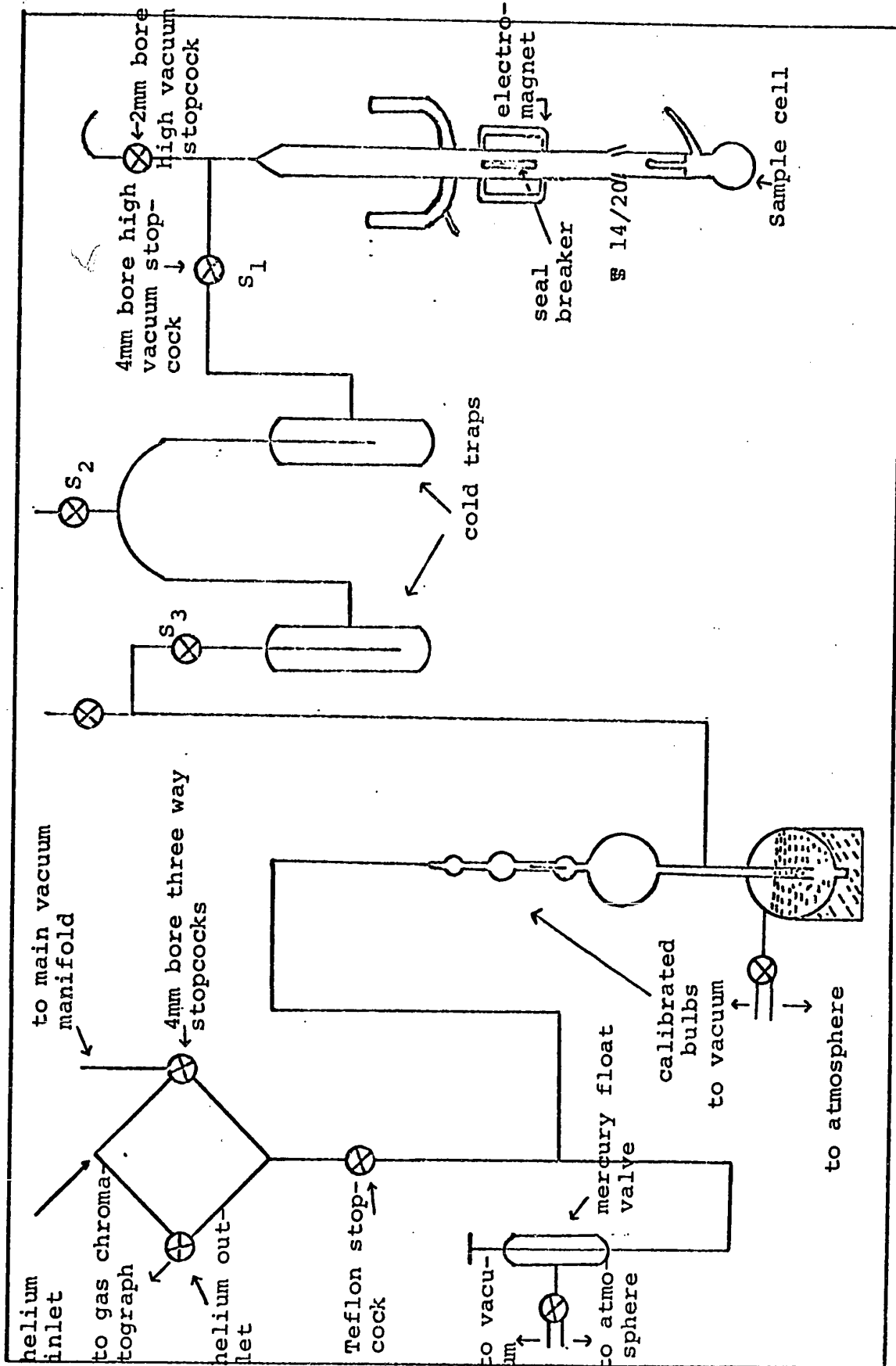


FIGURE II-3. Sample Analysis System

Figure II-3. After the system was completely evacuated, stopcocks  $S_1$ ,  $S_2$  and  $S_3$  were closed and the cold traps were immersed in liquid nitrogen. The sample cell was broken, and the noncondensable gases were collected in the Toepler-McLeod gauge through stopcocks  $S_1$  and  $S_3$ . This technique separated the hydrogen, carbon monoxide, methane and nitrogen from the sample. The total pressure and volume of these gases was measured in the Toepler-McLeod gauge and then they were directly transferred on to the gas chromatographic column through the gas sample (Figure II-3).

To analyse the gas mixture, a 2.5 m column packed with molecular sieve 13X was used, with helium carrier gas and a thermal conductivity detector.

The gas chromatographic unit consisted of the thermal conductivity detector with W-2 filaments and Gow Mac power supply. A recorder from E.H. Sargent and Co. was used. The detector temperature was maintained at 30°C. The detector current of 300 mA was used.

## R E S U L T S

### Part I Radiolysis of Liquid Methanol

#### (A) Gaseous Products at 25°

The yields of hydrogen, methane and carbon monoxide were independent of dose over the range  $4.4 \times 10^{17}$  to  $6.3 \times 10^{18}$   $\text{eV ml}^{-1}$  at 25°, for both samples A and B of methanol. The yields at 25° are presented in Table III-1 together with the results of other workers. The dose rates and total dose used by different workers are also included in Table III-1. The agreement among the different sets of results is poor. The observed values of  $G(\text{H}_2)$  from gamma irradiation vary from 4.1 to 5.4. The technique of purification considerably influences the hydrogen yields. This aspect has been discussed in detail elsewhere (39). Recently, it has been deduced from scavenging experiments that  $G(\text{H}_2) = 5.4$  from pure methanol at room temperature although the experimental value was 4.92 (107).

#### (B) Effect of Temperature on Gaseous Product Yields

All samples were given a dose of  $5.6 \times 10^{17}$   $\text{eV g}^{-1}$ . The irradiation temperature was varied over the range from -97° (freezing point of methanol) to 240° (critical temperature of methanol). The variation of the yields with temperature for both samples A and B are presented in Table III-2 and are plotted in Figures III-1 and III-2.

TABLE III-1

G Values of Products from  $\gamma$ -Radiolysis of Methanol at 25°

Product	This work		Ref. (107)	Ref. (98)	Ref. (96)	Ref. (39)	Ref. (41)	Ref. (19)	Ref. (108)	Ref. (109)
	Sample A	Sample B								
Hydrogen	5.0	5.40	4.92	4.48	4.20	4.60	4.99	5.40	4.1	5.39
Methane	0.45	0.45	0.38	---	---	0.32	0.44	0.80	0.39	0.54
Carbon Monoxide	0.20	0.20	0.14	---	---	0.15	0.12	0.15	0.13	0.11
Dose x 10 <sup>-18</sup> eV ml <sup>-1</sup>	0.44	0.44	22	0.3-60	0.55	10-500	30	1.6-12	0.016-.09	4-400
Dose rate x 10 <sup>-16</sup> eV ml <sup>-1</sup> min <sup>-1</sup>	22	22	15	7.5	1.7	20&30	15&80	0.2&3.0	0.16	9.4

TABLE III-2

Product Yields as a Function of Temperature

Temperature °C	<u>Sample A</u>			<u>Sample B</u>		
	G(H <sub>2</sub> )	G(CH <sub>4</sub> )	G(CO)	G(H <sub>2</sub> )	G(CH <sub>4</sub> )	G(CO)
-97°	3.5	0.37	0.12	4.50*	0.34*	0.14*
-45	3.88	0.28	0.16			
0	4.64	0.30	0.19			
25	5.0	0.49	0.20	5.40*	0.40*	0.20*
60	5.35	0.45	0.21			
90	5.72	0.37	0.25			
140	6.45	0.43	0.36			
150				6.48	0.44	0.32
160	6.64	0.43	0.37			
180	7.25	0.41	0.45			
200	7.42	0.52	0.53			
220	7.75	0.51	0.57	7.45	0.60	0.48
240	8.04	0.55	0.68			

---

\* These values were duplicated.

FIGURE III-1

The yield of hydrogen as a function of temperature:

⊙ , Sample A; △ , Sample B; -----, estimated values for absolutely pure methanol.

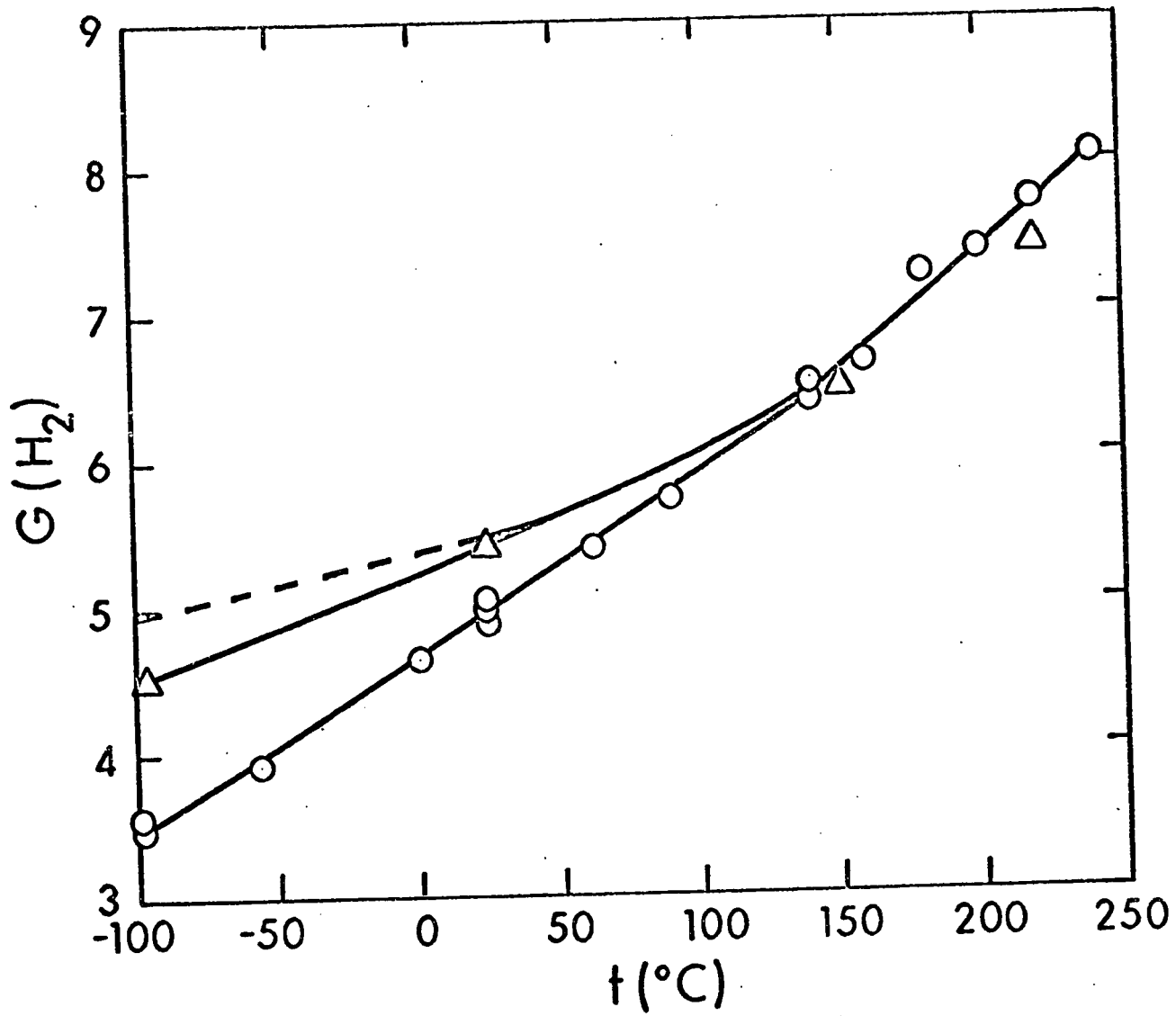
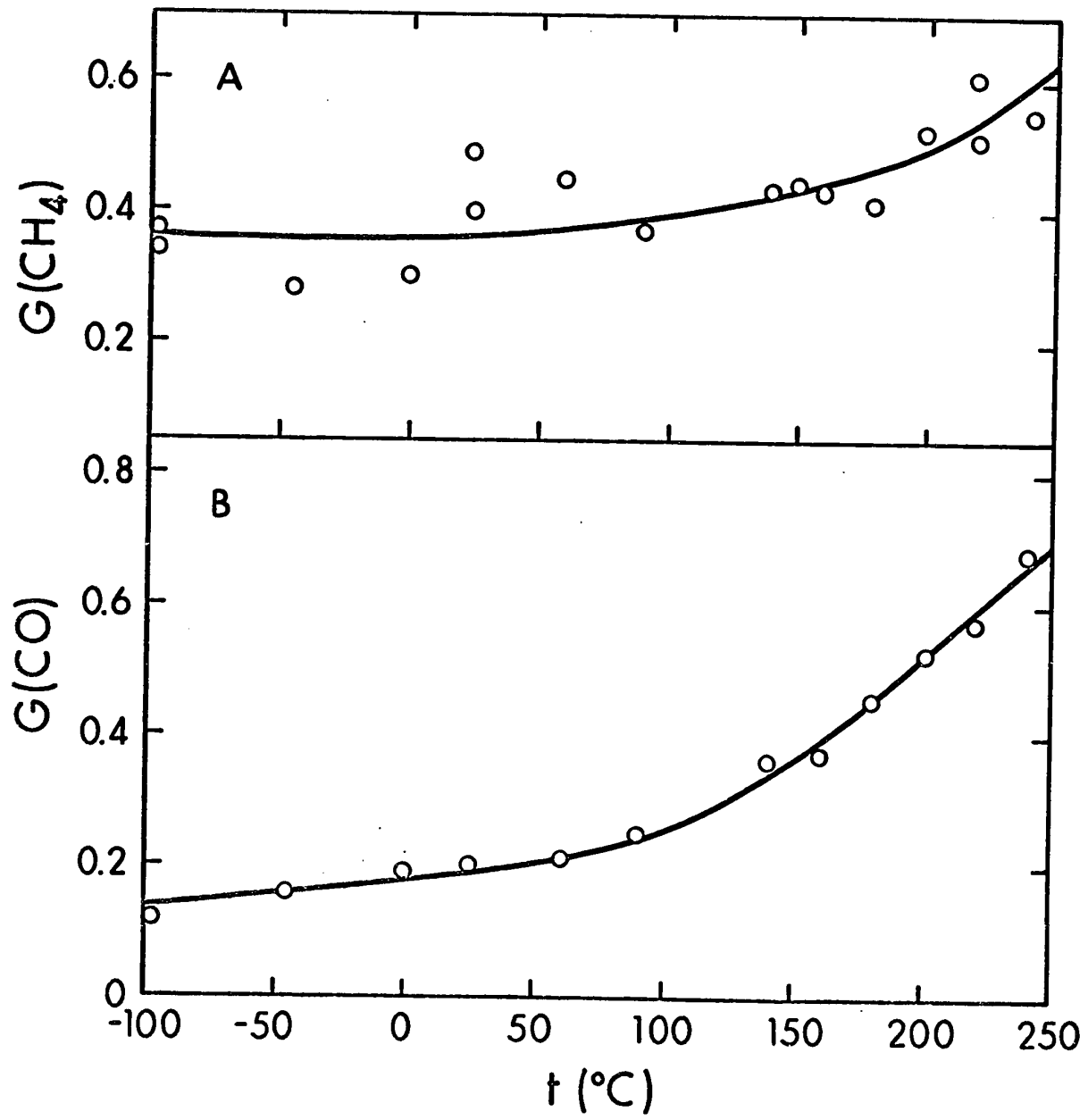


FIGURE III-2

Methane and carbon monoxide yields as a function of temperature in methanol.

A, methane; B, carbon monoxide.



Between  $-97^{\circ}$  and  $+240^{\circ}$  the hydrogen yield from sample B increased from  $G(H_2) = 4.5$  to  $8.0$ , while from A it increased from  $3.5$  to  $8.0$  (Figure III-1). Sample A evidently contained a trace of carbon dioxide, which was largely removed by the potassium hydroxide treatment. Kinetic analysis of later scavenger results indicate that Sample B of methanol contained about  $10^{-5}$  M of an electron scavenger, probably acetone, and Sample A contained about  $10^{-4}$  M electron scavenger, probably mostly carbon dioxide. (The kinetic calculations are presented in the Discussion Section). Sample-B methanol was used for experiments when less than  $10^{-2}$  M scavenger was added.

#### (C) Scavenger Studies in Liquid Methanol

Nitrous oxide, sulfuric acid and hydrochloric acid were used as electron scavengers in the radiolysis of methanol at  $-97^{\circ}$ ,  $25^{\circ}$  and  $150^{\circ}$ .

Whenever the symbol  $G$  is used, it refers to a product yield in a single component system, i.e. not a solution. For all scavenger solutions the yields are reported in  $g$  units, which are normal  $G$  values divided by the electron fraction of methanol in the solution. For the direct radiolysis of nitrous oxide in the more concentrated solutions a correction was made to the nitrogen yields. It was assumed that the energy absorbed by nitrous oxide was proportional to its electron fraction in the solution

and that  $G(N_2) = 12.9$  for direct radiolysis (110). The hydrogen yields from the more concentrated sulfuric acid solutions were similarly corrected for the direct radiolysis of sulfuric acid, using  $G(H_2)_{H_2SO_4} = 2.3$  (111). The hydrogen chloride solutions were so dilute that no correction to the yields was necessary.

#### 1. Calculation of the Scavenger Concentrations in Methanol

The concentrations of nitrous oxide in samples at  $-97^\circ$  were calculated by assuming that all the nitrous oxide was dissolved at that temperature. At  $25^\circ$  the value of the Bunsen absorption coefficient of nitrous oxide in methanol is  $\alpha = 2.92$  (112), where  $\alpha = (273.1/T) (C_{liquid}/C_{gas})$ , and  $C_{liquid}$  and  $C_{gas}$  are the concentrations of nitrous oxide in the liquid and gas phases, respectively. Thus the concentration of nitrous oxide in the sample can be calculated if the volume of the cell is known. The cell volumes were measured at the conclusion of each analysis. Available values of  $\alpha$  extend only from  $18^\circ$  to  $34^\circ$ , so the value used at  $150^\circ$  ( $\alpha = 0.62$ ) was obtained by a long extrapolation. An error in this value would shift the entire concentration scale for the  $150^\circ$  curves in Figures III-5 and III-6 by a constant factor, but the shapes of the curves would not be affected.

In acidic methanol, for kinetic analysis of the product yields, the concentration of protonated methanol

was needed. The dissociation constant of sulfuric acid in methanol is  $K_1 = 0.028$  (113). The value of the dissociation constant of hydrogen chloride in methanol  $K_{\text{diss}} = 0.25$ , was calculated from the equation given below that relates the acid dissociation constant to the dielectric constant of the medium (114), and using the known value  $K_{\text{diss}} = 0.015$  in ethanol (115).

$$\ln \frac{(K_{\text{HB}})_2}{(K_{\text{HB}})_1} = -\frac{e^2}{2kT} \left( \frac{1}{r_{\text{H}^+}} + \frac{1}{r_{\text{B}^-}} \right) \cdot \left( \frac{1}{D_2} - \frac{1}{D_1} \right)$$

where  $K_{\text{HB}}$  is the dissociation constant of a particular acid HB,  $e$  is the electronic charge in e.s.u.,  $k$  is the Boltzmann constant,  $T$  is the absolute temperature,  $r_{\text{H}^+}$  and  $r_{\text{B}^-}$  are the radii of dissociated species,  $D$  is the dielectric constant and subscripts 1 and 2 refers to the solvents 1 and 2 respectively. This equation is approximate and is used for lack of better information. The dissociation constants of weak acids in water and in aqueous organic mixed solvents do not change rapidly with temperature. Furthermore, some dissociation constants increase and others decrease with increasing temperature (116). It is therefore assumed, for the lack of better information, that the dissociation constants in methanol are independent of temperature.

At concentrations of 0.1 M and greater, hydrogen chloride reacted with methanol to form an appreciable

amount of methyl chloride. Methyl chloride is an electron scavenger which reduces the hydrogen yield, so sulfuric acid was used to make the strongly acidic solutions (24,25). Sulfuric acid added to methanol at 25° gives  $\text{CH}_3\text{OH}_2^+$  and  $\text{HSO}_4^-$  ions (117). On warming the solution, methyl hydrogen sulfate forms (117). By analogy with the near equality of the dissociation constants (118) of  $\text{CH}_3\text{CH}_2\text{COOH}$  ( $1.34 \times 10^{-5}$ ) and  $\text{CH}_3\text{COOH}$  ( $1.76 \times 10^{-5}$ ) in water, it is assumed that  $K_{\text{diss}}(\text{CH}_3\text{OSO}_2\text{OH}) \approx K_1(\text{HOSO}_2\text{OH})$ . Thus it was concluded that the concentration of oxonium ions was essentially the same at 150° as at 25° for a given concentration of added sulfuric acid. This conclusion was supported by conductance measurements. The conductance of pure methanol at 25° was  $7.0 \times 10^{-7}$  mho/cm; that of 0.75 M sulfuric acid in methanol at 25° was 0.030 mho/cm; that of the preceding solution after heating to 150° for half an hour, then cooling to 25° was 0.028 mho/cm. Thus the conductance was only slightly reduced by the heat treatment.

## 2. Effect of Scavengers on the Gaseous Product Yields at -97°, 25° and 150°.

The g values of gaseous products as functions of solute concentration are presented in Tables III-3 to III-8 and Figures III-3 to III-6. It is evident from the data in Figures III-3 to III-6 and Tables III-3 to III-8 that the addition of acid caused  $g(\text{H}_2)$  to increase in the same way

TABLE III-3

Product Yields as a Function of Nitrous Oxide Concentration at -97°

[N <sub>2</sub> O] Molar	g(H <sub>2</sub> )	g(N <sub>2</sub> ) total	g(N <sub>2</sub> ) corrected	g(H <sub>2</sub> ) + g(N <sub>2</sub> ) corrected	g(CH <sub>4</sub> )	g(CO)
5.80x10 <sup>-5</sup>	3.60	1.03	1.03	4.63	0.40	0.17
2.30x10 <sup>-4</sup>	3.30	1.45	1.45	4.75	0.33	0.14
7.52x10 <sup>-4</sup>	3.22	1.73	1.73	4.95	0.34	0.15
1.12x10 <sup>-3</sup>	3.15	1.80	1.80	4.95	0.38	0.14
4.10x10 <sup>-3</sup>	3.00	2.03	2.03	5.03	0.42	0.17
1.0 x10 <sup>-2</sup>	2.75	2.35	2.35	5.10	0.32	0.14
1.56x10 <sup>-2</sup>	2.85	2.30	2.30	5.15	0.29	0.14
6.00x10 <sup>-2</sup>	2.76	2.67	2.62	5.38	0.37	0.18
0.167	2.60	3.04	2.94	5.54	0.37	0.17
0.485	2.16	4.02	3.70	5.86	0.25	0.19
0.90	1.95	4.64	4.04	5.99	0.24	0.18
0.94	1.37	5.22	4.40	5.77	0.22	0.19
1.15	1.60	5.40	4.55	6.15	0.17	0.18
1.30	1.51	5.55	4.60	6.11	0.17	0.22
2.75	1.30	6.80	4.80	6.10	0.17	0.18
4.2	1.65	7.50	4.70	6.35	n.d.*	n.d.
7.0	1.65	8.80	4.30	5.95	n.d.	n.d.

\* n.d. not determined

TABLE III-4

Product Yields as a Function of Acid Concentration  
at -97°.

Acid	[Acid]M	[CH <sub>3</sub> OH <sub>2</sub> <sup>+</sup> ]M	g(H <sub>2</sub> )	g(CH <sub>4</sub> )	g(CO)
HCl	1.75x10 <sup>-4</sup>	1.75x10 <sup>-4</sup>	4.68	0.24	0.16
	2.0 x10 <sup>-3</sup>	2.0 x10 <sup>-3</sup>	4.90	0.30	0.15
	2.8 x10 <sup>-2</sup>	2.5 x10 <sup>-2</sup>	5.07	0.23	0.17
H <sub>2</sub> SO <sub>4</sub>	4.3 x10 <sup>-2</sup>	2.3 x10 <sup>-2</sup>	5.10	0.35	0.14
	0.75	0.137	5.40	0.24	0.16
	1.69	0.222	5.50	0.32	0.18

TABLE III-5

Product Yields as a Function of Nitrous Oxide Concentration at 25°

[N <sub>2</sub> O] Molar	g(H <sub>2</sub> )	g(N <sub>2</sub> ) total	g(N <sub>2</sub> ) corrected	g(H <sub>2</sub> ) + g(N <sub>2</sub> ) corrected	g(CH <sub>4</sub> )	g(CO)
5.6x10 <sup>-5</sup>	4.60	0.80	0.80	5.40	0.45	0.21
2.2x10 <sup>-4</sup>	4.10	1.30	1.30	5.40	0.42	0.22
5.6x10 <sup>-4</sup>	3.95	1.50	1.50	5.45	0.50	0.24
1.5x10 <sup>-3</sup>	3.50	1.96	1.96	5.46	0.42	0.21
5.8x10 <sup>-3</sup>	3.40	2.10	2.10	5.50	0.42	0.21
2.7x10 <sup>-2</sup>	2.84	2.76	2.76	5.60	0.52	0.20
7.5x10 <sup>-2</sup>	2.90	3.04	2.95	5.85	0.42	0.22
0.40	2.55	4.30	3.70	6.25	0.43	0.21
0.61	2.40	4.47	3.90	6.30	0.35	0.21
0.80	1.80	5.62	4.60	6.40	0.34	0.24
0.94	2.05	5.39	4.25	6.30	0.38	0.25
0.98	2.08	5.43	4.30	6.38	0.32	0.22

TABLE III-6

Product Yields as a Function of Acid Concentration at 25°

Acid	[Acid] Molar	[CH <sub>3</sub> OH <sub>2</sub> <sup>+</sup> ] Molar	g(H <sub>2</sub> )	g(CH <sub>4</sub> )	g(CO)
HCl	1.31x10 <sup>-3</sup>	1.30x10 <sup>-3</sup>	5.45	0.30	0.20
	1.24x10 <sup>-2</sup>	1.20x10 <sup>-2</sup>	5.53	0.27	0.21
	4.60x10 <sup>-2</sup>	4.0x10 <sup>-2</sup>	5.70	0.18	0.14
H <sub>2</sub> SO <sub>4</sub>	3.20x10 <sup>-2</sup>	1.88x10 <sup>-2</sup>	5.54	0.37	0.14
	0.375	9.7 x10 <sup>-2</sup>	5.85	0.29	0.23
	0.75	0.137	5.90	0.31	0.20
	1.5	0.194	6.00	0.46	0.28

TABLE III-6

Product Yields as a Function of Acid Concentration at 25°

Acid	[Acid] Molar	[CH <sub>3</sub> OH <sub>2</sub> <sup>+</sup> ] Molar	g(H <sub>2</sub> )	g(CH <sub>4</sub> )	g(CO)
HCl	1.31x10 <sup>-3</sup>	1.30x10 <sup>-3</sup>	5.45	0.30	0.20
	1.24x10 <sup>-2</sup>	1.20x10 <sup>-2</sup>	5.53	0.27	0.21
	4.60x10 <sup>-2</sup>	4.0x10 <sup>-2</sup>	5.70	0.18	0.14
H <sub>2</sub> SO <sub>4</sub>	3.20x10 <sup>-2</sup>	1.88x10 <sup>-2</sup>	5.54	0.37	0.14
	0.375	9.7 x10 <sup>-2</sup>	5.85	0.29	0.23
	0.75	0.137	5.90	0.31	0.20
	1.5	0.194	6.00	0.46	0.28

TABLE III-7

Product Yields as a Function of Nitrous Oxide Concentration at 150°

<u>[N<sub>2</sub>O] Molar</u>	<u>g(H<sub>2</sub>)</u>	<u>g(N<sub>2</sub>) total</u>	<u>g(N<sub>2</sub>) corrected</u>	<u>g(H<sub>2</sub>) + g(N<sub>2</sub>) corrected</u>	<u>g(CH<sub>4</sub>)</u>	<u>g(CO)</u>
4.2x10 <sup>-5</sup>	6.28	0.28	0.28	6.56	0.33	0.35
8.4x10 <sup>-5</sup>	6.17	0.35	0.35	6.52	0.33	0.35
1.88x10 <sup>-4</sup>	5.70	0.83	0.83	6.53	0.33	0.33
2.26x10 <sup>-4</sup>	5.97	0.60	0.60	6.57	0.35	0.30
6.6 x10 <sup>-4</sup>	5.27	1.30	1.30	6.57	0.35	0.34
1.86x10 <sup>-3</sup>	4.78	1.73	1.73	6.51	0.41	0.33
5.6 x10 <sup>-3</sup>	4.80	2.40	2.40	7.20	0.49	0.36
1.52x10 <sup>-2</sup>	4.08	2.82	2.77	6.85	0.58	0.34
0.145	3.26	3.95	3.57	6.83	0.55	0.36

TABLE III-8

Product Yields as a Function of Acid Concentration  
at 150°

<u>Acid</u>	<u>[Acid]</u> <u>Molar</u>	<u>[CH<sub>3</sub>OH<sub>2</sub><sup>+</sup>]</u> <u>Molar</u>	<u>g (H<sub>2</sub>)</u>	<u>G (CH<sub>4</sub>)</u>	<u>g (CO)</u>
HCl	6.5x10 <sup>-4</sup>	6.5x10 <sup>-4</sup>	6.53	0.56	0.29
H <sub>2</sub> SO <sub>4</sub>	4.3x10 <sup>-2</sup>	2.30x10 <sup>-2</sup>	6.80	0.61	0.36
	0.375	9.00x10 <sup>-2</sup>	6.70	0.70	0.46
	1.125	0.168	6.70	0.56	0.29

FIGURE III-3

The effect of acid or nitrous oxide concentration at  $-97^{\circ}$  in methanol.

O,  $N_2$  and  $\square$ ,  $(H_2 + N_2)$  from nitrous oxide solutions, corrected for direct radiolysis of nitrous oxide;  $\Delta$ ,  $H_2$  in the presence of HCl;  $\blacktriangle$ ,  $H_2$  in the presence of  $H_2SO_4$ , corrected for the direct radiolysis of the acid. S is  $N_2O$  or  $CH_3OH_2^+$ . The solid and broken lines through the nitrogen yields were calculated by the 1AP and 2AP treatments, respectively (see Table IV-1). The line through the  $(H_2 + N_2)$  points is the sum of the  $N_2$  and  $H_2$  (Fig. III-6) calculated curves.

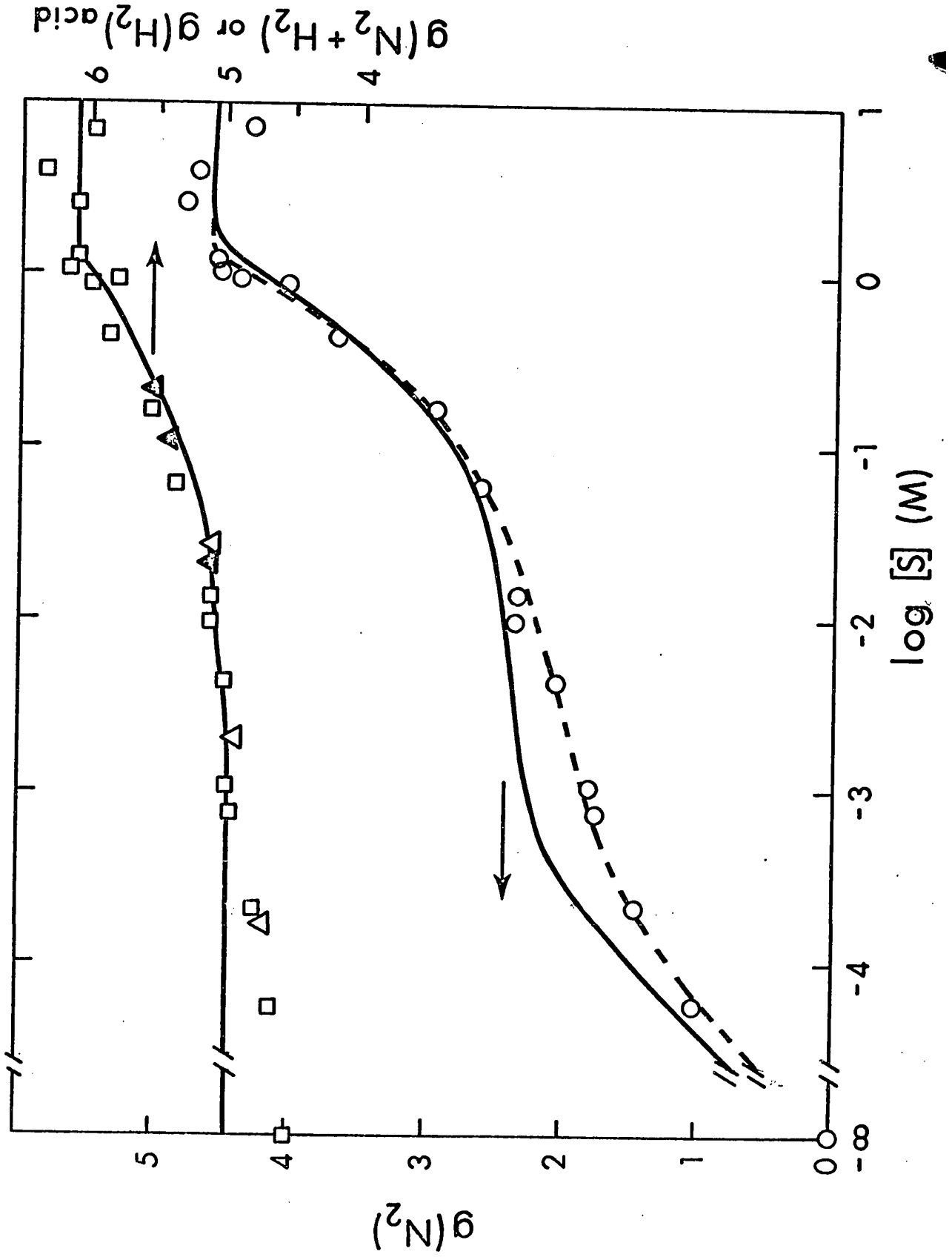


FIGURE III-4

The effect of acid or nitrous oxide concentration at 25° in methanol.

O, N<sub>2</sub> and □, (H<sub>2</sub> + N<sub>2</sub>) from nitrous oxide solutions, corrected for direct radiolysis of nitrous oxide; Δ, H<sub>2</sub> in the presence of HCl; ▲, H<sub>2</sub> in the presence of H<sub>2</sub>SO<sub>4</sub> corrected for the direct radiolysis of the acid. S is N<sub>2</sub>O or CH<sub>3</sub>OH<sub>2</sub><sup>+</sup>. The solid and broken lines through the nitrogen yields were calculated by the 1AP and 2AP treatments, respectively (see Table IV-1). The line through the (H<sub>2</sub> + N<sub>2</sub>) points is the sum of the N<sub>2</sub> and H<sub>2</sub> (Fig. III-6) calculated curves.

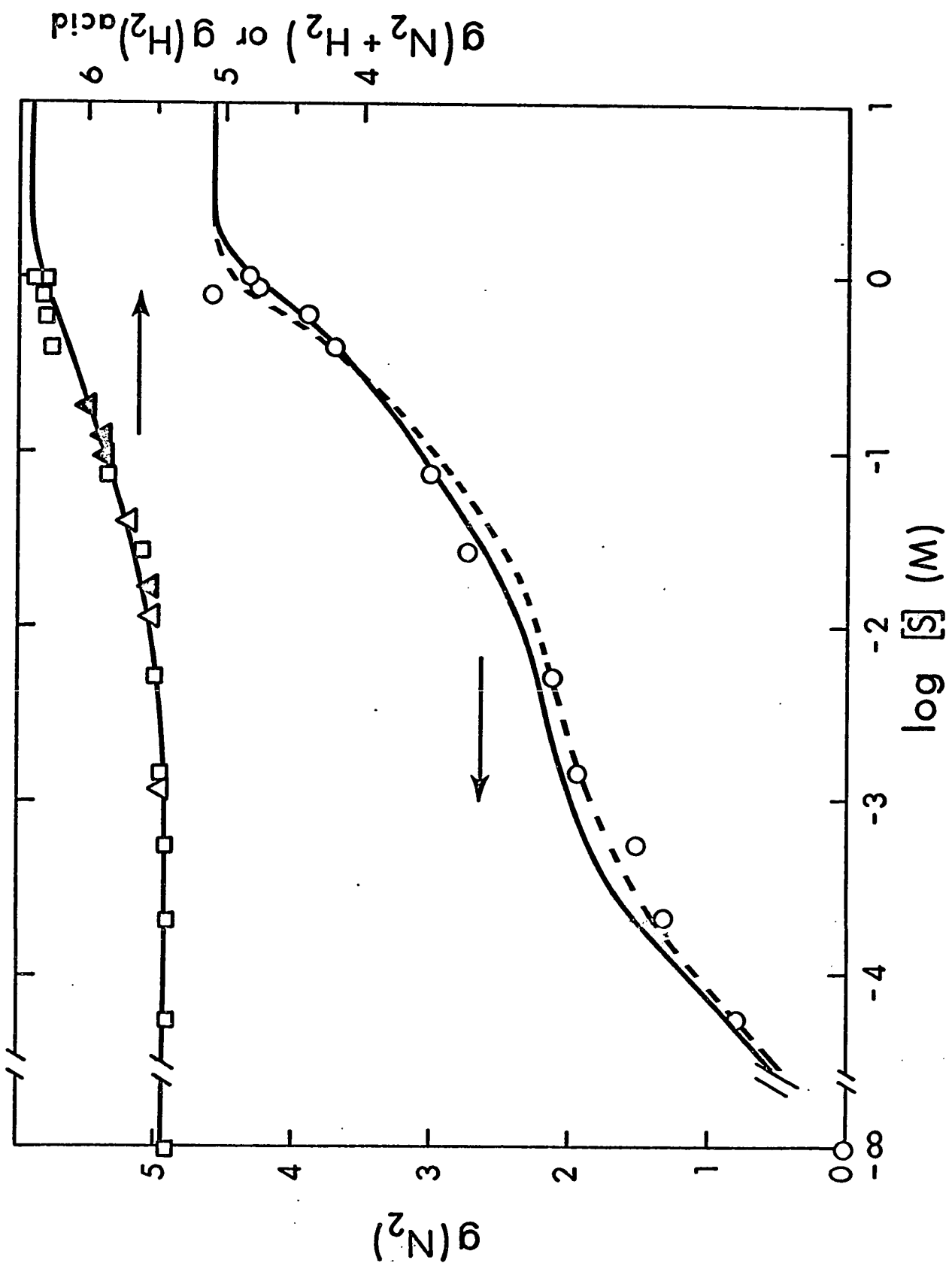


FIGURE III-5

.The effect of acid or nitrous oxide concentration at 150° in methanol.

O, N<sub>2</sub> and □, (H<sub>2</sub> + N<sub>2</sub>) from nitrous oxide solutions, corrected for direct radiolysis of nitrous oxide; Δ, H<sub>2</sub> in the presence of HCl; ▲, H<sub>2</sub> in the presence of H<sub>2</sub>SO<sub>4</sub>, corrected for the direct radiolysis of the acid. S is N<sub>2</sub>O or CH<sub>3</sub>OH<sub>2</sub><sup>+</sup>. The line through the nitrogen yields was calculated by the LAP treatment (see Table IV-1). The line through the (H<sub>2</sub> + N<sub>2</sub>) points is the sum of the N<sub>2</sub> and H<sub>2</sub> (Fig. III-6) calculated curves.

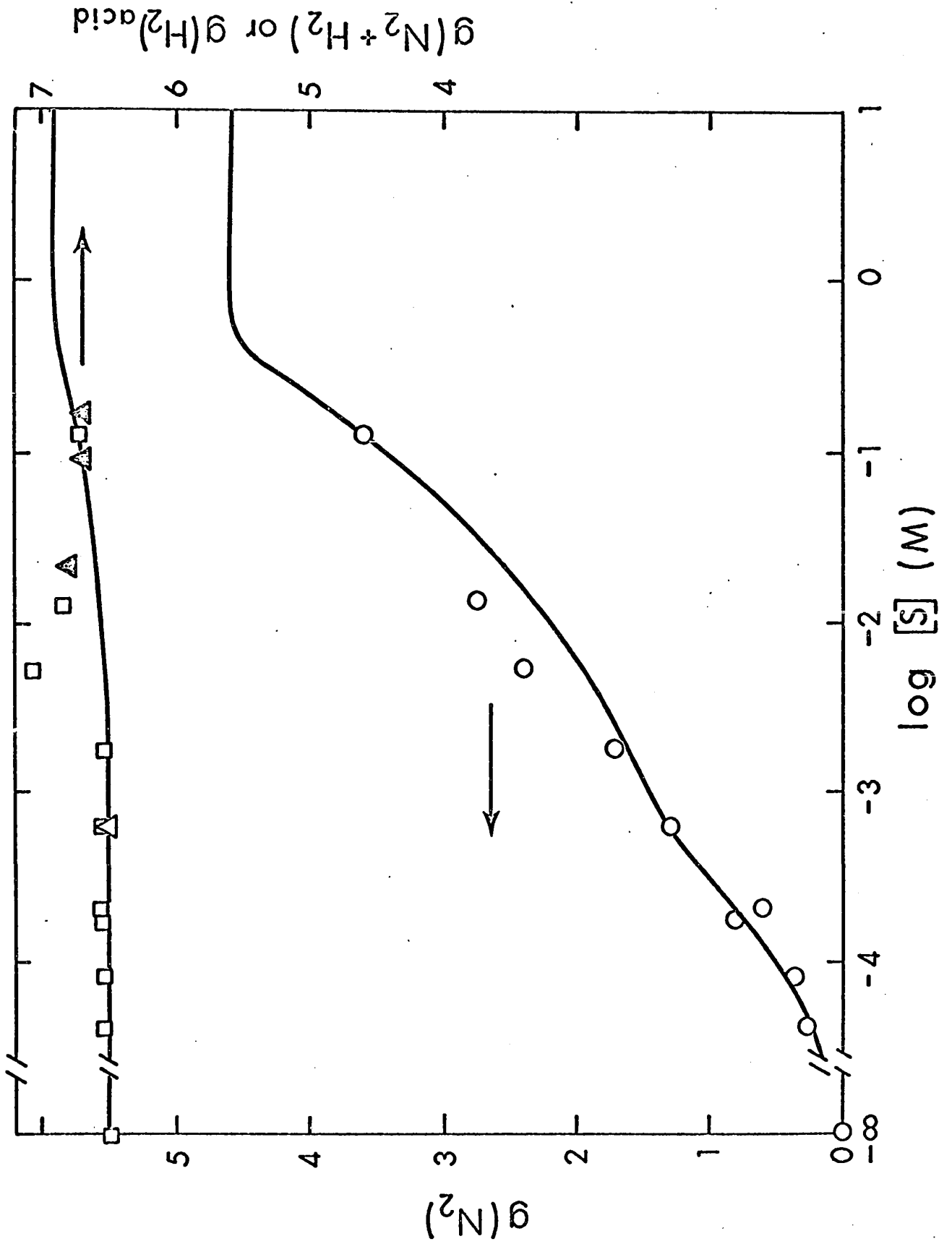
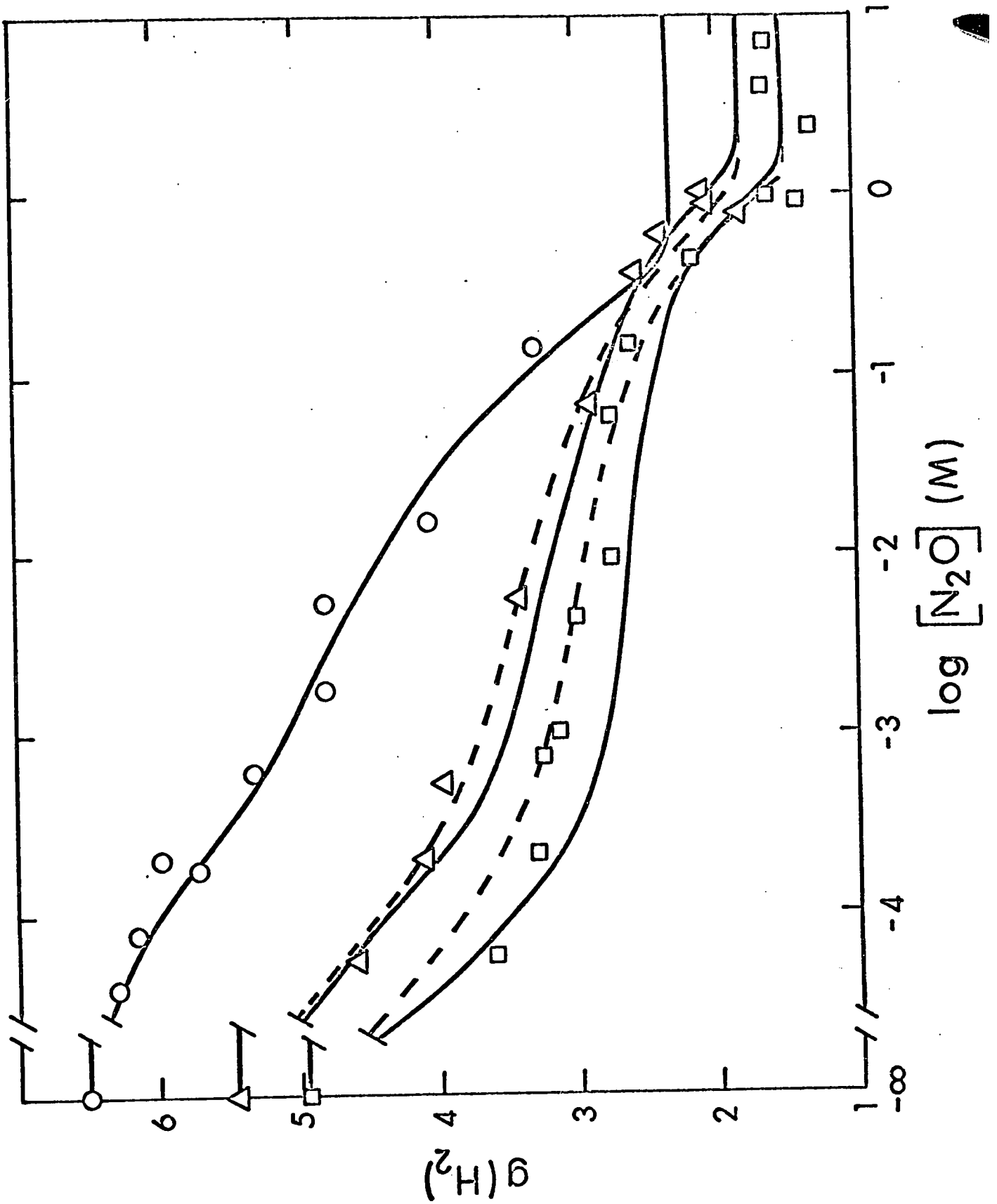


FIGURE III-6

The yield of hydrogen as a function of nitrous oxide concentration in methanol.

O, 150°; Δ, 25°; □, -97°. The solid and broken lines were calculated by the 1AP and 2AP treatments, respectively (see Tables IV-1 and IV-5).



as the addition of nitrous oxide caused  $g(\text{H}_2 + \text{N}_2)$  to increase. At  $-97^\circ$  these yields tended to level off at  $g = 4.9 - 5.0$  between  $10^{-3}$  and  $10^{-2}$  M nitrous oxide or  $\text{CH}_3\text{OH}_2^+$ , then increased again at higher solute concentrations (Figure III-3 and Tables III-3 and III-4). At  $25^\circ$ , these  $g$  values were essentially constant at  $5.4 - 5.5$  between  $10^{-3}$  and  $10^{-2}$  M scavenger, then increased with further increase of scavenger concentration (Figure III-4 and Tables III-5 and III-6). At  $150^\circ$  the yields equalled  $6.5$ , independent of scavenger concentration up to  $10^{-3}$  M, then increased slightly with increasing scavenger concentration (Figure III-5 and Tables III-7 and III-8).

The hydrogen yield decreased with increasing nitrous oxide concentration at all temperatures (Figure III-6 and Tables III-3, III-5 and III-7). Unfortunately, the apparatus was such that only at  $-97^\circ$  was it possible to obtain sufficiently concentrated solutions to observe a lower plateau in the hydrogen yield curve. The plateau occurred at  $g(\text{H}_2) = 1.5$  at  $-97^\circ$ . The corresponding plateau for the nitrogen yield occurred at  $g(\text{N}_2) = 4.6$  (Figure III-3). For  $25^\circ$  and  $150^\circ$ , the plateau values of hydrogen at very high solute concentrations were chosen such that reasonable upper limits of  $g(\text{H}_2 + \text{N}_2)$  curves were obtained (Figures III-4 and III-5). These values were  $g(\text{H}_2) = 1.8$  at  $25^\circ$  and  $g(\text{H}_2) = 2.3$  at  $150^\circ$  respectively (Figure III-6).

(D) Competition Between Nitrous Oxide and Acid at 25°

A study was made of the competition between acid and nitrous oxide at 25°. The concentrations of hydrogen chloride used were sufficiently low that methyl chloride formation was too slow to interfere with the nitrous oxide-acid competition. The values of  $g(\text{H}_2)$  and  $g(\text{N}_2)$  were between the values caused by the presence of either solute alone at the same concentration. These values are reported in Table III-9.

TABLE III-9

Competition Between Nitrous Oxide and Acid at 25°

<u>[N<sub>2</sub>O]</u> Molar	<u>[HCl]</u> Molar	<u>[CH<sub>3</sub>OH<sub>2</sub><sup>+</sup>]</u> Molar	<u>g(H<sub>2</sub>)</u>	<u>g(N<sub>2</sub>)</u>	<u>g(CH<sub>4</sub>)</u>	<u>g(CO)</u>
0.0164	0.104	0.080	5.30	0.31	0.44	0.18
0.0164	0.021	0.019	5.15	0.57	0.47	0.21
0.165	0.102	0.080	4.15	2.05	0.46	0.21

---

Part II Radiolysis of Liquid n-Propanol

The n-propanol from Fisher Co. retained a larger amount of impurities after purification than did that from J. T. Baker Co. after similar treatment. Therefore the purified n-propanol from the latter source was used throughout the experiments.

(A) Effect of Dose on the Gaseous Product Yields at 25°

The yields of methane and carbon monoxide were independent of dose over the range  $1.8 \times 10^{17}$  to  $1.5 \times 10^{19}$   $\text{eV ml}^{-1}$ . The yield of hydrogen was independent of the dose between  $1.8 \times 10^{17}$  and  $1.0 \times 10^{18}$   $\text{eV ml}^{-1}$  and then decreased slowly with increasing dose (Table III-10).

The yields of hydrogen, methane and carbon monoxide at a dose of  $4.5 \times 10^{17}$   $\text{eV g}^{-1}$  were  $G(\text{H}_2) = 4.5$ ,  $G(\text{CH}_4) = 0.08$  and  $G(\text{CO}) = 0.03$ . These values are compared with previously determined values in Table III-11. The total dose and dose rates used are also included in the Table.

The agreement between our values and that of Basson and van der Linde (42) is good. In both works the dose used is below  $1.0 \times 10^{18}$   $\text{eV ml}^{-1}$  where yields are independent of dose. The yield of hydrogen reported by Johnsen (119) is lower than ours because he used high dose ( $8 \times 10^{18}$   $\text{eV ml}^{-1}$ ). The reason for the disagreement in carbon monoxide yields is not known.

TABLE III-10

Effect of Dose on the Hydrogen Yield at 25°

<u>Dose</u> <u>eV ml<sup>-1</sup></u>	<u>G(H)<sub>2</sub></u>
2.00 x 10 <sup>17</sup>	4.45
3.80 x 10 <sup>17</sup>	4.50
1.00 x 10 <sup>18</sup>	4.45
3.65 x 10 <sup>18</sup>	4.30
7.30 x 10 <sup>18</sup>	4.18
1.46 x 10 <sup>19</sup>	4.12

---

TABLE III-11

Gaseous Product Yields at 25°

	<u>This work</u>	<u>Ref. (42)</u>	<u>Ref. (119)</u>
Hydrogen	4.5	4.4	4.09
Methane	0.08	0.14	0.10
Carbon Monoxide	0.03	nil	0.27
Dose, eV ml <sup>-1</sup>	3.8 x 10 <sup>17</sup>	1.0 x 10 <sup>18</sup>	8.0 x 10 <sup>18</sup>
Dose rate eV ml <sup>-1</sup> min <sup>-1</sup>	3.65 x 10 <sup>17</sup>	7.3 x 10 <sup>16</sup>	1.5 x 10 <sup>17</sup>

---

(B) Effect of Temperature on the Product Yields

All samples were irradiated to a dose of  $4.5 \times 10^{17}$  eV g<sup>-1</sup>. The temperature was varied over the range -120° (melting point -127°) to +264° (critical temperature). The variation of G(H<sub>2</sub>) with temperature is presented in Table III-12 and Figure III-7. The variation of the methane yield is also included in Table III-12. The carbon monoxide yield was independent of temperature.

Between -120° and +264° G(H<sub>2</sub>) increased from 4.08 to 5.85 (Figure III-7 and Table III-12). Results of the kinetic analysis of the scavenging studies indicate that this propanol contained about 10<sup>-5</sup> M of an electron scavenger, probably propionaldehyde (the kinetic calculations are similar to those that are presented for methanol in Section IV).

(C) Scavenging Studies in Liquid n-Propanol

Nitrous oxide, sulfuric acid and hydrogen chloride were used as electron scavengers at -120°, 25° and 140°. For all scavenger solutions the yields are reported in g units, defined in the methanol section (Part I). Corrections for nitrogen and hydrogen yields from the direct radiolysis of nitrous oxide and acid, respectively, in the more concentrated solutions were made. The method of corrections used is the same as in the case of methanolic solutions.

TABLE III-12

Effect of Temperature on the Gaseous Product Yields

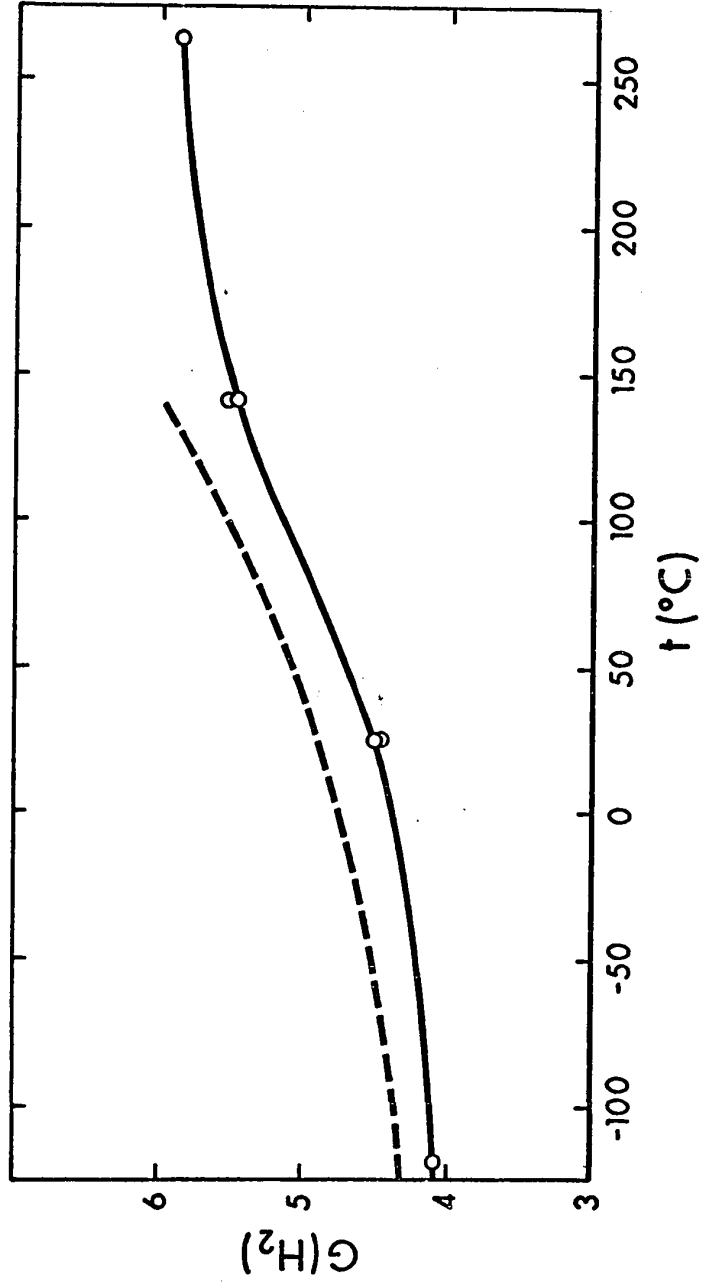
<u>Temperature (°C)</u>	<u>G(H<sub>2</sub>)</u>	<u>G(CH<sub>4</sub>)</u>
-120°	4.08	0.02
25°	4.50	0.08
140°	5.50	0.12
264°	5.85	0.15

---

FIGURE III-7

The yield of hydrogen as a function of temperature:

O, purified n-propanol;-----, estimated values  
for absolutely pure n-propanol.



1. Calculation of the Scavenger Concentrations in n-Propanol.

The solubility of nitrous oxide in n-propanol is not known, so the available data for ethanol were used to estimate the solubility of nitrous oxide in n-propanol. At  $-120^{\circ}$ , all the nitrous oxide was assumed to be dissolved. At  $25^{\circ}$  the value of the Bunsen absorption coefficient of nitrous oxide in ethanol is  $\alpha = 2.57$ . Available values of  $\alpha$  extend only from  $18^{\circ}$  to  $36^{\circ}$ , so the value used at  $140^{\circ}$  ( $\alpha = 0.55$ ) was obtained by a long extrapolation. From the  $\alpha$  values, the concentrations of nitrous oxide in n-propanol were calculated. An error in these values would shift the concentration scales of Figures III-8 to III-11, but the shape of each curve would be unaffected.

The concentrations of hydrogen chloride in the samples were computed assuming that all the hydrogen chloride was dissolved in the propanol. The dissociation constant  $K_{\text{diss}} = 1.10 \times 10^{-3}$  for hydrogen chloride in n-propanol was estimated from the value  $K_{\text{diss}} = 0.015$  in ethanol (115) using the same equation (114) as that used in case of methanol. The dissociation constant  $K_{\text{diss}} = 1.2 \times 10^{-4}$  for sulfuric acid in n-propanol was estimated by using the same value of the ratio  $K_{\text{HCl}}/K_{\text{H}_2\text{SO}_4}$  as in methanol. These values of the dissociation constants of the acids in n-propanol may be inaccurate, but are used for lack of better information. As in methanol, the dissociation constants are

assumed to be independent of temperature in n-propanol.

For the reason stated in methanol, hydrogen chloride was used to make low concentration solutions and sulfuric acid was used to make the strongly acidic solutions.

2. Effects of Scavengers on the Hydrogen Yields at -120°, 25° and 140°

The g values of hydrogen and nitrogen are presented as functions of solute concentration in Tables III-13 to III-18 and Figures III-8 to III-11. It is evident from the data in the Tables and Figures that the addition of acid caused  $g(H_2)$  to increase more than the addition of nitrous oxide caused  $g(H_2 + N_2)$  to increase at the same scavenger concentration. This difference between  $g(H_2)$  from acidic solutions and  $g(H_2 + N_2)$  from nitrous oxide solutions amounts to 0.4 - 0.5 g units in the lower concentration region at all temperatures (Figures III-8 to III-10). Part of the apparent discrepancy between  $g(H_2)$  and  $g(H_2 + N_2)$  from more concentrated solutions of acid and nitrous oxide respectively, may be caused by the lack of true knowledge of the dissociation constant of sulfuric acid in n-propanol. At -120° the value of  $g(H_2 + N_2)$  from nitrous oxide solutions tended to level off at 4.3 at  $10^{-3}$  M nitrous oxide, then increased again at higher solute concentrations (Figure III-8 and Table III-13). The corresponding  $g(H_2)$  from acidic solutions levelled off at

TABLE III-13

Product Yields as a Function of Nitrous Oxide Concentration at  $-120^{\circ}$ 

[N <sub>2</sub> O] Molar	g(H <sub>2</sub> )	g(N <sub>2</sub> ) total	g(N <sub>2</sub> ) d.r.*	g(N <sub>2</sub> ) sec.**	g(N <sub>2</sub> ) corrected	g(H <sub>2</sub> )+g(N <sub>2</sub> ) corr.
$5.80 \times 10^{-5}$	3.90	0.23	-	-	0.23	4.13
$2.30 \times 10^{-4}$	3.72	0.57	-	-	0.57	4.29
$7.05 \times 10^{-4}$	3.36	0.92	-	-	0.92	4.28
$2.04 \times 10^{-3}$	3.30	1.00	-	-	1.00	4.30
$7.68 \times 10^{-3}$	3.04	1.57	-	-	1.57	4.61
$3.28 \times 10^{-2}$	3.00	1.83	-	-	1.83	4.83
$6.00 \times 10^{-2}$	3.13	2.55	0.05	-	2.50	5.63
0.238	2.70	3.36	0.15	-	3.21	5.91
0.910	2.24	4.88	0.57	0.03	4.28	6.52
2.20	1.93	6.00	1.40	0.11	4.49	6.42
3.00	2.22	6.20	1.87	0.24	4.09	6.31
3.90	1.95	7.10	2.45	0.40	4.25	6.20
7.00	2.11	9.95	4.40	1.25	4.30	6.41

\* d.r., Direct Radiolysis of N<sub>2</sub>O\*\* sec., Secondary Reaction of N<sub>2</sub>O

TABLE III-14

Yield of Hydrogen as a Function of Acid  
Concentration at -120°

Acid	[Acid] Molar	[n-PrOH <sub>2</sub> <sup>+</sup> ] Molar	g(H <sub>2</sub> ) <sub>total</sub>	g(H <sub>2</sub> ) <sub>cor.</sub>
HCl	1.53x10 <sup>-4</sup>	1.30x10 <sup>-4</sup>	4.55	4.55
	1.02x10 <sup>-3</sup>	6.50x10 <sup>-4</sup>	4.77	4.77
	4.28x10 <sup>-3</sup>	1.60x10 <sup>-3</sup>	4.80	4.80
H <sub>2</sub> SO <sub>4</sub>	1.88x10 <sup>-2</sup>	1.50x10 <sup>-3</sup>	4.77	4.77
	0.188	4.70x10 <sup>-3</sup>	5.53	5.48
	1.13	1.10x10 <sup>-2</sup>	6.07	5.79
	3.76	2.12x10 <sup>-2</sup>	6.50	5.50

TABLE III-15

Product Yields as a Function of Nitrous Oxide Concentration at 25°

[N <sub>2</sub> O] Molar	g(H <sub>2</sub> )	g(N <sub>2</sub> ) total	g(N <sub>2</sub> ) d.r.*	g(N <sub>2</sub> ) sec.**	g(N <sub>2</sub> ) corrected	g(H <sub>2</sub> ) + g(N <sub>2</sub> ) cor.
6.30x10 <sup>-5</sup>	4.00	0.50	-	-	0.50	4.50
1.47x10 <sup>-4</sup>	4.04	0.80	-	-	0.80	4.84
4.32x10 <sup>-4</sup>	3.95	0.90	-	-	0.90	4.85
1.44x10 <sup>-3</sup>	3.70	1.27	-	-	1.27	4.97
7.48x10 <sup>-3</sup>	3.47	2.13	-	-	2.13	5.60
3.76x10 <sup>-2</sup>	3.00	2.51	0.03	-	2.48	5.48
0.187	2.72	3.46	0.10	-	3.36	6.08
0.766	2.21	4.85	0.45	0.24	4.16	6.37
1.02	2.30	5.28	0.73	0.40	4.15	6.45
1.37	1.84	6.00	1.04	0.70	4.26	6.10

\* d.r., Direct Radiolysis of N<sub>2</sub>O

\*\* sec., Secondary Reaction of N<sub>2</sub>O

TABLE III-16

Yield of Hydrogen as a Function of Acid Con-  
centration at 25°

Acid	[Acid] Molar	[n-ProH <sub>2</sub> <sup>+</sup> ] Molar	g(H <sub>2</sub> ) <sub>total</sub>	g(H <sub>2</sub> ) <sub>corrected</sub>
HCl	1.31x10 <sup>-4</sup>	1.15x10 <sup>-4</sup>	5.26	5.26
	9.40x10 <sup>-4</sup>	6.10x10 <sup>-4</sup>	5.35	5.35
	4.44x10 <sup>-3</sup>	1.73x10 <sup>-3</sup>	5.54	5.54
	2.80x10 <sup>-2</sup>	5.00x10 <sup>-3</sup>	5.84	5.84
H <sub>2</sub> SO <sub>4</sub>	1.88x10 <sup>-2</sup>	1.50x10 <sup>-3</sup>	5.75	5.75
	0.188	4.70x10 <sup>-3</sup>	5.98	5.93
	3.76	2.12x10 <sup>-2</sup>	7.44	6.50

TABLE III-17

Product Yields as a Function of Nitrous Oxide Concentration at 140°

[N <sub>2</sub> O] Molar	g(H <sub>2</sub> )	g(N <sub>2</sub> ) total	g(N <sub>2</sub> ) d.r.*	g(N <sub>2</sub> ) sec.**	g(N <sub>2</sub> ) corrected	g(H <sub>2</sub> )+g(N <sub>2</sub> ) cor
7.0 x10 <sup>-5</sup>	5.27	0.29	-	-	0.29	5.56
2.74x10 <sup>-4</sup>	5.26	0.54	-	-	0.54	5.80
8.0 x10 <sup>-4</sup>	5.33	0.66	-	-	0.66	5.99
4.5 x10 <sup>-3</sup>	5.14	0.96	-	-	0.96	6.10
1.89x10 <sup>-2</sup>	4.25	2.14	-	-	2.14	6.39
7.8 x10 <sup>-2</sup>	3.37	3.24	0.09	0.06	3.09	6.46
0.21	3.26	4.97	0.28	0.35	4.34	7.60
0.44	3.16	6.53	0.53	1.70	4.30	7.46

\* d.r., Direct Radiolysis of N<sub>2</sub>O

\*\* sec., Secondary Reaction of N<sub>2</sub>O

TABLE III-18

Yield of Hydrogen as a Function of Acid

Concentration at 140°

<u>Acid</u>	<u>[Acid] Molar</u>	<u>[n-PrOH<sub>2</sub><sup>+</sup>] Molar</u>	<u>g(H<sub>2</sub>)<sub>total</sub></u>	<u>g(H<sub>2</sub>)<sub>corrected</sub></u>
HCl	5.68x10 <sup>-4</sup>	4.20x10 <sup>-4</sup>	6.25	6.25
	1.13x10 <sup>-3</sup>	6.90x10 <sup>-4</sup>	6.35	6.35
<hr/>				
H <sub>2</sub> SO <sub>4</sub>	3.76x10 <sup>-2</sup>	2.07x10 <sup>-3</sup>	6.48	6.48
	0.188	4.70x10 <sup>-3</sup>	6.48	6.43
	1.13	1.10x10 <sup>-2</sup>	7.24	6.95
	4.88	2.42x10 <sup>-2</sup>	8.14	6.90

FIGURE III-8

The effect of acid and nitrous oxide concentration at  $-120^{\circ}$  in n-propanol. O,  $N_2$  and  $\square$ ,  $(H_2 + N_2)$  from nitrous oxide solutions, corrected for the direct radiolysis and secondary reaction of nitrous oxide;  $\blacktriangle$  and  $\blacktriangledown$ ,  $H_2$  in the presence of HCl and  $H_2SO_4$  respectively, corrected for the direct radiolysis of acids. S is  $N_2O$  or  $n-PrOH_2^+$ . The solid and broken lines through the nitrogen yields were calculated by the 1AP and 2AP treatments, respectively (see Table IV-7). The line through the  $(H_2 + N_2)$  points is the sum of  $N_2$  and  $H_2$  (Fig. III-11) calculated curves.

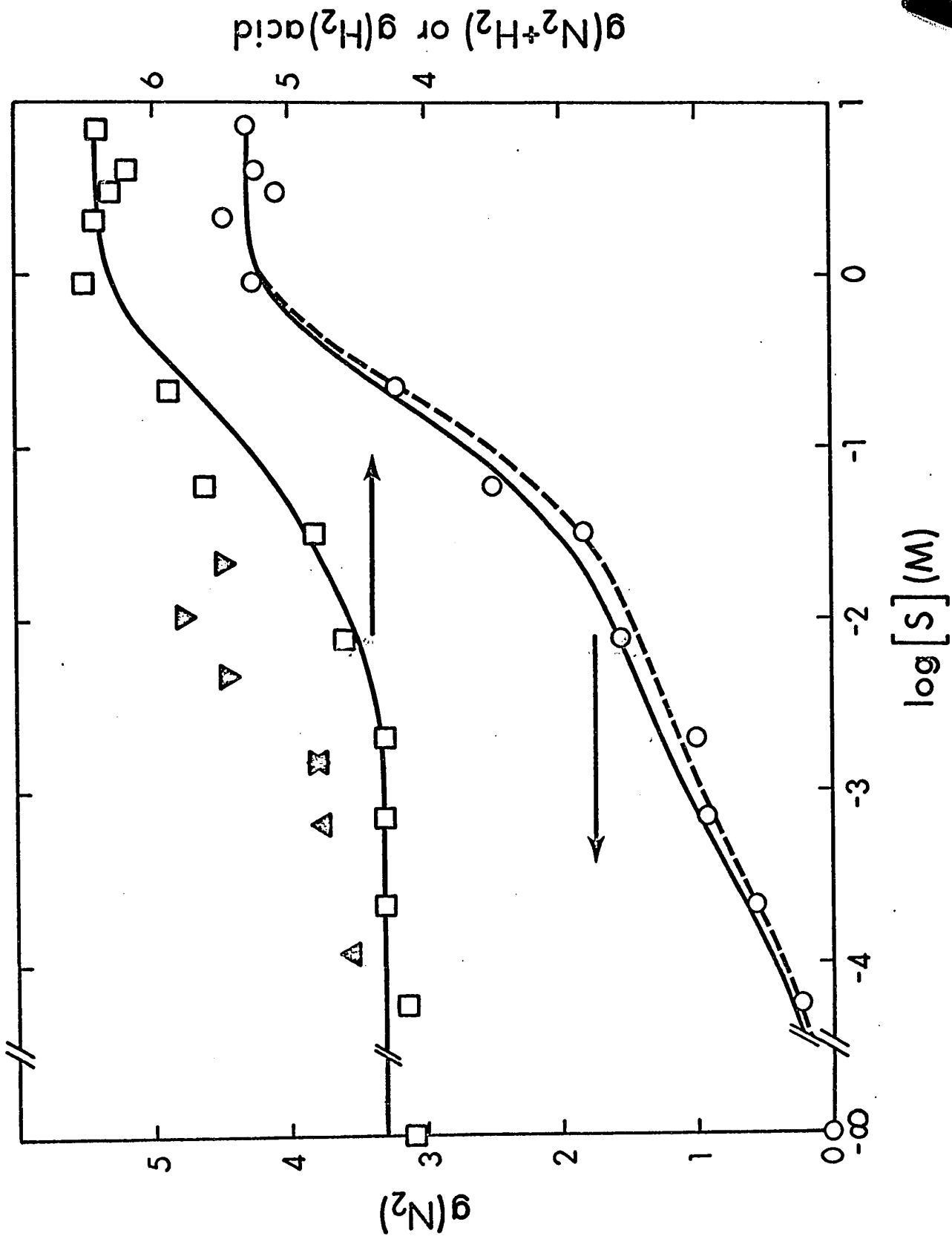


FIGURE III-9

The effect of acid and nitrous oxide concentration at 25° in n-propanol.

O, N<sub>2</sub> and □, (H<sub>2</sub> + N<sub>2</sub>) from nitrous oxide solutions, corrected for the direct radiolysis and secondary reaction of nitrous oxide; ▲ and ▼, H<sub>2</sub> in the presence of HCl and H<sub>2</sub>SO<sub>4</sub> respectively, corrected for the direct radiolysis of acids. S is N<sub>2</sub>O or n-PrOH<sub>2</sub><sup>+</sup>. The line through the nitrogen yields was calculated by the LAP treatment (see Table IV-7). The line through the (H<sub>2</sub> + N<sub>2</sub>) points is the sum of the N<sub>2</sub> and H<sub>2</sub> (Fig. III-11) calculated curves.

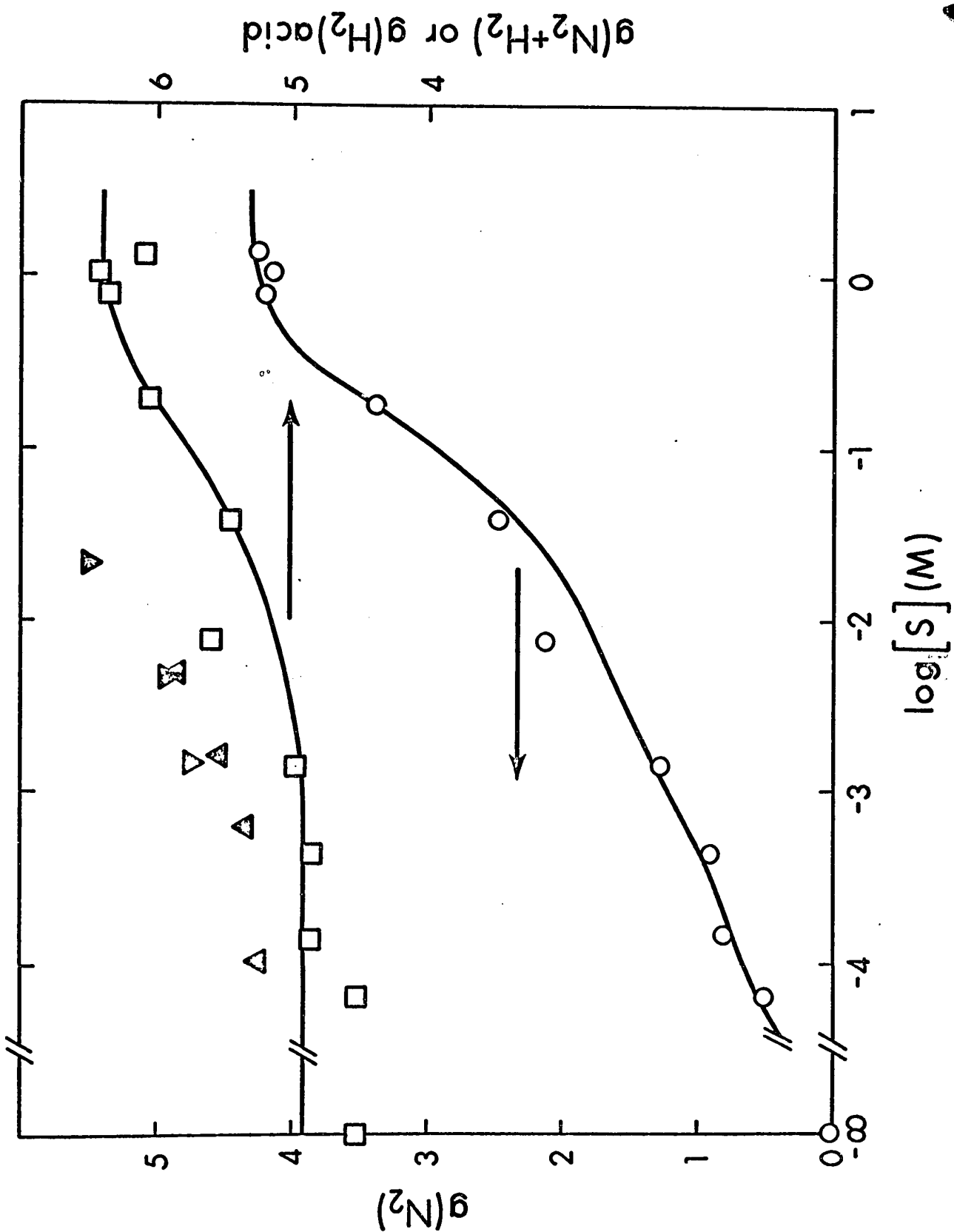


FIGURE III-10

The effect of acid and nitrous oxide concentration at 140° .

O, N<sub>2</sub> and □, (H<sub>2</sub> + N<sub>2</sub>) from nitrous oxide solutions, corrected for the direct radiolysis and secondary reaction of nitrous oxide; ▲ and ▼, H<sub>2</sub> in the presence of HCl and H<sub>2</sub>SO<sub>4</sub> respectively, corrected for the direct radiolysis of acids. S is N<sub>2</sub>O or n-PrOH<sub>2</sub><sup>+</sup>. The line through the nitrogen yields was calculated by the LAP treatment (see Table IV-7). The line through the (H<sub>2</sub> + N<sub>2</sub>) points is the sum of the N<sub>2</sub> and H<sub>2</sub> (Fig. III-11) calculated curves.

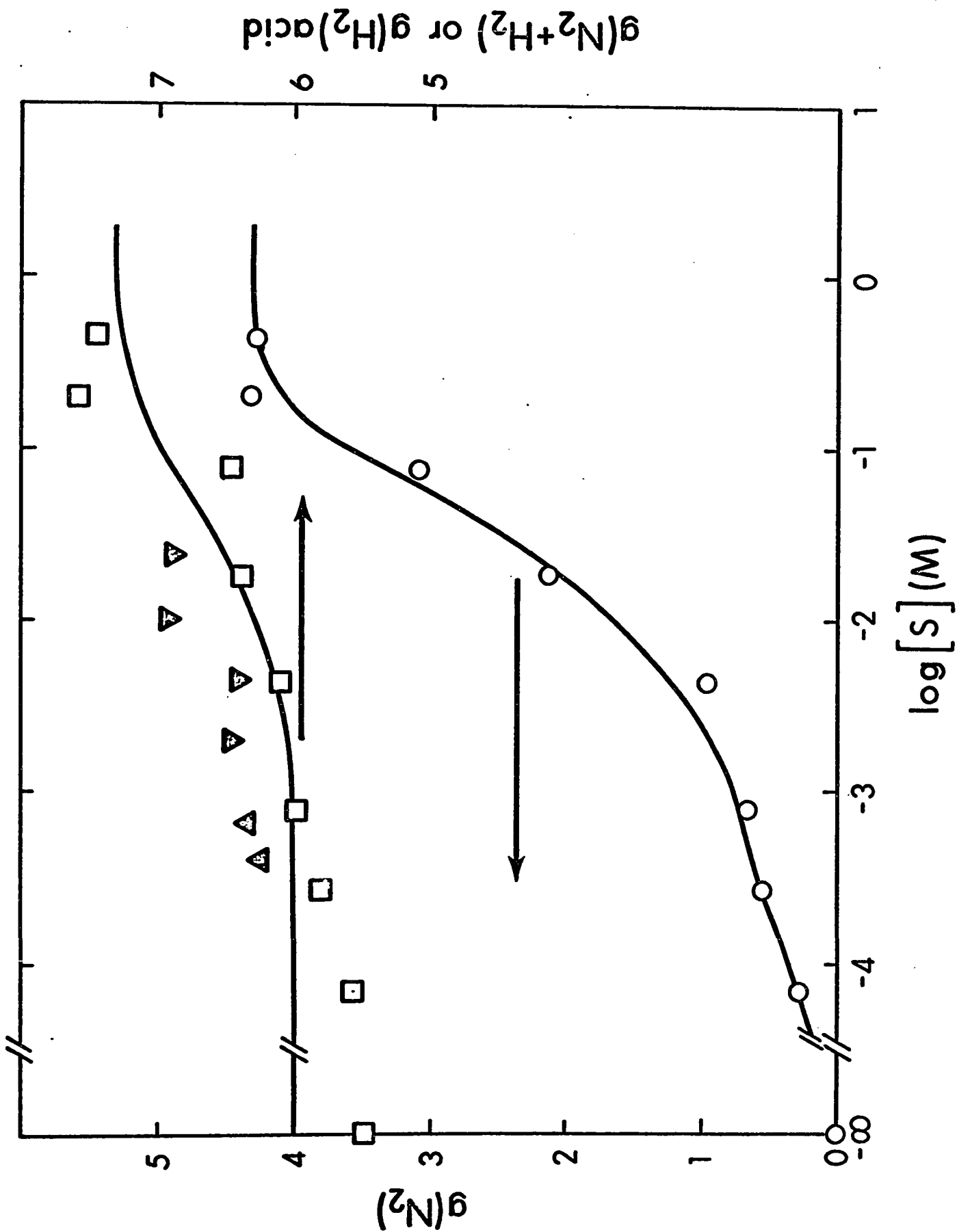
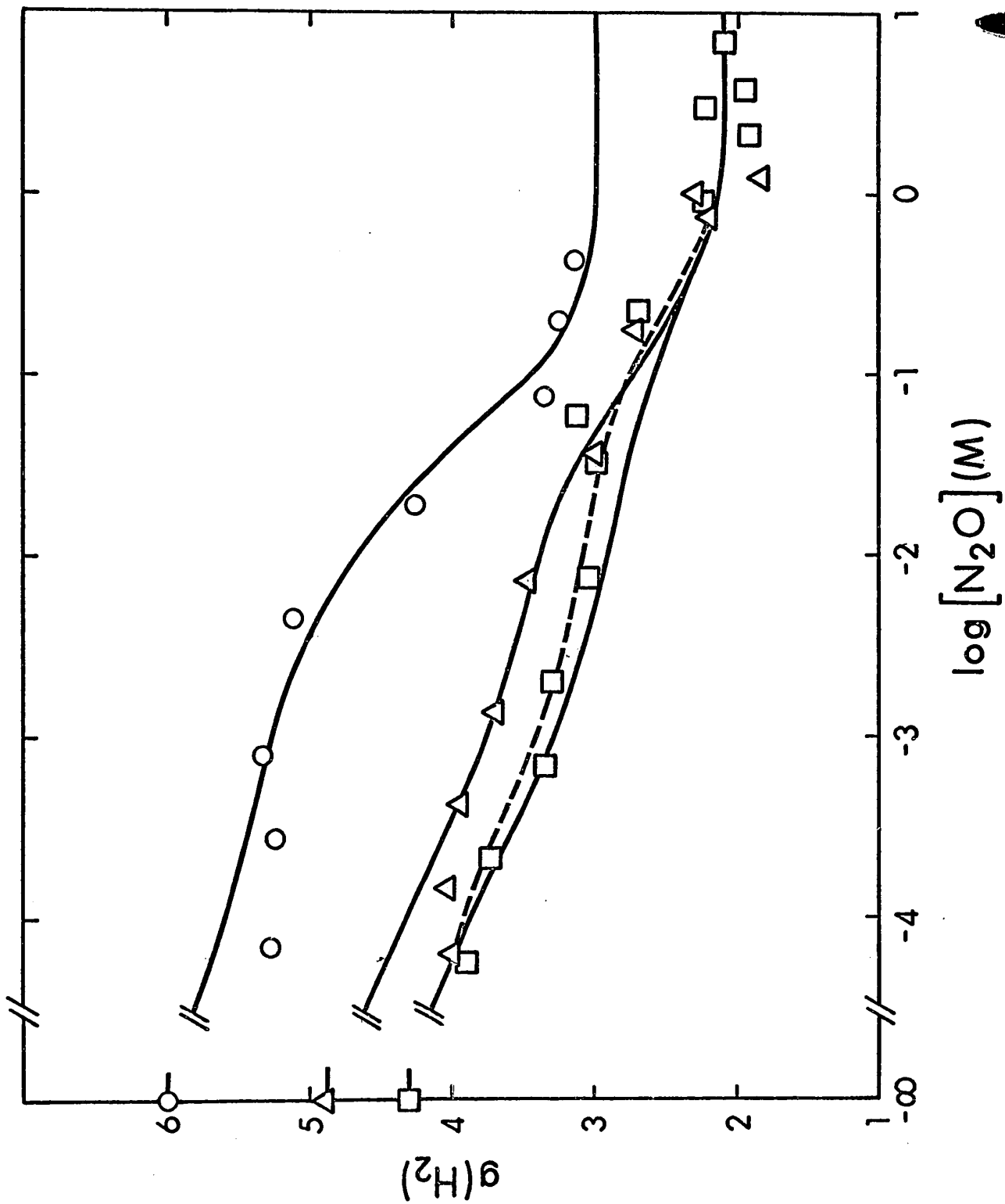


FIGURE III-11

The yield of hydrogen as a function of nitrous oxide concentration.

O, 140°; Δ, 25°; □, -120°. The solid and broken lines were calculated by the 1AP and 2AP treatments, respectively (See Tables IV-7 and IV-11).



4.7 - 4.8 at  $10^{-3}$  M acid and increased with further increase of acid concentration (Figure III-8 and Table III-14). At  $25^{\circ}$   $g(H_2 + N_2)$  was essentially constant at 4.9 in the vicinity of  $10^{-3}$  M nitrous oxide, then increased with further increase of nitrous oxide concentration (Figure III-9 and Table III-15). The corresponding  $g(H_2)$  from acidic solutions was about 5.3 - 5.4 at  $10^{-3}$  M acid, and increased at higher acid concentrations (Figure III-9 and Table III-16). At  $140^{\circ}$   $g(H_2 + N_2)$  equalled about 6.0 at  $10^{-3}$  M nitrous oxide, and increased with increasing nitrous oxide concentration (Figure III-10 and Table III-17). The corresponding  $g(H_2)$  from acidic solutions was 6.3 - 6.4 at  $10^{-3}$  M acid, and increased with increasing acid concentration (Figure III-10 and Table III-18). Above a certain concentration of nitrous oxide the nitrogen yield increased rapidly with increasing nitrous oxide concentration at all temperatures e.g. above  $\sim 4$  M nitrous oxide at  $-120^{\circ}$ ; above  $\sim 1$  M nitrous oxide at  $25^{\circ}$  and above  $\sim 0.2$  M at  $140^{\circ}$  (Tables III-13, III-15 and III-17). The rapid increase in nitrogen formation was most probably due to a secondary reaction of nitrous oxide, so the nitrogen yields were corrected by a method which is given in Section IV.

The hydrogen yield decreased with increasing nitrous oxide concentration at all temperatures (Figure III-11 and Tables III-13, III-15 and III-17). Unfortunately, the apparatus was such that only at  $-120^{\circ}$  was it possible to

obtain sufficiently concentrated solutions to observe a lower plateau in the hydrogen-yield curve. The plateau occurred at  $g(\text{H}_2) = 2.1$  at  $-120^\circ$  (Figure III-11). The corresponding plateau value for the nitrogen yield was at about  $g(\text{N}_2) = 4.3$  (Figure III-8). For  $25^\circ$  and  $140^\circ$ , the hypothetical plateau values of hydrogen were chosen such that reasonable upper limits of the  $g(\text{H}_2 + \text{N}_2)$  curves were obtained (Figures III-9 and III-10). These plateau values were  $g(\text{H}_2) = 2.1$  at  $25^\circ$  and  $g(\text{H}_2) = 3.0$  at  $140^\circ$  (Figure III-11).

(D) Competition Between Nitrous Oxide and Acid at  $25^\circ$

A study was made of the competition between acid and nitrous oxide in order to attempt to distinguish the hydrogen precursors. The concentrations of hydrogen chloride used were sufficiently low that n-propylchloride formation was too slow to interfere with the acid-nitrous oxide competition. The values of  $g(\text{H}_2)$  and  $g(\text{N}_2)$  were between the values caused by the presence of either solute alone at the same concentration. These values are reported in Table III-19.

TABLE III-19

Competition Between Nitrous Oxide and Acid at 25°

<u>[N<sub>2</sub>O]</u> Molar	<u>[HCl]</u> Molar	<u>[n-PrOH<sub>2</sub><sup>+</sup>]</u> Molar	<u>g(H<sub>2</sub>)</u>	<u>g(N<sub>2</sub>)</u>
0.0296	0.0240	0.0044	4.66	1.45
0.0264	0.0078	0.0024	4.06	1.67
0.0826	0.0240	0.0044	3.95	2.35

---

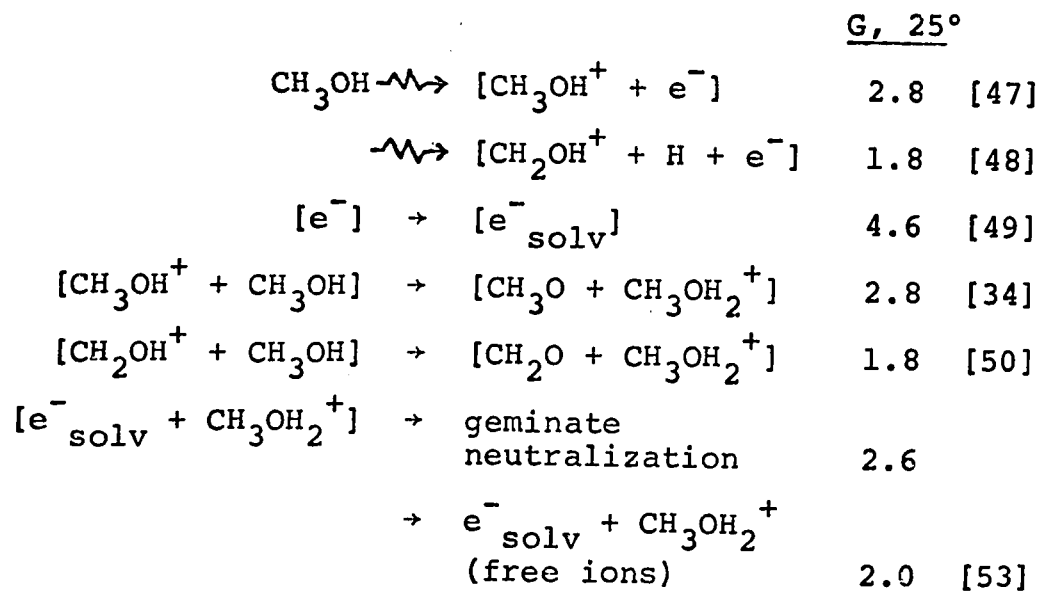
D I S C U S S I O N

Many of the reactions in the Discussion have been previously mentioned in the Introduction. The numbers of these reactions in the Discussion are the same as in the Introduction.

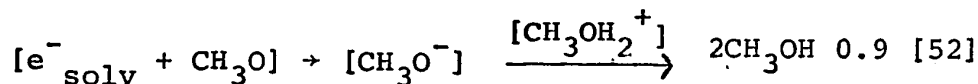
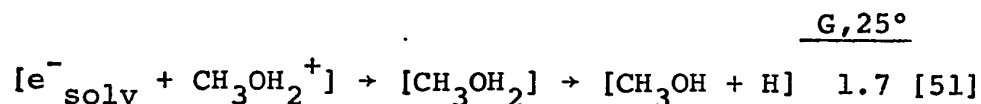
(A) Methanol

1. Pure Methanol

The mechanism which follows is similar to those proposed for ethanol (24) and iso-propanol (25), with a few exceptions which will be discussed later. It is largely based upon the considerations of the fate of ionic species in irradiated liquids (21,22). The yield specified at the right side of each reaction refers to irradiation at 25° and is based on experimental results and theoretical considerations (discussed later). Square brackets around reactants or products denote that the species are inside a spur.

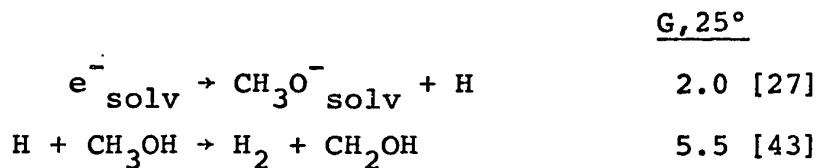


The ions that undergo geminate neutralization can apparently participate in two types of reaction, only one of which results in hydrogen formation. The competition between these two types of reaction is slightly temperature dependent, the activation energy of the hydrogen forming reaction being roughly 1 kcal/mole greater than that which does not form hydrogen. There are many feasible reactions between the intermediates in spurs and a number of competitions can be envisaged that might have a small temperature dependence. Only one example is given here:

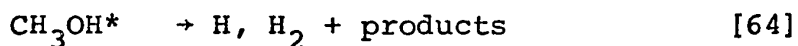


The stipulated yields of reactions [34] and [50] to [53] are those that would be required if reaction [52] were the only one that consumed electrons without producing hydrogen.

The other reactions in pure methanol that are relevant to the present work are



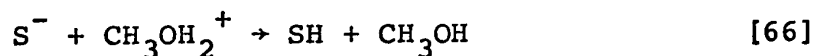
If the reactions



occur, the estimated yield of reaction [48] would have to

be decreased by an amount equal to the yield of reaction [64] and the estimated yield of reaction [47] would have to be increased by the same amount to maintain the total G value of ion pairs equal to 4.6 .

The presence of a low concentration of an impurity S that can react with electrons can prevent some of the free ion solvated electrons from forming hydrogen.



In the methanol used in the present experiments, two probable identities of S are carbon dioxide and acetone.

One may estimate the concentration of electron scavenging impurity in the methanol as follows. It is assumed that reactions of the free ions can be described by homogeneous kinetics. Then the competition for solvated electrons between reactions [27] and [65] leads to the kinetic expression

$$\frac{1}{\Delta G(\text{H}_2)} = \frac{1}{G(e^-_{\text{solv}})_{\text{fi}}} \left( 1 + \frac{k_{27}}{k_{65}[\text{S}]} \right) \quad (\text{IV-i})$$

where  $\Delta G(\text{H}_2)$  is the difference between  $G(\text{H}_2)$  in absolutely pure methanol and in the presence of [S],  $G(e^-_{\text{solv}})_{\text{fi}}$  is the yield of free ion solvated electrons, [S] is the concentration of electron scavenging impurity in moles/litre, and  $k_{27}$  and  $k_{65}$  are the rate constants of the respective reactions. The hydrogen yields in absolutely pure methanol

and in Sample B of methanol are taken from Fig. III-4, p. 57, and are 5.0 and 4.5 respectively at  $-97^\circ$ . The yield of free ion solvated electrons at  $-97^\circ$  is found to be 1.9 (see Table IV-1 under the heading 2AP, and Discussion Section A-3a). The value of  $k_{27}$  at  $-97^\circ$  is estimated from those of the ratios  $k_{26}/k_{54}$  and  $k_{54}/k_{27}$  as given below. The value of  $k_{26}$  at  $-97^\circ$  is estimated from the value at  $23^\circ$  (16) and the activation energy  $E_{26} = 2.8$  kcal/mole (see Discussion Section A-3)), and is found to be  $1.5 \times 10^9$  l/mole sec. At  $0^\circ$  and ionic strength  $\mu = 1 \times 10^{-4}$  M,  $k_{26}/k_{54} = 7.9$  (72), and the same value is assumed to be valid at  $-97^\circ$  because  $E_{26} \sim E_{54}$  (see Discussion Section A-6). The value of  $k_{54}/k_{27}$  at  $-97^\circ$  is  $1.7 \times 10^4$  l/mole (see Table IV-1). Combination of these values yields  $k_{27} = 1.1 \times 10^4$  sec $^{-1}$  at  $-97^\circ$ . In aqueous solution, the value of  $k_{65}$  when S is carbon dioxide is nearly equal to that when S is acetone ( $\sim 8 \times 10^9$  l/mole sec at  $25^\circ$ ) (17). The same value is assumed in methanol at  $25^\circ$ . This value when adjusted to  $-97^\circ$  using  $E_{65} \sim E_{26} = 2.8$  kcal/mole (see Discussion Section A-5) gives  $k_{65} = 3.1 \times 10^8$  l/mole sec. For Sample B of methanol one obtains

$$\frac{1}{5.0-4.5} = \frac{1}{1.9} \left( 1 + \frac{1.1 \times 10^4}{3.1 \times 10^8 [S]} \right)$$

$$\text{and } [S] \sim 1 \times 10^{-5} \text{ M.}$$

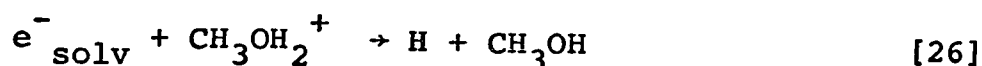
In a similar way one can estimate that the concentration of

impurities in Sample A of methanol is  $\approx 1 \times 10^{-4}$  M.

## 2. Effects of Electron Scavengers

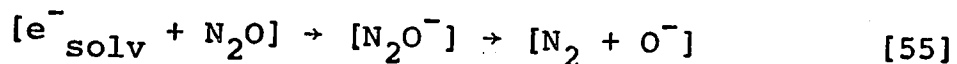
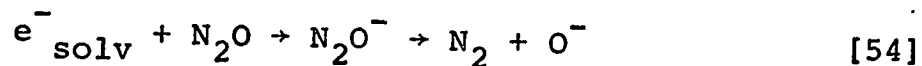
The plots of  $g(\text{H}_2 + \text{N}_2)$  against nitrous oxide concentration coincide with those of  $g(\text{H}_2)$  against  $\text{CH}_3\text{OH}_2^+$  concentration at  $-97^\circ$ ,  $25^\circ$  and  $150^\circ$ , within experimental error (Figs. III-3 to III-5 p.62,63,64 ). This indicates that both scavengers react with the same species, namely solvated electrons, and that there is no "species X" formed in the radiolysis of methanol. In the radiolysis of ethanol an unidentified species, designated X, is apparently formed which reacts with acid but not with nitrous oxide (24). The results in Fig. III-5 (p. 64) also indicate that a secondary reaction which generates large amounts of nitrogen from nitrous oxide, such as the one that occurs at high temperature in iso-propanol (25), does not occur in methanol.

The addition of acid causes reactions [27] and [65] to be replaced by [26].



A sufficiently high concentration of  $\text{CH}_3\text{OH}_2^+$  causes reaction [52] to be replaced by [51]. The increase of hydrogen yield with increasing acid concentration (Figs. III-3 to III-5, p. 62,63,64 ) is explained by these replacements of reactions [52] and [65]. In a similar way, the addition of nitrous oxide causes the value of  $g(\text{H}_2 + \text{N}_2)$  to increase

with increasing nitrous oxide concentration, by the occurrence of reactions [54] and [55].



### 3. Scavenging Kinetics, Nitrogen Yields

The experiments covered wide ranges of scavenger concentration ( $6 \times 10^{-5}$  to 7 M), temperature (176° to 423°K) and dielectric constant (73 to 15). The most stringent test of the kinetics model was provided by trying to fit the entire set of results by using only one adjustable parameter.

#### (a) One-Adjustable-Parameter Treatment

The yield of free ion solvated electrons at each temperature was calculated by a method that is summarized in Appendix A, but which is described in detail elsewhere (22). The yields are listed under the heading 1 AP in Table IV-1.

It was assumed that reactions of the free ions could be described by homogeneous kinetics. Values of  $k_{54}/k_{27}$  reported in Table IV-1, were obtained from conventional plots of  $1/g(\text{N}_2)$  vs  $1/[\text{N}_2\text{O}]$ , using only the data for nitrous oxide concentrations less than  $10^{-2}$  M (Fig. IV-1). The nitrogen yields from solutions with concentrations up to  $3 \times 10^{-3}$  M were then calculated from an equation similar

TABLE IV-1

Quantities Relevant to the Reactions of Solvated Electrons in Methanol

t(°C)	density (g/cc)	ε	k <sub>54</sub> /k <sub>27</sub> (ℓ/mole)	1AP <sup>a</sup>		2AP <sup>b</sup>	
				G(e <sup>-</sup> solv) <sup>c</sup> fi (V/cm <sup>2</sup> )	β <sub>-</sub> (V/cm <sup>2</sup> )	G(e <sup>-</sup> solv) <sup>d</sup> fi (V/cm <sup>2</sup> )	β <sub>-</sub> (V/cm <sup>2</sup> )
-97	0.907	73	1.7 x 10 <sup>4</sup>	2.4	1.0 x 10 <sup>13</sup>	1.9	2.8 x 10 <sup>13</sup>
+25	0.791	33	1.1 x 10 <sup>4</sup>	2.2	2.5 x 10 <sup>13</sup>	2.0	4.2 x 10 <sup>13</sup>
150	0.650	15	4 x 10 <sup>3</sup>	1.8	1.3 x 10 <sup>14</sup>	1.9	-----

a. One-adjustable-parameter treatment.

b. Two-adjustable-parameters treatment.

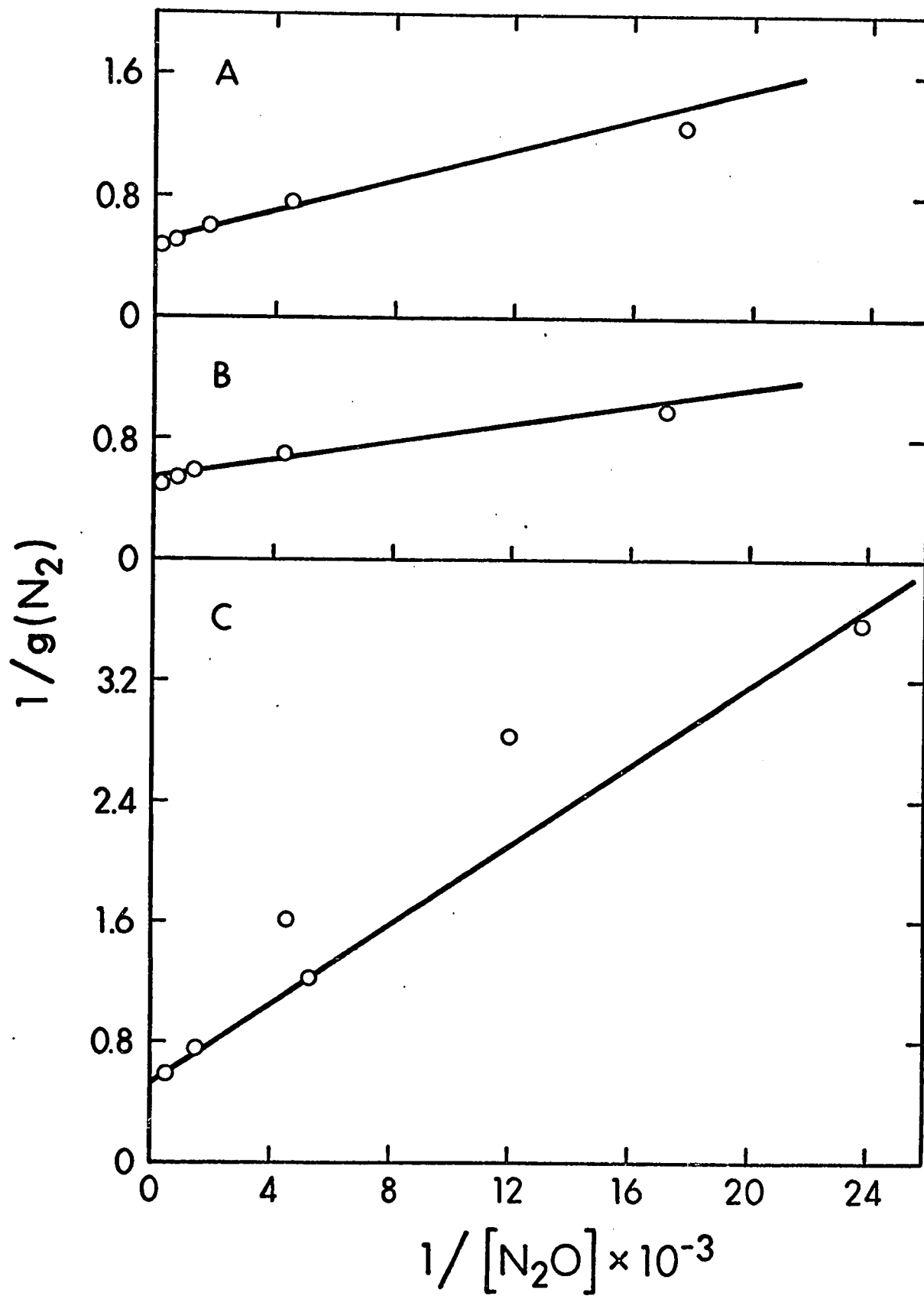
c. Calculated from equation (A1)

d. Estimated from homogeneous kinetics plots of results at [N<sub>2</sub>O] < 10<sup>-2</sup> M.

FIGURE IV-1

Plots of  $1/g(N_2)$  against  $1/[N_2O]$  for methanol.

A, 25°; B, -97° C, 150°.



to (IV-i).

$$g(N_2) = G(e^-_{\text{solv}})_{fi} \cdot \frac{k_{54} [N_2O]}{k_{27} + k_{54} [N_2O]} \quad (\text{IV-ii})$$

The model of nonhomogeneous kinetics for the reactions of ions in spurs (22) was applied when the solute concentration was greater than  $2 \times 10^{-3}$  M. The details of the model will not be described here, but the relevant equations are presented in Appendix A for convenience.

The nitrogen yields from the more concentrated nitrous oxide solutions at  $-97^\circ$  indicated that  $g(\text{total ionization}) = 4.6$  (Fig. III-3, p. 62), so this value was used in equations (Ai) and (Aiv) for all temperatures. Other workers have obtained similar values of  $G(\text{total ionization})$ : Dainton and coworkers (120) estimated  $G(e^-)_{\text{total}} = 5.0$  in methanol glass at  $77^\circ\text{K}$ ; Leblanc and Herman (121) measured the  $W$  value for methanol vapor and obtained  $W = 23.6 \pm 0.4$  eV which corresponds to  $G(e^-) = 4.2 \pm 0.1$

The density of methanol at each temperature must be known for the estimation of the initial spectrum of ion-electron separation distances,  $N(y)$ , at each temperature. The value of the dielectric constant is needed in equations (Aiii) and (Aviii) in Appendix A. These quantities are reported in Table IV-1.

The adjustable parameter used in fitting the model to the nitrogen yields was  $\beta_-$  (see equations Avi and Avii), and the best values are listed in Table IV-1.

The results of the calculations of the one-adjustable-parameter treatment are represented by the full lines through the nitrogen yields in Figs. III-3 to III-5 (p. 62,63,64 ). The calculated curves are too high in the homogeneous kinetics region (solute concentrations  $< 10^{-2}M$ ) at 25° and -97°. The reason for the lack of agreement is as follows. The homogeneous kinetics plots (Fig. IV-1) that were used to obtain the values of  $k_{54}/k_{27}$  also gave values of  $G(e^-_{\text{solv}})_{fi}$ , and these were lower at 25° and -97° than those calculated from equation (Ai) (see Table IV-1). The difference between the two independently obtained sets of values was 20% at -97°, 10% at 25° and 5% (negligible) at 150°. The reported values of  $k_{54}/k_{27}$  are related to the homogeneous kinetics values of  $G(e^-_{\text{solv}})_{fi}$ , but the model values were used in equation (IV-ii). Thus the calculated nitrogen yields at low nitrous oxide concentrations were 20% too high at -97° and 10% too high at 25°. To obtain better agreement between calculation and experiment, a second adjustable parameter is needed and either  $k_{54}/k_{27}$  or  $G(e^-_{\text{solv}})_{fi}$ , could be used. It is preferable to use the latter. In the nonhomogeneous kinetics model calculations, the static dielectric constant was used. However, alcohols have unusually long dielectric relaxation times, and this may require that the complex dielectric constant be used in the calculations. The effects of the use of complex dielectric constants in various liquids has

been discussed elsewhere (106). If the time  $t_{gn}$  required for geminate neutralization to occur approaches or becomes less than the dielectric relaxation time  $\tau$  of the liquid between the ions of a pair, the value of  $G(e^-_{solv})_{fi}$  decreases. This situation is feasible for a fraction of the ion pairs generated in alcohols, because of their unusually long dielectric relaxation times (106). The effect in methanol would be more important at low than at high temperatures because the activation energy  $E_\tau$  for dielectric relaxation ( $E_\tau = 3.7$  kcal/mole (122)) is probably greater than that of ion migration. The activation energy  $E_\tau$  for dielectric relaxation has been estimated from the Arrhenius plot in Fig. IV-2. The activation energy for viscous flow in methanol is 2.3 kcal/mole (123), that for self diffusion is 2.8 kcal/mole (123) and that for the diffusion of phenol in methanol is 3.2 kcal/mole (124) (these values along with others are reported in Table IV-2). Hence the activation energy for the migration of the radiolytic ions is probably about 2.8 kcal/mole. Thus the value of  $\tau$  increases more rapidly with decreasing temperature than does that of  $t_{gn}$ , so the lack of complete dielectric relaxation could be the cause of the crudely calculated value of  $G(e^-_{solv})_{fi}$  being 10% too high at 25° and 20% too high at -97°.

FIGURE IV-2

- A. Arrhenius plot for dielectric relaxation  
in methanol.
  
- B. Arrhenius plot of  $[G(H_2)_{t^\circ} - G(H_2)_{-97^\circ}]$   
in methanol.

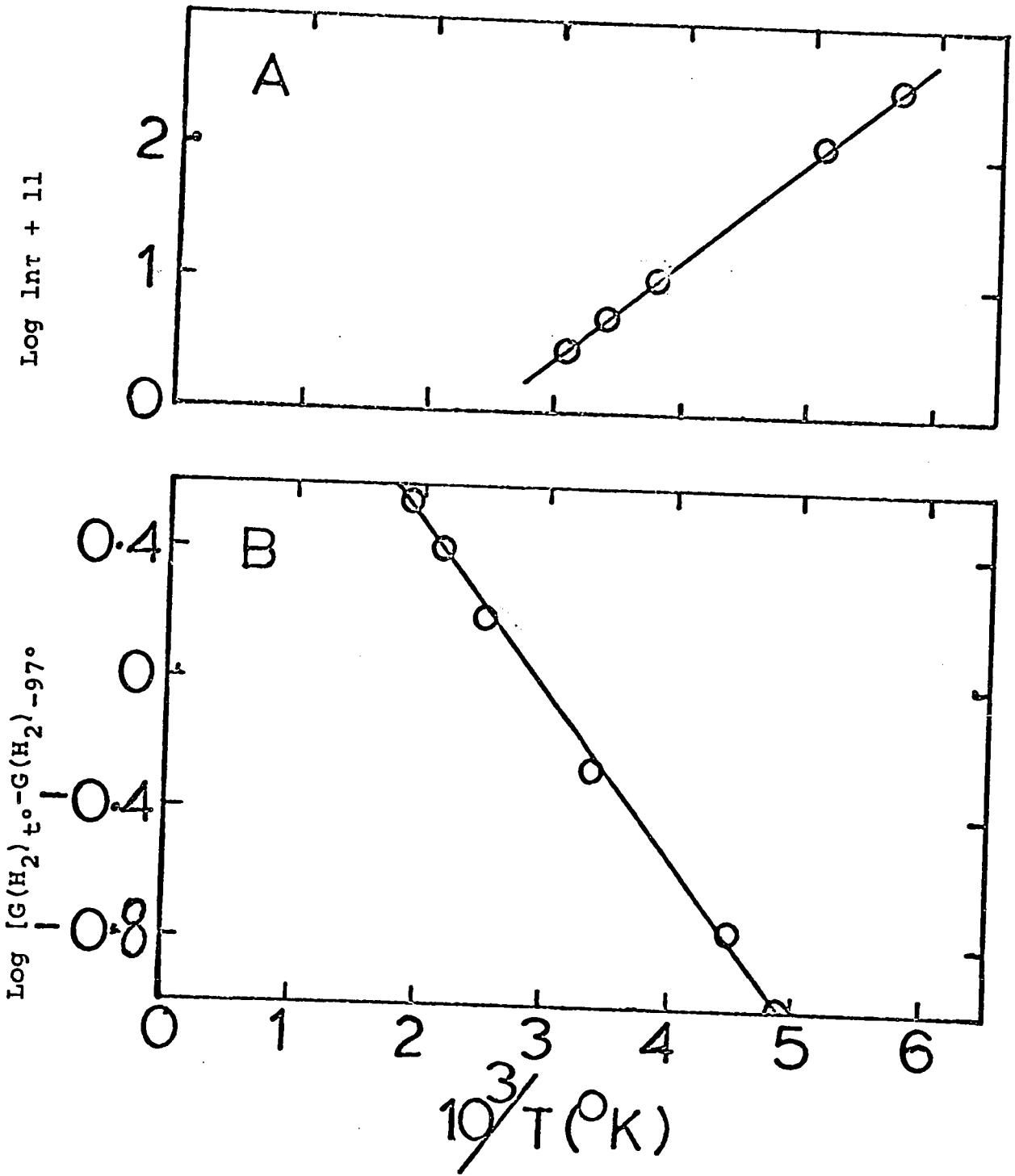


FIGURE IV-2

TABLE IV-2

Some Relevant Data for Methanol

$t(^{\circ}\text{C})$	$\tau_{\text{sec}}^{\text{a}}$	$E_{\text{T}}$ kcal/mole	$E_{\text{self diffusion}}$ k/cal/mole	$E_{\text{viscous flow}}$ kcal/mole	$E_{27-E_{54}}$ kcal/mole	$E_{\text{self-diff}} +$ $(E_{27-E_{54}})$ kcal/mole
-97	$3.3 \times 10^{-9}$	} 3.7	2.8	2.3	0.9	3.7
+25	$4.9 \times 10^{-11}$					
150	$7.3 \times 10^{-12}$					

a. Calculated from data in Ref. (122).

(b) Two-Adjustable-Parameters Treatment

The value of  $G(e^-_{\text{solv}})_{\text{fi}}$  is used indirectly as an adjustable parameter. The time averaged complex dielectric constant is used in equation (Aiii) and the value of the ratio  $\tau/t_{\text{gn}}$  is chosen such that the value of  $G(e^-_{\text{solv}})_{\text{fi}}$  calculated from equation (Ai) is equal to the value obtained from the homogeneous kinetics treatment of the low solute concentration results.

The complex dielectric constant can be expressed in the form (106)

$$\epsilon(t) = \epsilon_0 + \frac{\epsilon_\infty - \epsilon_0}{1 + (\tau/t)^2} \quad (\text{IV-iii})$$

where  $\epsilon(t)$  is the dielectric constant of the medium at time  $t$  after the instantaneous application of an electric field,  $\epsilon_0$  and  $\epsilon_\infty$  are the  $t = 0$  and  $t = \infty$  values, respectively. It can be shown that the time averaged value of the dielectric constant,  $\epsilon_{\text{ave}}$ , during the period  $t_{\text{gn}}$  is

$$\epsilon_{\text{ave}} = \epsilon_\infty - (\epsilon_\infty - \epsilon_0) \frac{\tau}{t_{\text{gn}}} \tan^{-1} \frac{t_{\text{gn}}}{\tau} \quad (\text{IV-iv})$$

The values of  $t_{\text{gn}}$  and  $\tau$  in various liquids are discussed elsewhere (106). It will suffice here to indicate the magnitude of the effect required to reduce the calculated value of  $G(e^-_{\text{solv}})_{\text{fi}}$  from 2.4 to 1.9 at  $-97^\circ$  and from 2.2 to 2.0 at  $25^\circ$ . For ion pairs with  $y = 20 \text{ \AA}$ ,  $\frac{\tau}{t_{\text{gn}}} = 0.14$  at  $-97^\circ$

and 0.10 at 25°. The dielectric relaxation of the medium between a pair of suddenly created ions is perturbed by the electric fields of the ions. The "perturbed" values of  $\tau$  that should be used in equation (IV-iv) for radiolytic systems are probably smaller than the "unperturbed" values that are measured by microwave spectroscopy, perhaps by as much as an order of magnitude (106). It is important to mention that the perturbation of the relaxation time rapidly becomes negligible with increasing distance between a singly charged ion and the molecule on which the ion exerts a torque. For  $y = 20 \text{ \AA}$ , therefore  $t_{gn} = \tau(\text{unperturbed}) \approx 3 \times 10^{-9} \text{ sec}$  at  $-97^\circ$  and  $\approx 5 \times 10^{-11} \text{ sec}$  at  $25^\circ$  (122).

The values of  $\epsilon_{ave}$  obtained from equation (IV-iv), and which gave the correct values of  $G(e^-_{solv})_{fi}$  when used in equations (Aiii) and (Ai), were then used in equation (Aiv) to calculate the nitrogen yields. The  $N(y)$  spectra and values of  $\epsilon_{ave}$  are listed in Table IV-3.

Thus in the two-adjustable-parameters treatment one adjustable parameter is  $\beta_*$  and the other may be considered to be either  $\epsilon_{ave}$  or  $(\tau/t_{gn})$ . This refinement of the kinetics model led to the calculation of the dashed curves in Figs. III-3 and III-4 (p. 62, 63) which are in good agreement with the measured nitrogen yields. The appropriate values of  $\beta_*$  are listed under the heading 2AP in Table IV-1.

The two-adjustable-parameters treatment was not applied to the  $150^\circ$  system because satisfactory results

TABLE IV-3

N( $\gamma$ ) Spectra and Values of  $\epsilon_{ave}$  in Methanol at  
Different Temperatures

N( $\gamma$ )	-97°		25°		150°	
	$\gamma$ (Å)	$\epsilon_{ave}$	$\gamma$ (Å)	$\epsilon_{ave}$	$\gamma$ (Å)	$\epsilon_{ave}$
2150	15	45	17	27	20	15
1100	17	53	20	29	23	15
600	20	60	23	31	28	15
476	28	73	32	33	38	ditto
270	47	73	54	33	64	
116	76	73	89	33	104	
64	110	73	128	33	151	
41	148	73	172	33	203	
28	192	73	223	ditto	262	
21	239	73	277		326	
16	290	73	337		397	
13	346	73	401		473	
15	421	73	488		576	
14	535	73	621		732	
76	>680	73	>790		>930	

$\Sigma N(\gamma) = 5000$

were obtained with one adjustable parameter. This is interpreted to mean that dielectric relaxation was sufficiently rapid relative to geminate neutralization at 150° that  $\epsilon_{\text{ave}} \approx \epsilon_{\text{static}}$ , even with the smallest values of  $y$  used in the model.

#### 4. Competition Between Nitrous Oxide and Acid

The presence of both acid and nitrous oxide in the methanol creates a competition between reactions [26] and [54]. The resulting nitrogen yield at a given nitrous oxide concentration is smaller than would be observed in the absence of acid. The nitrogen yield can be calculated from equation (IV-v).

$$g(\text{N}_2) = g(\text{N}_2)_0 \left[ 1 + \frac{k_{26} [\text{CH}_3\text{OH}_2^+]}{k_{54} [\text{N}_2\text{O}]} \right]^{-1} \quad (\text{IV-v})$$

where  $g(\text{N}_2)_0$  is the yield of nitrogen that would be obtained from a simple nitrous oxide solution with a nitrous oxide concentration equal to  $([\text{N}_2\text{O}] + \frac{k_{26}}{k_{54}} [\text{CH}_3\text{OH}_2^+])$ . The value of the ratio  $k_{26}/k_{54}$  varies with the ionic strength of the solution (72), so it is important to use the value for the appropriate ionic strength. The calculated and experimental values of  $g(\text{N}_2)$  are reported in Table IV-4 and they are in good agreement. This indicates that the present results agree with those of Buxton, Dainton and Hammerli (72). It also implies that the "species X" that reacts with acid but not with nitrous oxide, and that seems to be formed during

TABLE IV-4.

Competition Between Nitrous Oxide and Acid at 25°

[N <sub>2</sub> O] (M)	[HCl] (M)	[CH <sub>3</sub> OH <sub>2</sub> <sup>+</sup> ] (M)	k <sub>26</sub> /k <sub>54</sub>	a	b	c	g(N <sub>2</sub> ) expt. g(H <sub>2</sub> )
				g(N <sub>2</sub> ) <sub>o</sub>	g(N <sub>2</sub> ) <sub>o</sub>	g(N <sub>2</sub> ) <sub>calc</sub>	
0.0164	0.104	0.080	1.7	3.5	3.5	0.37	0.31 5.3
0.0164	0.021	0.019	3.4	3.2	3.2	0.65	0.57 5.15
0.165	0.102	0.080	1.7	3.9	3.9	2.10	2.05 4.15

- a. value at 0° at the appropriate ionic strength, obtained from ref. 72 and assumed to be the same at 25°.
- b. yield that would be obtained from a simple nitrous oxide solution with [N<sub>2</sub>O] equal to the present value of  $\{[N_2O] + \frac{k_{14}}{k_{15}} [CH_3OH_2^+]\}$ .
- c. using eqn. (IV-v).

the radiolysis of liquid ethanol (24), is not formed during the radiolysis of methanol.

#### 5. Hydrogen Yields

Evidently a small amount of electron scavenger remained in our most pure methanol (Sample B). At nitrous oxide or  $\text{CH}_3\text{OH}_2^+$  concentrations between  $10^{-3}$  and  $10^{-2}$  M, the scavenging of free ion solvated electrons is virtually complete and scavenging in spurs is negligible. Assuming that in absolutely pure methanol all the free-ion solvated electrons would react to form hydrogen, the value of  $G(\text{H}_2)$  in absolutely pure methanol would be equal to the value of  $g(\text{H}_2)$  in a solution with a  $\text{CH}_3\text{OH}_2^+$  concentration between  $10^{-3}$  and  $10^{-2}$  M, or equal to  $g(\text{H}_2 + \text{N}_2)$  in a solution with a nitrous oxide concentration between  $10^{-3}$  and  $10^{-2}$  M. Thus, from the upper curves in Figs. III-3 to III-5 (p. 62,63,64) it appears that in absolutely pure methanol  $G(\text{H}_2) = 4.95$  at  $-97^\circ$ ,  $5.45$  at  $25^\circ$  and  $6.5$  at  $150^\circ$ . The estimated yield as a function of temperature is represented by the uppermost curve in Fig. III-1 (p. 50).

The scavenging reactions of the impurities in Samples A and B become less efficient as the temperature increases. The impurities in Sample A could not compete with hydrogen forming reactions at temperatures above  $140^\circ$  and those in Sample B could not compete above about  $30^\circ$ . Kinetic analysis of the results in Fig. III-1 (p.50) shows that  $(E_{27} - E_{65})$  is about 1 kcal/mole. This is essentially the

same as the value  $E_{27} - E_{54} = 0.9$  kcal/mole that can be derived from the values of  $k_{54}/k_{27}$  in Table IV-1. Thus  $E_{65} \approx E_{54}$ , as expected.

Two workers (19,109) have previously measured the value  $G(H_2) = 5.4$  for "pure" methanol at room temperature, although many workers have obtained lower values (39-41, 99,107). The only previously reported low temperature value,  $G(H_2) = 4.15$  at  $-78^\circ$  (19), is lower than the presently measured  $G(H_2) = 4.5$  at  $-97^\circ$  and is much lower than our estimate of  $G(H_2) = 5.0$  for absolutely pure methanol at  $-97^\circ$ . This emphasizes the extreme difficulty of obtaining pure methanol and throws serious doubt on all yields of free ion solvated electrons ( $G \approx 1$ ) that have been estimated from changes in the hydrogen yield. Recently, Seki and Imamura (107) deduced from scavenging experiments that  $G(H_2) = 5.4$  from pure methanol at room temperature (although they measured the value 4.92) and they also deduced that  $G(e^-_{\text{solv}})_{\text{fi}} = 2.0$ . The present work indicates that  $G(e^-_{\text{solv}}) = 4.6$  and that  $G(e^-_{\text{solv}})_{\text{fi}} = 2.0$ .

To further check the model, the hydrogen yields from the nitrous oxide solutions were calculated as a function of nitrous oxide concentration. The one-adjustable-parameter and two-adjustable-parameters treatment were applied, using the same values of  $\beta_-$  and of  $k_{54}/k_{27}$  (Table IV-1) that were used for the calculation of  $g(N_2)$ . According to the proposed mechanism all free ion solvated electrons

ultimately form hydrogen in pure methanol, but only a fraction, equal to  $k_{51}/k_{52}$ , of the electrons that undergo geminate neutralization lead to hydrogen formation. The values of  $k_{51}/k_{52}$  and  $G(H_2)_{51}$  were obtained as described in Appendix B and are reported in Table IV-5 along with other relevant data.

For nitrous oxide concentrations below  $3 \times 10^{-3}$  M, where essentially only free ions were being scavenged, the hydrogen yields  $g(H_2)$  were calculated with the aid of equation (IV-ii), since under these circumstances

$$g(N_2) = \Delta g(H_2) = G(H_2)_0 - g(H_2) \quad \text{(IV-vi)}$$

For nitrous oxide concentrations greater than  $3 \times 10^{-3}$  M, where essentially all the free ions were scavenged, the hydrogen yields were calculated with the aid of equation (IV-vii).

$$\begin{aligned} \Delta g(H_2) &= G(H_2)_0 - g(H_2) \\ &= G(H_2)_{fi} + G(H_2)_{51} \left[ \frac{g(N_2) - G(H_2)_{fi}}{G(\text{total ionization}) - G(H_2)_{fi}} \right] \end{aligned} \quad \text{(IV-vii)}$$

where  $G(H_2)_{fi} = G(e^-_{solv})_{fi}$ ,  $g(N_2)$  was calculated from equation (Aiv),  $G(\text{total ionization}) = 4.6$  and  $G(H_2)_{51}$  was determined as described in Appendix B.

The hydrogen yields calculated from the one-adjustable-parameter treatment are represented by the full curves in Fig. III-6 (p. 65). The results of the two-adjustable-parameters calculations are represented by the dashed curve. The

TABLE IV-5

Relevant Data for the Calculation of the Hydrogen Yields

t(°C)	LAP <sup>a</sup>			2AP <sup>b</sup>				
	G(H <sub>2</sub> ) <sub>o</sub>	g(H <sub>2</sub> ) <sub>min</sub> <sup>c</sup>	G(H <sub>2</sub> ) <sub>fi</sub> <sup>d</sup>	G(H <sub>2</sub> ) <sub>51</sub> <sup>c</sup>	k <sub>51</sub> /1.52 <sup>c</sup>	G(H <sub>2</sub> ) <sub>fi</sub> <sup>d</sup>	G(H <sub>2</sub> ) <sub>51</sub> <sup>c</sup>	k <sub>51</sub> /k <sub>52</sub> <sup>c</sup>
-97	4.9 <sub>5</sub>	1.5	2.4	1.1	1.0	1.9	1.6	1.5
+25	5.4 <sub>5</sub>	1.8	2.2	1.5	1.7	2.0	1.7	1.9
150	6.5	2.3	1.8	2.4	6.0	---	---	---

a. One-adjustable-parameter treatment

b. Two-adjustable-parameters treatment

c. Estimated by the method illustrated in Appendix B

d. G(H<sub>2</sub>)<sub>fi</sub> = G(e<sup>-</sup> solv)<sub>fi</sub>. Values taken from Table IV-1.

same values of  $\beta_-$  and  $\epsilon_{ave}$  were used in the calculation of both the nitrogen and hydrogen yields, and the calculated yields agree well with those measured experimentally (Fig. III-6, p. 65). The fact that the measured values of  $g(H_2)$  at  $-97^\circ$  are lower than the calculated values at very low nitrous oxide concentrations is attributed to the presence of a trace of impurity in the alcohol.

#### 6. Effect of Temperature on the Hydrogen-Forming Reactions

The yield of free ions in methanol varies only slightly, if at all, with temperature. This is mainly because the changes in liquid density, and hence in  $\gamma$  values, and in dielectric constant nearly balance the change in  $T$  in equations (Aii) and (Aiii) in Appendix A.

The value of the ratio  $k_{51}/k_{52}$  increases from about 1.5 at  $-97^\circ$  to about 6.0 at  $150^\circ$  (Table IV-5). Thus, over this temperature range the average difference between the activation energies of reactions [51] and [52] is  $(E_{51} - E_{52}) = 0.8$  kcal/mole.

The minimum value of the hydrogen yield obtained by the addition of nitrous oxide is designated  $g(H_2)_{min}$  (see Fig. III-3, p. 62). The yield of  $g(H_2)_{min}$  has been attributed to reactions [48] and [64]. The estimated values of  $g(H_2)_{min}$  at different temperatures are included in Table IV-5. The temperature variation of these reactions corresponds to  $E_{48,64} = 0.2$  kcal/mole.

The relatively small temperature dependence of the

hydrogen yield that has been attributed to reactions [48], [51] and [64] might actually be due to the increasing importance of other reactions that are negligible at  $-97^{\circ}$  but that have larger activation energies. However, the maximum possible value of the activation energy of such reactions is only 2.3 kcal/mole, calculated from an Arrhenius plot of  $[G(H_2)_{t^{\circ}} - G(H_2)_{-97^{\circ}}]$  for temperatures up to  $240^{\circ}$  (Fig. IV-2). These low values of the activation energies seem to imply that they refer to secondary effects such as solvent rearrangements and "cage" effects, rather than to actual primary decomposition reactions of molecules or radicals.

Reaction [54] is essentially diffusion controlled in water (18) and is nearly the same in methanol (72). Thus the activation energy of reaction [54] probably equals that of diffusion, i.e.  $E_{54} \approx 2.8$  kcal/mole. It was pointed out in the preceding section that  $(E_{27} - E_{54}) = 0.9$  kcal/mole. Hence

$$E_{27} \approx 3.7 \text{ kcal/mole} = E_{\tau} \quad (\text{IV-viii}).$$

which means that the activation energy for the decomposition of solvated electrons in methanol, reaction [27], is approximately the same as that of dielectric relaxation.

The value of  $k_{27}$  at  $25^{\circ}$  can be estimated as follows: The value of  $k_{26}$  at  $23^{\circ}$  is  $3.9 \times 10^{10}$  l/mole sec in a solution with ionic strength  $\mu = 1 \times 10^{-4}$  M(16). Assuming

that  $E_{26} = 2.8$  kcal/mole, at  $25^\circ$   $k_{26} = 4.0 \times 10^{10}$  l/mole sec. At  $0^\circ$  and  $\mu = 1 \times 10^{-4}$  M,  $k_{26}/k_{54} = 7.9$  (72), and the same value will be assumed to be valid at  $25^\circ$ . The value of  $k_{54}/k_{27}$  at  $25^\circ$  is  $1.1 \times 10^4$  l/mole (Table IV-1). Combination of these values gives  $k_{27} = 4.6 \times 10^5$  sec $^{-1}$  at  $25^\circ$ , which corresponds to a half-life of 1.5  $\mu$ sec at this temperature. Previously reported values of the half-life of reaction [27] can be converted to values at  $25^\circ$  by using  $E_{27} = 3.7$  kcal/mole. The converted values 1.4  $\mu$ sec (20) and 1.7  $\mu$ sec (125) agree well with the present result of 1.5  $\mu$ sec. The value of 7.5  $\mu$ sec recently derived from hydrogen scavenging studies (126) is dependent on the value used for  $G(e^-_{\text{soln}})_{\text{fi}}$ . The estimated half-life would have been much smaller if the yield  $G(e^-_{\text{soln}})_{\text{fi}} = 2.0$  rather than the reported yield of 1.3 had been used.

From the values of  $k_{27}$  and  $E_{27}$ , the entropy of activation  $\Delta S^\ddagger_{27}$  can be estimated by the use of equation (IV-ix) (127).

$$k_{27} = \frac{e\kappa T}{h} e^{\Delta S^\ddagger/R} e^{-E/RT}$$

$$= 10^{13} e^{\Delta S^\ddagger/R} e^{-E/RT} \quad \text{(IV-ix)}$$

Substituting the values of  $k_{27} = 4.6 \times 10^5$  sec $^{-1}$  and  $E_{27} = 3.7$  kcal/mole into equation (IV-ix) yields  $\Delta S^\ddagger_{27} = -21$  cal/degree mole. This large negative value is nearly the same as the values in water, ethanol, n-propanol and isopropanol (Table IV-6).

TABLE IV-6

Entropies of Activation of the First Order Decay of  
Solvated Electrons

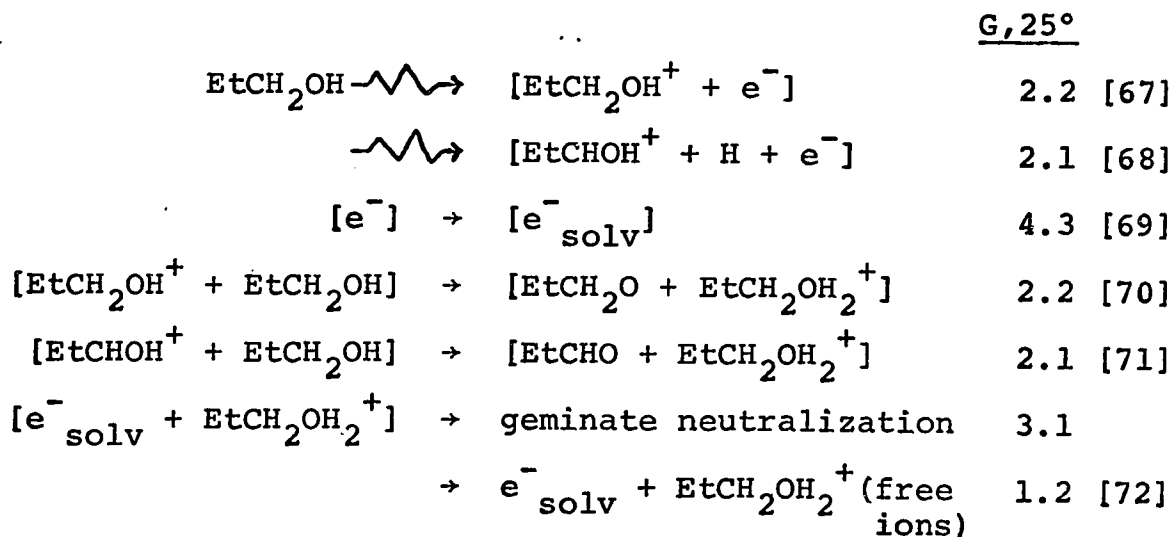
Solvent	$k_{27}(\text{sec}^{-1})^a$	$E_{27}(\text{kcal/mole})^{1a}$	$\Delta S_{27}^\ddagger(\text{cal/deg mole})^a$
Water	$9 \times 10^2$ <sup>b</sup>	6.7 <sup>c</sup>	-23
Methanol	$4.6 \times 10^5$	3.7	-21
Ethanol	$1.2 \times 10^5$ <sup>d</sup>	4.6 <sup>d</sup>	-21
n-Propanol	$4.9 \times 10^5$ <sup>e</sup>	4.3 <sup>e</sup>	-19
iso-Propanol	$3.1 \times 10^5$ <sup>d</sup>	5.3 <sup>d</sup>	-17

- a. Subscript 27 refers to the decay of solvated electrons in each solvent corresponding to reaction [27] in methanol.
- b. Calculated from the data in Ref. (16), p.251.
- c. Value taken from Ref. (128).
- d. Values taken from Discussion Section C-3.
- e. Values taken from Discussion Section B-7.

(B) n-Propanol

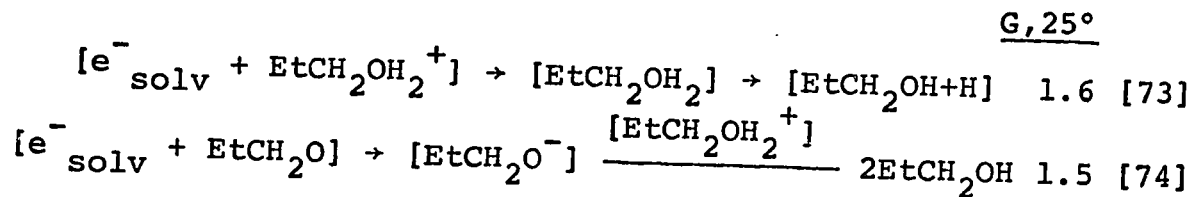
1. Pure n-Propanol

The results obtained are consistent with the mechanism proposed for methanol (previous section), ethanol (24) and iso-propanol (25), with a few exceptions which will be discussed later. The yield specified after each of the following reactions refers to irradiation at 25° and is based on the experimental yields and theoretical considerations. Square brackets around reactants or products indicate that the species are inside a spur.



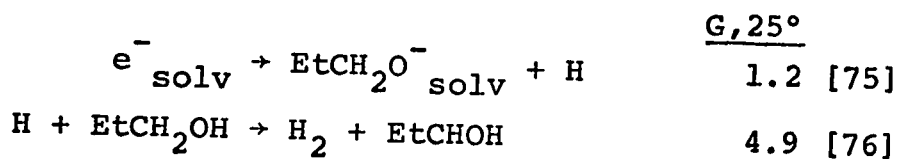
The ions that undergo geminate neutralization appear to be involved in two types of reaction, only one of which produces hydrogen. The competition between these two types of reaction is slightly temperature dependent, the activation energy of the hydrogen producing reaction being roughly 1 kcal/mole greater than that which does not produce hydrogen. One of the many feasible reactions between the intermediates

in spurs that might have a small temperature dependence is presented here:

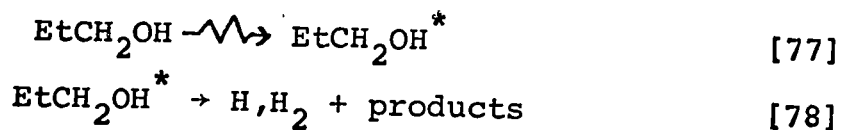


The stipulated yields of reactions [70] to [74] are those that would be required if reaction [74] were the only one that consumed electrons without producing hydrogen.

The other reactions that are relevant to the present work are

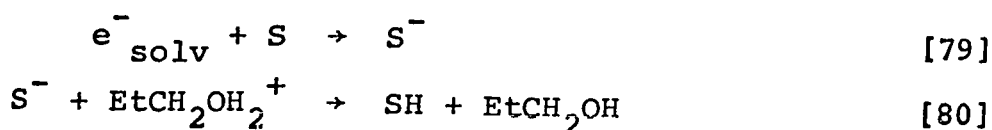


If the reactions



take place, the estimated yield of reaction [68] would have to be decreased by an amount equal to the yield of reaction [78] and the estimated yield of reaction [67] would have to be increased by the same amount to maintain the total G value of ion pairs equal to 4.3

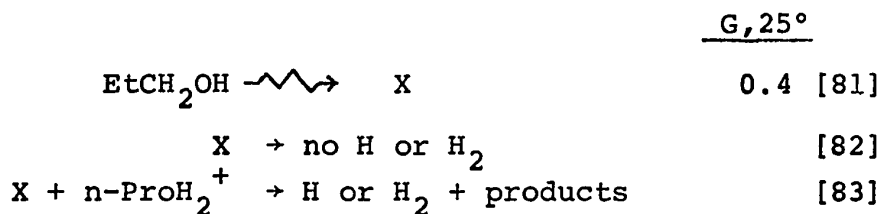
The presence of a low concentration of an electron scavenging impurity S can prevent some of the free ion solvated electrons from forming hydrogen.



In the n-propanol used in the present experiments, the probable identity of S is propionaldehyde.

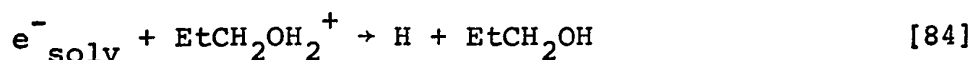
## 2. Effects of Electron Scavengers

The plots of  $g(\text{H}_2 + \text{N}_2)$  against nitrous oxide concentration are lower than those of  $g(\text{H}_2)$  against  $\text{n-PrOH}_2^+$  concentration at all temperatures studied (see Figs. III-8 to III-10, p. 83,84,85). In order to explain the acid effect adequately, it is necessary to postulate a species to be represented by the symbol X, as in ethanol (24), which reacts with hydrogen ions to give either H or  $\text{H}_2$ . This species does not react with nitrous oxide to form nitrogen and in the absence of acid does not give rise to hydrogen.



The results in Table III-17 (p. 81) also indicate that a secondary reaction that generates a large amount of nitrogen from nitrous oxide, such as the one that occurs in iso-propanol (25), can also occur in n-propanol.

The addition of acid would cause reactions [75] and [79] to be replaced by [84].

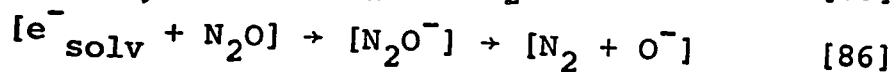
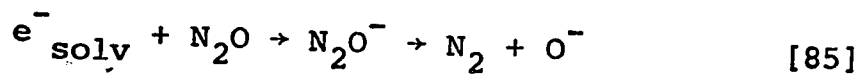


It has been mentioned above that a small amount of acid causes the hydrogen yield to increase by reaction [83].

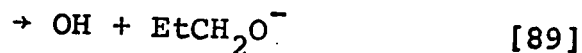
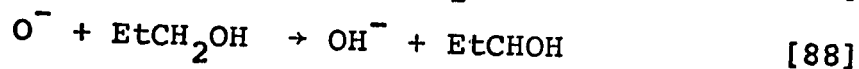
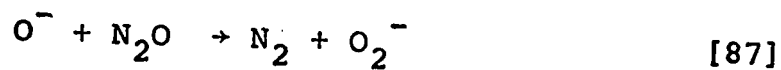
It is apparent from Figs. III-8 to III-10 (p. 83,84,85) that neither high temperatures nor high concentrations of nitrous oxide interfere with reaction [83]. Because of this, it appears that X is not a solvated electron.

A sufficiently high concentration of acid would cause reaction [74] to be replaced by [73]. The increase of hydrogen yield with increasing acid concentration is explained by these replacements of reactions [74] and [79].

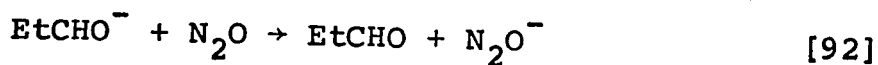
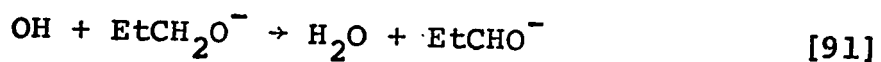
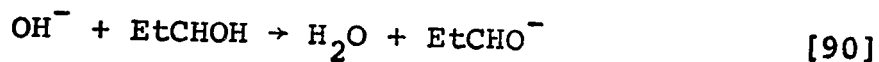
In a similar way (except for species X), the addition of nitrous oxide would cause the value of  $g(\text{H}_2 + \text{N}_2)$  to increase with increasing nitrous oxide concentration, by the occurrence of reactions [85] and [86].



Reactions [85] and [86] increase the value of  $g(\text{H}_2 + \text{N}_2)$  only to the extent that they interfere with reactions [74] and [79]. Such an increase in  $g(\text{H}_2 + \text{N}_2)$  should not give a yield greater than 6.4 ( $G(\text{total ionization}) = 4.3 + g(\text{H}_2)_{\text{min}}$  (see Table IV-11 for values of  $g(\text{H}_2)_{\text{min}}$ )) at  $-120^\circ$  and  $25^\circ$ ; and 7.3 at  $140^\circ$ . At  $140^\circ$ ,  $g(\text{H}_2 + \text{N}_2)$  rises rapidly above 0.1 M nitrous oxide concentration, which suggests the extensive occurrence of a secondary reaction at above 0.1 M nitrous oxide (see Table III-17, p. 81). Such a secondary reaction might be reaction [87] in competition with reaction [88] or [89].



However, reaction [87] apparently does not occur in methanol or ethanol (24) and it probably cannot compete with reactions [88] or [89] in n-propanol. The large nitrogen yields at high temperatures and high nitrous oxide concentrations might be due to occurrence of a short chain reaction similar to that proposed for nitrous oxide - methylcyclohexane vapour mixtures (129). This would involve reaction [88] or [89] followed by [90] or [91] and then [92].



A similar series of reactions has been proposed by Sherman to explain a chain reaction found in alkaline solutions of nitrous oxide in iso-propanol (101). There is a great need for knowledge of values of electron affinities of molecules and radicals, in the vapour phase and in solvents of various polarities, to help to decide the feasibility of reactions such as [92].

Because of the occurrence of what is most probably a secondary reaction of nitrous oxide, it is necessary to apply a correction to the experimental nitrogen yields in

order to obtain a reasonable measure of the number of solvated electrons scavenged. The correction was applied as follows. The order of the secondary reaction of nitrous oxide was chosen to be two. The reason for this choice is twofold. Firstly, the true order of this reaction may be between 1 and 2 because some of the secondary reaction may occur in the spurs. Secondly, the mechanism proposed for this reaction supports second order. The contributions from such reactions are estimated on this basis and are included in Table III-13, III-15 and III-17 (p. 77,79,81). The corrected values of the nitrogen yields are plotted in Figs. III-8 to III-10 (p. 83,84,85 ). The experimental points thus obtained are in good agreement with the calculated curves.

### 3. Scavenging Kinetics, Nitrogen Yields

The scavenging kinetics treatment and calculation of the nitrogen yields are similar to those for methanol discussed in the previous section (see Discussion Section A-3). The experiments covered wide ranges of scavenger concentration ( $6 \times 10^{-5}$  to 7M), temperature (153° to 413°K) and dielectric constant (45.7 to 8.1). As in the methanol system, one-adjustable-parameter and two-adjustable-parameters treatments were applied.

#### (a) One-Adjustable-Parameter Treatment

The yield of free ion solvated electrons at each temperature was calculated by a method that is summarized

in Appendix A, but which is described in detail elsewhere (22). The yields are reported under the heading IAP in Table IV-7.

It was assumed that reactions of the free ions could be described by homogeneous kinetics. Values of  $k_{85}/k_{75}$ , reported in Table IV-7, were obtained from conventional plots of  $\frac{1}{g(N_2)}$  vs  $\frac{1}{[N_2O]}$ , using only data for nitrous oxide concentrations less than  $10^{-3}$  M (Fig. IV-3). The nitrogen yields in the concentration region below  $10^{-3}$  M were computed using an equation similar to (IV-ii).

$$g(N_2) = G(e^-_{solv})_{fi} \cdot \frac{k_{85}[N_2O]}{k_{75} + k_{85}[N_2O]} \quad (IV-x)$$

The model of nonhomogeneous kinetics for the reactions of ions in spurs (22) was applied when the solute concentrations were greater than  $10^{-3}$  M (for calculations see Appendix A).

The nitrogen yields from the more concentrated nitrous oxide solutions at  $-120^\circ$  indicated that  $g(\text{total ionization}) = 4.3$  (Fig. III-8, p. 83), so this value was used in equations (Ai) and (Aiv) for all temperatures. Alder and Bothe (130) measured the W value for n-propanol vapour and obtained  $W = 24.5$  eV which corresponds to  $G(e^-)_{total} = 4.1$ . Their measured W values for several compounds are 1 to 2 eV greater than those obtained by other workers (121,131). The agreement between W values in the gas phase and in the liquid phase is reasonable.

TABLE IV-7

Quantities Relevant to the Reactions of Solvated Electrons in n-Propanol.

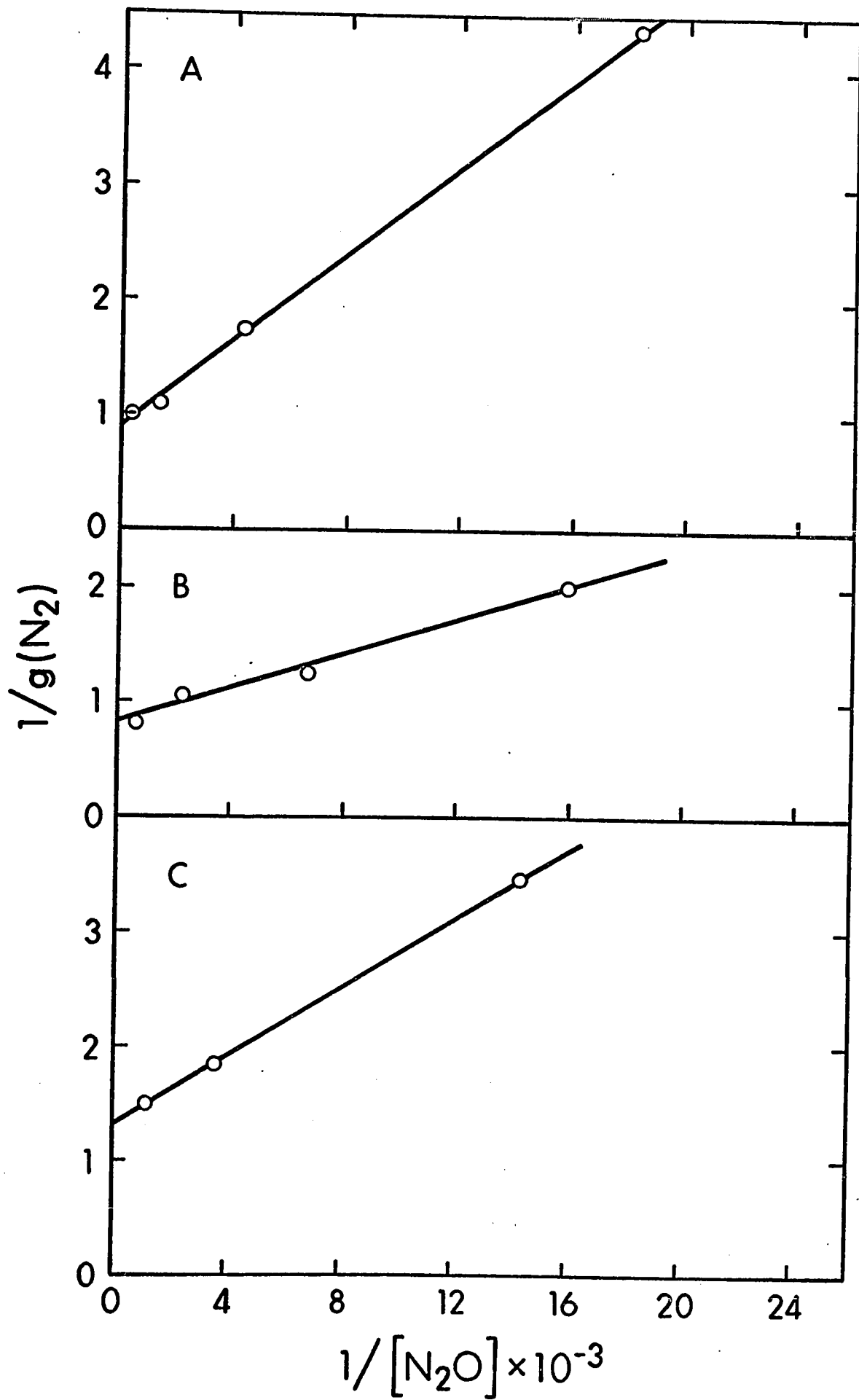
t(°C)	density g/ml	ε	k <sub>85</sub> /k <sub>75</sub> (l/mole)	LAP		2AP	
				a	b	c	d
				G(e <sup>-</sup> solv) fi	β <sub>-</sub> (v/cm <sup>2</sup> )	G(e <sup>-</sup> solv) fi	β <sub>-</sub> (v/cm <sup>2</sup> )
-120	0.913	45.7	4.7 x 10 <sup>3</sup>	1.3	3.9 x 10 <sup>13</sup>	1.1	4.6 x 10 <sup>13</sup>
+25	0.800	20.31	1.06 x 10 <sup>4</sup>	1.3	6.4 x 10 <sup>13</sup>	1.2	---
140	0.688	8.1	8.9 x 10 <sup>3</sup>	0.8	2.2 x 10 <sup>14</sup>	0.8	---

- a. one-adjustable-parameter treatment.
- b. two-adjustable-parameters treatment
- c. calculated from the model.
- d. estimated from homogeneous kinetics plots of results at [N<sub>2</sub>O] < 10<sup>-3</sup> M.

FIGURE IV-3

Plots of  $1/g(N_2)$  against  $1/[N_2O]$  for  
n-propanol.

A,  $-120^\circ$ ;    B,  $25^\circ$ ;    C,  $140^\circ$ .



The density of n-propanol at each temperature must be known for the estimation of the initial spectrum of ion-electron separation distances,  $N(y)$ . The value of the dielectric constant is required in equations (Aiii) and (Aviii) in Appendix A. These quantities are listed in Table IV-7.

The adjustable parameter used in fitting the model to the nitrogen yields was  $\beta_*$ , and the best values are reported in Table IV-7.

The results of the calculations of the one-adjustable-parameter treatment are represented by the full lines through the nitrogen yields in Figs. III-8 to III-10 (p.83, 84, 85 ). The calculated curve is little high in the homogeneous kinetics region at  $-120^\circ$  (Fig. III-8, p. 83). The reason for the lack of agreement is the same as discussed in the methanol section (see Discussion Section A-3a). The homogeneous kinetics plots (Fig. IV-3) that were used to obtain the values of  $k_{85}/k_{75}$  also gave values of  $G(e^-_{\text{solv}})_{fi}$ , and this was lower at  $-120^\circ$  than that calculated from the model (Table IV-7). The reported values of  $k_{85}/k_{75}$  are related to the homogeneous kinetics values of  $G(e^-_{\text{solv}})_{fi}$ , but the model values were used in equation (IV-x). Thus the calculated nitrogen yields at low concentrations of nitrous oxide were 15% too high at  $-120^\circ$ . To obtain better agreement between calculation and experiment a second adjustable parameter is needed and, as in methanol, the com-

plex dielectric constant is used. The activation energy  $E_t$  6.1 kcal/mole for dielectric relaxation has been estimated from the Arrhenius plot in Fig. IV-4A. The activation energies for viscous flow and self diffusion in n-propanol are each 4.3 kcal/mole (123) these values along with others are listed in Table IV-8). Hence the activation energy for the migration of the radiolytic ions is probably about 4.3 kcal/mole. Thus the value of the dielectric relaxation time  $\tau$  increases more rapidly with decreasing temperature than does that of  $t_{gn}$ , the time required for geminate neutralization. So, the lack of complete dielectric relaxation could be the cause of the crudely calculated value of  $G(e^-_{solv})_{fi}$  being too high at  $-120^\circ$ .

(b) Two-Adjustable-Parameters Treatment

The time averaged complex dielectric constant is used in the model calculation and the value of the ratio  $\tau/t_{gn}$  is chosen such that the value of  $G(e^-_{solv})_{fi}$  calculated from the model is equal to the value obtained from the homogeneous kinetics plots (Fig. IV-3).

The time averaged values of complex dielectric constant were calculated by using equation (IV-iv). It will suffice here to indicate the magnitude of the effect required to reduce the calculated value of  $G(e^-_{solv})_{fi}$  from 1.3 to 1.1 at  $-120^\circ$ . For ion pairs with  $y = 14 \text{ \AA}$ ,  $\tau/t_{gn} = 0.20$ ; for  $y = 16 \text{ \AA}$ ,  $\tau/t_{gn} = 0.10$ ; and for  $y = 19 \text{ \AA}$ ,  $\tau/t_{gn} = 0.05$ .

FIGURE IV-4

- A. Arrhenius plot for dielectric relaxation  
in n-propanol.
- B. Arrhenius plot of  $[G(H_2)_{t^\circ} - G(H_2)_{-120^\circ}]$   
in n-propanol.

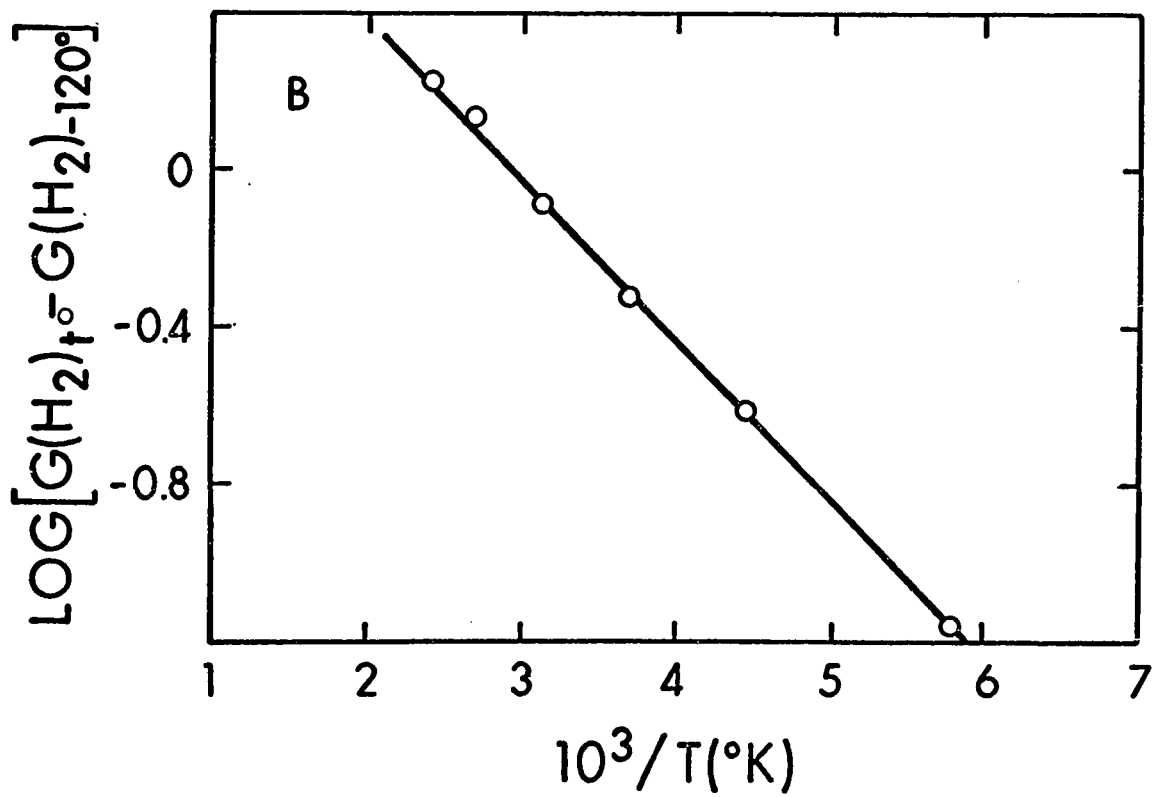
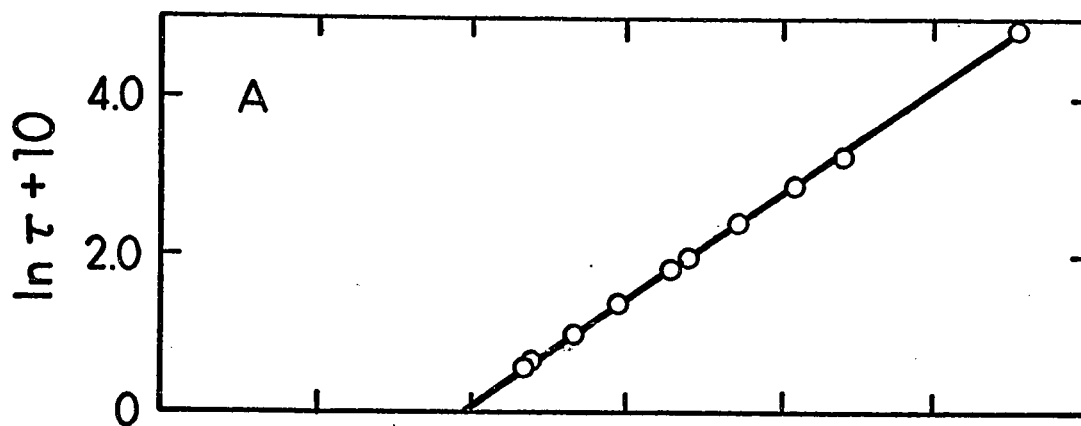


TABLE IV-8

Some Relevant Data for n-Propanol

t(°C)	$\tau$ sec <sup>a</sup>	$E_t$ kcal/mole	$E_{\text{self diffusion}}$ kcal/mole	$E_{\text{viscous flow}}$ kcal/mole	$E_{75-E85}$ kcal/mole	$E_{\text{self diff}} + (E_{75-E85})$ kcal/mole
-120	$6.5 \times 10^{-6}$	6.1	4.3	4.3	0.0	4.3
+25	$3.7 \times 10^{-10}$					
140	$2.8 \times 10^{-11}$					

a. Calculated from data in Ref. (122).

The values of  $\epsilon_{ave}$  obtained from equation (IV-iv), and which gave the correct values of  $G(e^-_{solv})_{fi}$  when used in model calculations, were then used to calculate the nitrogen yields. The  $N(y)$  spectra and values of  $\epsilon_{ave}$  are listed in Table IV-9.

Thus in the two-adjustable-parameters treatment, one adjustable parameter is  $\beta_-$  and the other may be considered to be either  $\epsilon_{ave}$  or  $(\tau/t_{gn})$ . This refinement of the kinetics model led to the dashed curve in Fig. III-9 (p. 84). The appropriate value of  $\beta_-$  is reported under the heading 2AP in Table IV-7.

The two-adjustable-parameters treatment was not applied to the 25° and 140° systems because satisfactory results were obtained with one-adjustable-parameter. This is interpreted to mean that dielectric relaxation was sufficiently rapid relative to geminate neutralization at 25° and 140° that  $\epsilon_{ave} = \epsilon_{static}$  even with the smallest values of  $y$  used in the model.

#### 4. Competition Between Nitrous Oxide and Acid

The presence of both acid and nitrous oxide in the n-propanol would cause a competition between reactions [84] and [85]. The resulting nitrogen yield at a given nitrous oxide concentration is smaller than would be observed in the absence of acid. The nitrogen yields are calculated from equation (IV-xi) and are reported in Table IV-10.

TABLE IV-9

N( $\gamma$ ) Spectra and Values of  $\epsilon_{ave}$  in n-Propanol at Different Temperatures

<u>N(<math>\gamma</math>)</u>	<u>-120°</u>		<u>25°</u>		<u>140°</u>	
	<u><math>\gamma</math>(Å)</u>	<u><math>\epsilon_{ave}</math></u>	<u><math>\gamma</math>(Å)</u>	<u><math>\epsilon_{ave}</math></u>	<u><math>\gamma</math>(Å)</u>	<u><math>\epsilon_{ave}</math></u>
2150	14	35	17	20.3	19	8.1
1100	16	40	19	20.3	22	8.1
600	19	43	22	20.3	26	8.1
476	27	45.7	31	ditto	36	ditto
270	45	45.7	52		60	
116	74	45.7	85		99	
64	106	ditto	123		142	
41	143		165		192	
28	185		214		248	
21	230		266		308	
16	280		323		375	
13	334		385		447	
15	406		468		544	
14	517		596		692	
76	<600		<700		<800	

$\Sigma N(\gamma) = 5000$

TABLE IV-10

Competition Between Nitrous Oxide and Acid at 25°C

$[N_2O]M$	$[HCl]M$	$[n-PrOH_2^+]M$	$k_{84}/k_{85}$ <sup>a</sup>	$g(N_2)$ <sup>b</sup>	$g(N_2)$ calc	$g(N_2)$ expt.	$g(H_2)$
0.0296	0.0240	0.0044	5.0	2.55	1.46	1.45	4.66
0.0264	0.0078	0.0024	5.6	2.40	1.60	1.67	4.06
0.0826	0.0240	0.0044	5.0	3.00	2.37	2.35	3.95

a. Using the same ratio as in methanol (Trans. Faraday Soc., p.1191 (1967))

b. Yield that would be obtained from a simple nitrous oxide solution with  $[N_2O]$  equal to the present value of  $\{[N_2O] + k_{84}/k_{85} [n-PrOH_2^+]\}$ .

c. Using equation (IV-xi) in the text.

$$g(N_2) = g(N_2)_0 \left[ 1 + \frac{k_{84} [n\text{-PrOH}_2^+]}{k_{85} [N_2O]} \right]^{-1} \quad (\text{IV-xi})$$

where  $g(N_2)_0$  is the yield of nitrogen at a nitrous oxide concentration equal to  $([N_2O] + \frac{k_{84}}{k_{85}} [n\text{-PrOH}_2^+])$ . The value of  $\frac{k(e^-_{\text{solv}} + H^+)}{k(e^-_{\text{solv}} + N_2O)}$  in methanol has been reported to be 7.9 at zero ionic strength and 1.7 at an ionic strength of 0.1 (72). The value of this rate constant ratio is not known in any other alcohols. It is, therefore, assumed for lack of anything better, that this ratio in n-propanol has the same value as in methanol. The calculated values of  $g(N_2)$  obtained using the value for this ratio at the appropriate ionic strength are in very good agreement with the experimental values (see columns 6 and 7 of Table IV-10). Thus the results indicate that nitrous oxide and acid compete for the same species. Although nitrous oxide does not compete with acid for species X, acid competes for all of the species with which nitrous oxide reacts.

These results also support the suggestion that a species X exists.

##### 5. Hydrogen Yields

Evidently a small amount of electron scavenger remained in our purified n-propanol. At nitrous oxide concentrations  $\approx 10^{-3}$  M, the scavenging of free ion solvated electrons is virtually complete and scavenging in the spurs

is negligible. Assuming that in absolutely pure n-propanol all the free ion solvated electrons would react to form hydrogen, the value of  $G(H_2)$  in absolutely pure n-propanol would be equal the value of  $g(H_2 + N_2)$  in a solution with nitrous oxide concentration  $\approx 10^{-3}$  M. Thus, from the upper curves in Figs. III-8 to III-10 (p. 83, 84, 85) it appears that in absolutely pure n-propanol  $G(H_2) = 4.3$  at  $-120^\circ$ , 4.9 at  $25^\circ$  and 6.0 at  $140^\circ$ . The estimated yield as a function of temperature is presented by the dashed curve in Fig. III-7 (p. 74).

The identity of the species X which reacts in the presence of acid to give hydrogen is elusive. The entity responsible for the observed effects must undergo reactions similar to [82] and [83]. The suggestion made earlier that this entity is not the solvated electron is further supported by the fact that acid increases the overall reduction yield by 0.4 - 0.5 g units, and this is true even under conditions where the solvated electrons, including those which normally undergo geminate neutralization, are scavenged by nitrous oxide.

The reaction of the electron scavenging impurity becomes slightly more efficient as the temperature increases (see Fig. III-7, p. 74). Kinetic analysis of the results in Fig. III-7 (p. 74) indicates that the difference between the activation energies of reactions [79] and [75] is about 1 kcal/mole. The ratio  $k_{85}/k_{75}$  seems to be independent of

temperature, so  $E_{85} = E_{75}$  (see Table IV-7).

Only one laboratory has previously measured the value  $G(H_2) = 4.4$  for pure n-propanol at room temperature (42), although other workers have obtained lower values (see Ref. 42). This emphasizes the extreme difficulty of obtaining pure n-propanol and throws serious doubt on yields of free ions that have been estimated from changes in the hydrogen yield.

To further check the model, the hydrogen yields from the nitrous oxide solutions were calculated as a function of nitrous oxide concentration. The one-adjustable-parameter and two-adjustable-parameters treatments were applied, using the same values of  $\beta_-$  and  $k_{85}/k_{75}$  (Table IV-7) that were used for the calculation of  $g(N_2)$ . According to the proposed mechanism, all free ion solvated electrons ultimately form hydrogen in n-propanol, but only a fraction equal to  $k_{73}/k_{74}$  of the electrons that undergo geminate neutralization lead to hydrogen formation. The values of  $k_{73}/k_{74}$  are listed in Table IV-11 along with other relevant data. For nitrous oxide concentrations below  $10^{-3}$  M, where essentially only free ions were being scavenged, the hydrogen yields  $g(H_2)$  were calculated with the aid of equation (IV-x), since under these circumstances

$$g(N_2) = \Delta g(H_2) = G(H_2)_0 - g(H_2) \quad (IV-vi)$$

For nitrous oxide concentrations greater than  $10^{-3}$  M, where

TABLE IV-11

Relevant Data for the Calculation of the Hydrogen Yields

t(°C)	$G(H_2)_0$	$g(H_2)_{min}^c$	1AP <sup>a</sup>			2AP <sup>b</sup>		
			$G(H_2)_{fi}^d$	$G(H_2)_{73}^e$	$k_{73}/k_{74}^c$	$G(H_2)_{fi}^d$	$G(H_2)_{73}^e$	$k_{73}/k_{74}^c$
-120°	4.3	2.1	1.3	0.9	0.4	1.1	1.1	0.5
+25	4.9	2.1	1.3	1.5	1.0	1.2	1.6	1.1
140	6.0	3.0	0.8	2.2	1.7	-----	---	-----

a. One-adjustable parameter treatment.

b. Two-adjustable-parameters treatment.

c. For the definition of  $g(H_2)_{min}$  and  $k_{73}/k_{74}$  see Appendix B.

d.  $G(H_2)_{fi} = G(e^-_{solv})_{fi}$ . Values taken from Table IV-7

e.  $G(H_2)_{73} = G(H_2)_0 - G(H_2)_{min} - G(H_2)_{fi}$  at a particular temperature.

essentially all the free ions were scavenged, the hydrogen yields were calculated with the aid of an equation similar to (IV-vii), namely,

$$\begin{aligned} \Delta g(\text{H}_2) &= G(\text{H}_2)_0 - g(\text{H}_2) \\ &= G(\text{H}_2)_{fi} + G(\text{H}_2)_{73} \cdot \left( \frac{g(\text{N}_2) - G(\text{H}_2)_{fi}}{G(\text{total ionization}) - G(\text{H}_2)_{fi}} \right) \end{aligned}$$

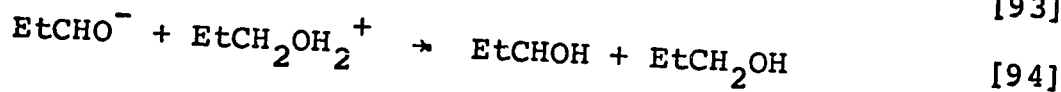
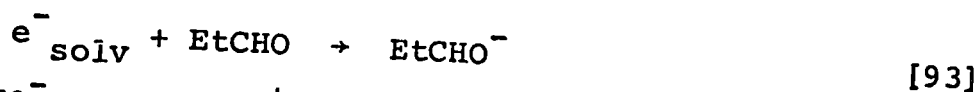
(IV-xi)

where  $G(\text{H}_2)_{fi} = G(e^-_{\text{solv}})_{fi}$ ,  $g(\text{N}_2)$  was calculated from equation (Aiv) in Appendix A,  $G(\text{total ionization}) = 4.3$  and  $G(\text{H}_2)_{73}$  was determined as defined in the foot-note of Table IV-11 (see also Appendix B for a similar determination in methanol).

The hydrogen yields calculated from the one-adjustable-parameter treatment are represented by the full curves in Fig. III-11 (p. 86). The results of the two-adjustable-parameters calculations at  $-120^\circ$  are represented by the dashed curve (Fig. III-11, p. 86). The same values of  $\beta_-$  and  $\epsilon_{\text{ave}}$  were used in the calculation of both the nitrogen and hydrogen yields, and the calculated yields agree well with those measured experimentally (Fig. III-11, p. 86).

#### 6. Effect of Dose on the Hydrogen Yields

The radiolytic product propionaldehyde is a good electron scavenger (17,42). Reaction [93] is responsible for the observed dose dependence of  $G(\text{H}_2)$ , (See Table III-10, p. 70).



7. Effect of Temperature on the Hydrogen-Forming Reactions

The yield of free ions in n-propanol varies slightly with temperature. This variation may be understood in terms of the variation of the values of the quantities in equations (Aii) and (Aiii) in Appendix A.

The value of the ratio  $k_{73}/k_{74}$  increases from about 0.5 at  $-120^\circ$  to 1.7 at  $140^\circ$  (Table IV-11). Thus, over this temperature range the average difference between the activation energies of reactions [73] and [74] is  $(E_{73} - E_{74}) = 0.6$  kcal/mole.

The yield  $g(\text{H}_2)_{\text{min}}$  has been attributed to reactions [68] and [78] and its temperature variation corresponds to  $E_{68,78} = 0.8$  kcal/mole between  $25^\circ$  and  $140^\circ$ .

The relatively small temperature dependence of the hydrogen yield, that has been attributed to reactions [68], [73] and [78], might actually be due to the increasing importance of other reactions that are negligible at low temperature but that have larger activation energies. However, the maximum possible value of the activation energy of such reactions is only 1.9 kcal/mole, calculated from an Arrhenius plot of  $[G(\text{H}_2)_{t^\circ} - G(\text{H}_2)_{-120^\circ}]$  (Fig. IV-4B). These low values of the activation energies seem to imply that they refer to secondary effects, such as solvent

rearrangements and "cage" effects, rather than to actual primary decomposition reactions of molecules or radicals.

Reaction [85] is essentially diffusion controlled in water (18) and is nearly the same in methanol (72). It is assumed to be the same in n-propanol. Thus the activation energy of reaction [85] probably equals that of diffusion, i.e.,  $E_{85} \approx 4.3$  kcal/mole. It was pointed out earlier that  $E_{75} \approx E_{85}$  and hence

$$E_{75} \approx 4.3 \text{ kcal/mole}$$

which means that the activation energy for the decomposition of solvated electrons in n-propanol, reaction [75] is approximately the same as that for diffusion.

The value of  $k_{75}$  at 25° can be estimated from the ratio of  $k_{85}/k_{75}$ . The rate constants for the reactions of oxygen, naphthalene and benzylchloride with solvated electrons in water, methanol and ethanol are the same and show no solvent effect (18). It appears that all of these rate constants are only slightly lower than diffusion controlled. Hence it seems likely that  $k_{85}$  is also independent of these solvents and has the same value in n-propanol and iso-propanol also. Actually, the values of  $k_{85}$  in water and in methanol are almost the same ( $5.3 \times 10^9$  and  $5.1 \times 10^9$  l/mole sec respectively at 25°, after adjusting for the temperature difference (17,18)), and are nearly diffusion controlled. Using the value  $k_{85} = 5.2 \times 10^9$  l/mole sec and from the ratio  $k_{85}/k_{75}$  ( $1.06 \times 10^4$  l/mole)

at 25° from Table IV-7 we get  $k_{75} = 4.9 \times 10^5 \text{ sec}^{-1}$  at 25°, which corresponds to a half-life of 1.4  $\mu$  sec at this temperature.

It is important to note that the viscosity of n-propanol is double that of water and if there is any viscosity effect on  $k_{85}$ , then our estimated value of the half-life of reaction [75] will be too low. The other reported values of the half-life of reaction [75] are 2.0 (20) and 0.7  $\mu$  sec (126). Since none of these estimates is of great accuracy, the agreement is satisfactory.

From the values of  $k_{75}$  and  $E_{75}$ , the entropy of activation  $\Delta S_{75}^\ddagger$  can be estimated by the use of equation (IV-xi). This value is found to be -19 cal/deg mole. This large negative value is nearly the same as the values in water, methanol, ethanol and iso-propanol (Table IV-6).

(C) Ethanol and iso-Propanol

The effects of high temperature, acid and nitrous oxide on the radiolysis of liquid ethanol (24,132) and iso-propanol (25) have been studied in this laboratory. The nonhomogeneous kinetics model (22) was applied to these systems to calculate the nitrogen yields from nitrous oxide solutions at different temperatures. The value of the total ionization was taken as  $G(\text{total ionization}) = 4.0$ . Equation (Ai) in the Appendix A was used to calculate the yield of free ions while the nitrogen yields in the nonhomogeneous kinetics region were obtained from an equation analogous to (IV-x). The rate constant ratio  $\frac{k(e^-_{\text{solv}} + N_2O)}{k(e^-_{\text{solv}} \rightarrow H + RO^-)}$  was varied to obtain the best fit of the calculated curve to the experimental points in both ethanol and iso-propanol.

The values of  $\beta_1$  in equation (Avi) in Appendix A were adjusted to fit the calculated values to the experimental points in nonhomogeneous kinetics regions. The treatment used, thus involved two-adjustable-parameters.

The yields of hydrogen were not calculated from the model and the effects of temperature on different reactions were not discussed in detail.

It is our purpose to test the kinetics model for these two systems in as much detail as were methanol and n-propanol in the previous sections A and B.

The reaction mechanisms for ethanol (24,132) and iso-

propanol (25) are similar to those proposed for methanol and n-propanol in the previous sections A and B with a few exceptions which are discussed below. The reaction mechanism proposed for n-propanol in the previous section B will be used as an example for ethanol and iso-propanol though the specific reaction products depend upon the alcohol.

In the radiolysis of ethanol, as in n-propanol, an unidentified species designated X is apparently formed which reacts with acid to form hydrogen but not with nitrous oxide to produce nitrogen (24,132). The results also indicate that a secondary reaction that generates large amounts of nitrogen from nitrous oxide, such as those that occur in n-propanol and iso-propanol (25), does not occur in ethanol. It has been suggested that there is a species Y in ethanol, which is sensitive to temperature but not to nitrous oxide or acid. The identity of this species will be discussed later. The results from iso-propanol indicate that there is no species like X in this alcohol (25).

1. Scavenging Kinetics, Nitrogen Yields

The scavenging kinetics treatment and calculation of the nitrogen yields are similar to those for methanol and n-propanol discussed in the previous sections A and B. As in the methanol and n-propanol systems, one-adjustable-parameter and two-adjustable-parameters treatments were applied.

(a) One-Adjustable-Parameter Treatment

The yield of free ion solvated electrons at each temperature was calculated by a method that is summarized in Appendix A. The yields are listed under the heading LAP in Tables IV-12 and IV-13 for ethanol and iso-propanol, respectively.

It was assumed that reactions of the free ions could be described by homogeneous kinetics. Values of  $k_{85}/k_{75}$ , reported in Tables IV-12 and IV-13, were obtained from conventional plots of  $\frac{1}{g(N_2)}$  vs  $\frac{1}{[N_2O]}$ , using only data for nitrous oxide concentrations less than  $10^{-3}$  M (Figs. IV-5 and IV-6). In the case of iso-propanol at  $25^\circ$ , the  $\frac{1}{g(N_2)}$  points are scattered (See Fig. IV-6B). Thus the curve was drawn in such a way that the yield of  $G(e^-_{solv})_{fi}$  obtained from the intercept equalled the calculated value and the value of the rate constant ratio  $k_{85}/k_{75}$  gave the best fit to the experimental points for the nitrogen and the hydrogen curves (see Figs. IV-12 and IV-17). The nitrogen yields in the concentration region below  $10^{-3}$  M were computed using equation (IV-x). The model for the reactions of ions in spurs (22) was applied when the solute concentration was greater than  $10^{-3}$  M (for calculations see Appendix A).

Unfortunately, the concentrations of nitrous oxide used were not sufficient to observe a plateau in the nitrogen yield curves at any temperature in either ethanol or

TABLE IV-12

Quantities Relevant to the Reactions of Solvated Electrons in Ethanol

t(°C)	Density (g/cc)	ε	k <sub>85</sub> /k <sub>75</sub>	1AP <sup>a</sup>			2AP <sup>b</sup>	
				G(e <sup>-</sup> solv) <sup>c</sup> fi	β <sub>-</sub> <sup>c</sup> (V/cm <sup>2</sup> )	G(e <sup>-</sup> solv) <sup>d</sup> fi	β <sub>-</sub> <sup>d</sup> (V/cm <sup>2</sup> )	
-112	0.903	60.0	4.0 x 10 <sup>4</sup>	1.9	2.8 x 10 <sup>13</sup>	1.7	4.0 x 10 <sup>13</sup>	
+25	0.788	24.6	4.2 x 10 <sup>4</sup>	1.6	6.3 x 10 <sup>13</sup>	1.5	-----	
90	0.725	16.0 (18.0)	3.4 x 10 <sup>4</sup>	1.4	2.3 x 10 <sup>14</sup>	1.4	-----	
-145	0.691	10.2 (16.0)	6.7 x 10 <sup>4</sup>	1.1	4.2 x 10 <sup>14</sup>	1.2	-----	

a. One-adjustable-parameter treatment

b. Two-adjustable-parameters treatment

c. Calculated from equation (Ai) in Appendix A.

d. Estimated from homogeneous kinetics plots of results at [N<sub>2</sub>O] < 10<sup>-3</sup> M.

e. Values under brackets were used in Ref. (24,132).

TABLE IV-13

Quantities Relevant to the Reactions of Solvated Electrons in iso-Propanol

t(°C)	Density (g/cc)	ε	k <sub>85</sub> /k <sub>75</sub>	LAP <sup>a</sup>		2AP <sup>b</sup>	
				G(e <sup>-</sup> solv) fi <sup>c</sup>	β <sub>-</sub> (V/cm <sup>2</sup> )	G(e <sup>-</sup> solv) fi <sup>d</sup>	β <sub>-</sub> (V/cm <sup>2</sup> )
-85	0.872	41.5	6.5 x 10 <sup>4</sup>	1.6	3.7 x 10 <sup>13</sup>	1.2	7.9 x 10 <sup>13</sup>
+25	0.781	19.4	1.7 x 10 <sup>4</sup>	1.3	5.8 x 10 <sup>13</sup>	1.3	-----
140	0.657	7.0 (8.3) e	1.6 x 10 <sup>4</sup>	0.8	1.6 x 10 <sup>14</sup>	1.0	-----

a. One-adjustable-parameter treatment.

b. Two-adjustable-parameters treatment.

c. Calculated from equation (A<sub>i</sub>) in Appendix A.

d. Estimated from homogeneous kinetics plots of results at [N<sub>2</sub>O] < 10<sup>-3</sup> M.

e. Value under bracket was used in Ref. (25).

FIGURE IV-5

Plots of  $1/g(N_2)$  against  $1/[N_2O]$  for ethanol.

A,  $-112^\circ$ ; B,  $25^\circ$ ; C,  $90^\circ$ ; D,  $145^\circ$ .

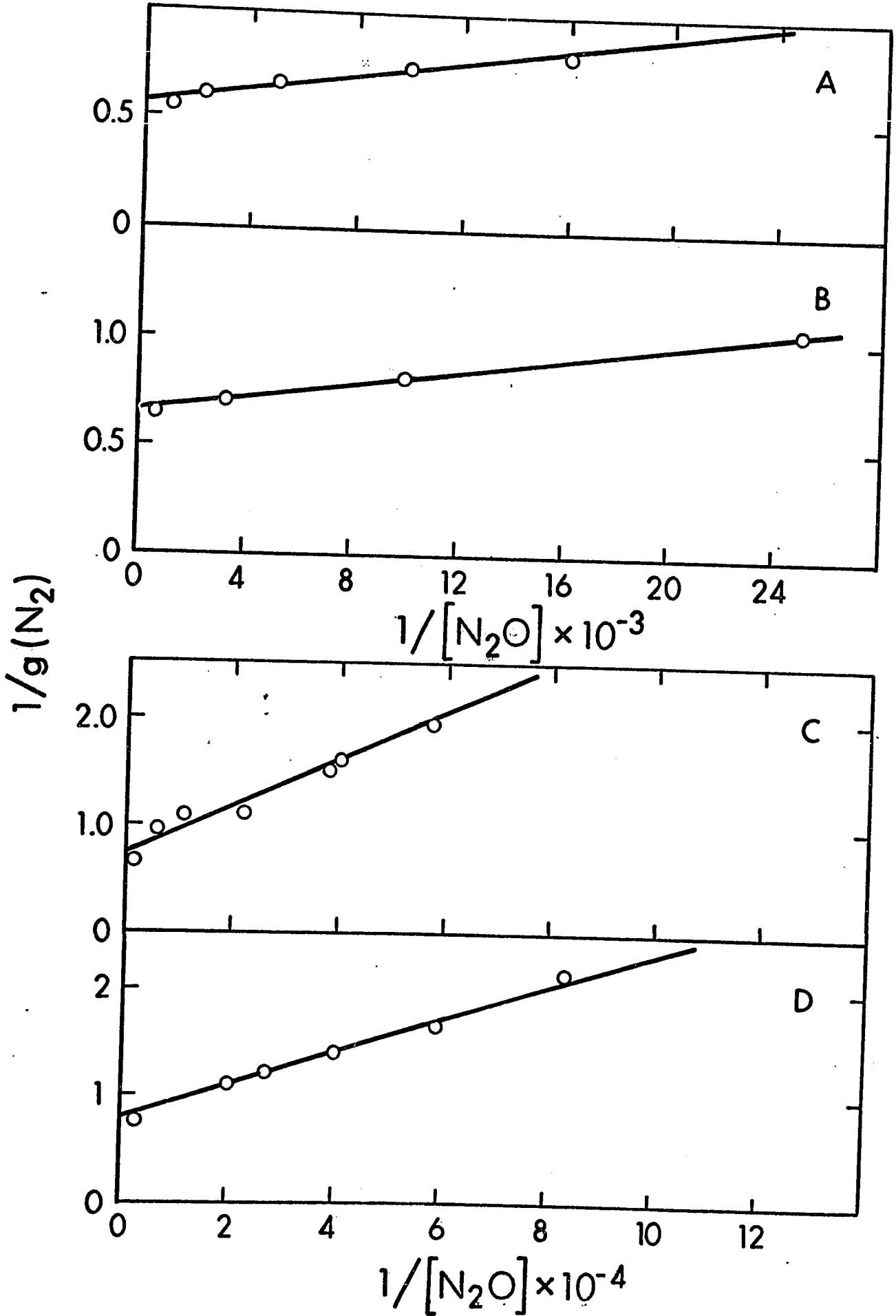
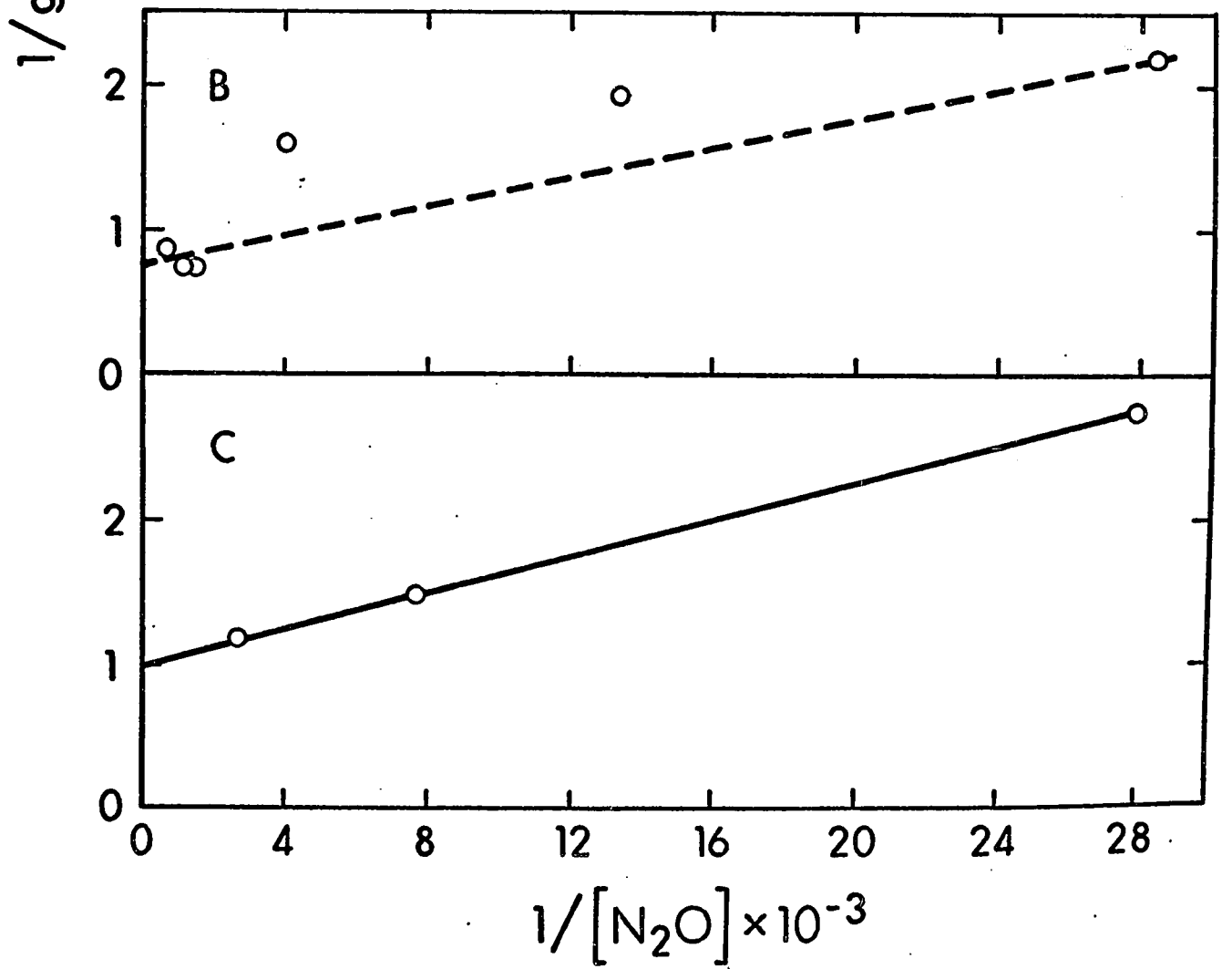
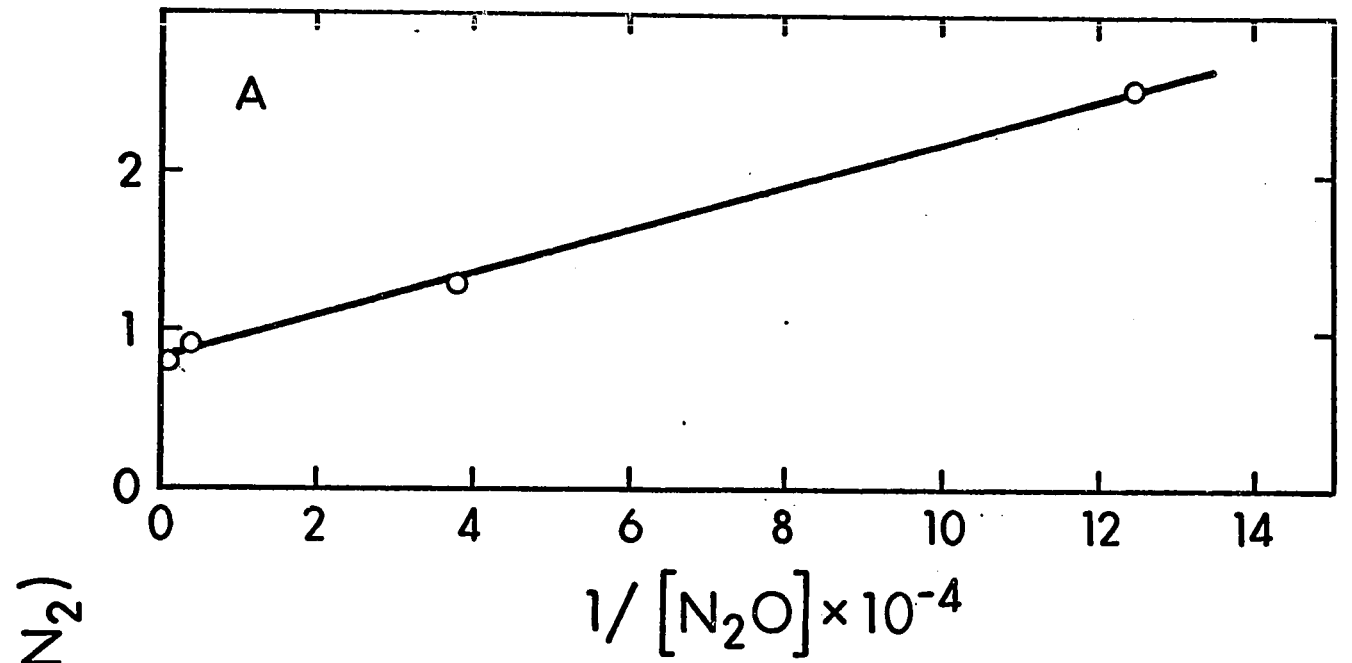


FIGURE IV-6

Plots of  $1/g(N_2)$  against  $1/[N_2O]$  for isopropanol.

- A,  $-85^\circ$ ;
- B,  $25^\circ$ , the dashed curve has been drawn in such a way that the value of  $G(e^-_{\text{solv}})$  obtained from the intercept equals that from model calculation.
- C,  $140^\circ$



iso-propanol (see Figs. IV-7 to IV-13). So, the value of  $g(\text{total ionization})$  was not obtained experimentally. Alder and Bothe (130) measured the  $W$  values for ethanol and iso-propanol vapours and obtained  $W = 25.1$  and  $24.2$  eV which correspond to  $G(e^-)_{\text{total}} = 4.0$  and  $4.1$  respectively. Their measured  $W$  values for several compounds are 1 to 2 eV greater than those obtained by other workers (121,131). So, on the basis of our n-propanol results, we assume the value of  $G(e^-)_{\text{total}} = 4.3$  both in ethanol and iso-propanol, which agrees well with corresponding gas phase values. This value was used in equation (Ai) and (Aiv) for all temperatures.

Densities and dielectric constants of ethanol and iso-propanol at each temperature must be known for the kinetics calculations. They are reported in Tables IV-12 and IV-13 respectively.

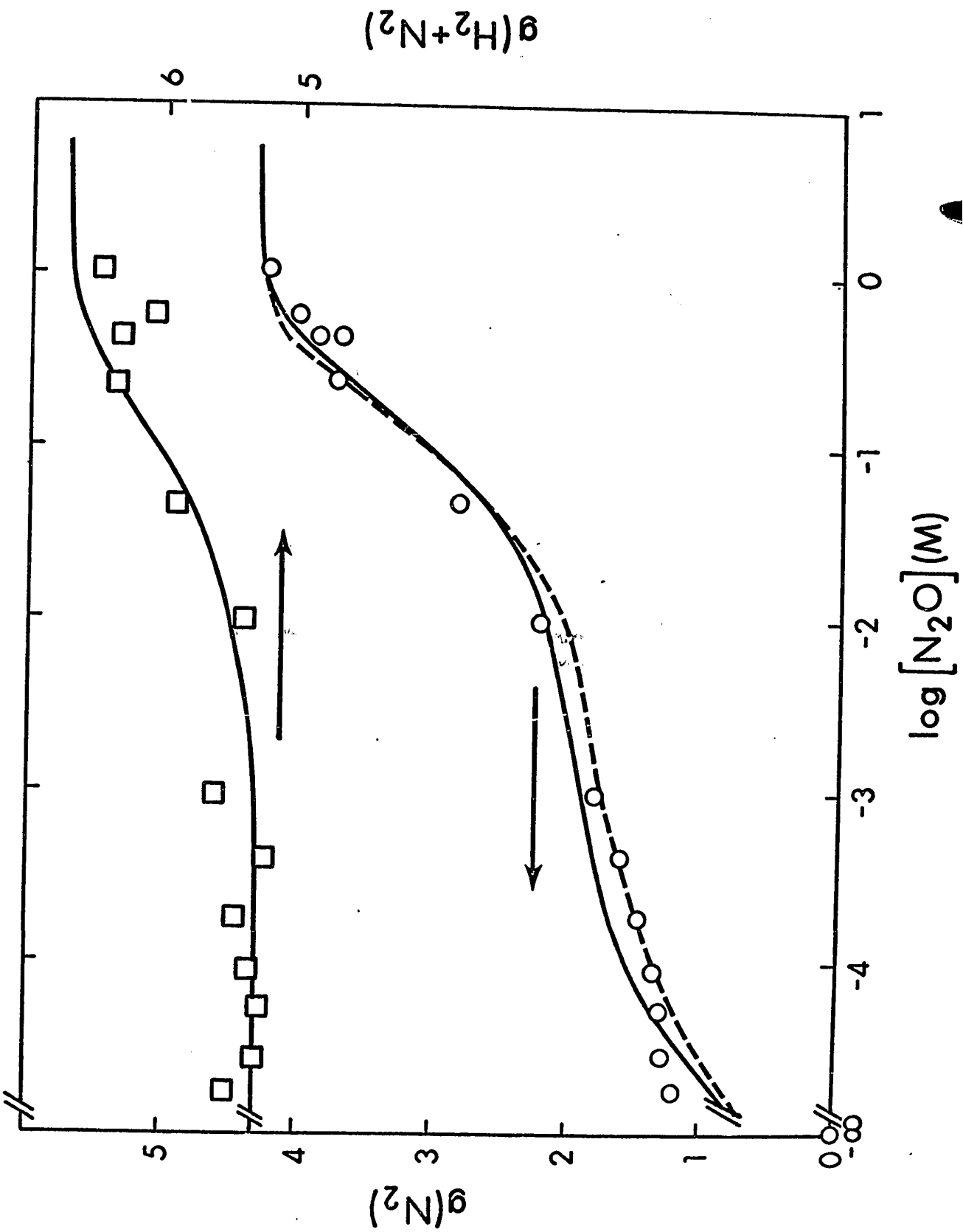
The adjustable parameter used in fitting the model to the nitrogen yields was  $\beta_*$ , and the best values are represented in Tables IV-12 and IV-13.

The results of the calculations of the one-adjustable-parameter treatment are represented by the full lines through the nitrogen yields in Figs. IV-7 to IV-10 (in ethanol) and Figs. IV-11 to IV-13 (in iso-propanol). The calculated curves are little high in the homogeneous kinetics regions at the lowest temperatures used (Figs. IV-7 and IV-11). The reason for the lack of agreement has been discussed in sections A and B. To obtain better agreement between

FIGURE IV-7

The effect of nitrous oxide concentration at  $-112^{\circ}$  in ethanol.

O, N<sub>2</sub> and  $\square$ , (H<sub>2</sub> + N<sub>2</sub>) from nitrous oxide solutions, corrected for direct radiolysis of nitrous oxide. The solid and broken lines through the nitrogen yields were calculated by the 1AP and 2AP treatments, respectively (See Table IV-12). The line through the (H<sub>2</sub> + N<sub>2</sub>) points is the sum of the N<sub>2</sub> and H<sub>2</sub> (Fig. IV-16) calculated curves.



$g(H_2+N_2)$

FIGURE IV-8

The effect of nitrous oxide concentration at 25° in ethanol.

O, N<sub>2</sub> and  $\square$ , (H<sub>2</sub> + N<sub>2</sub>) from nitrous oxide solutions, corrected for direct radiolysis of nitrous oxide. The line through the nitrogen yields was calculated by the LAP treatment (see Table IV-12). The line through the (H<sub>2</sub> + N<sub>2</sub>) points is the sum of the N<sub>2</sub> and H<sub>2</sub> (Fig. IV-16) calculated curves.

$g(\text{H}_2 + \text{N}_2)$

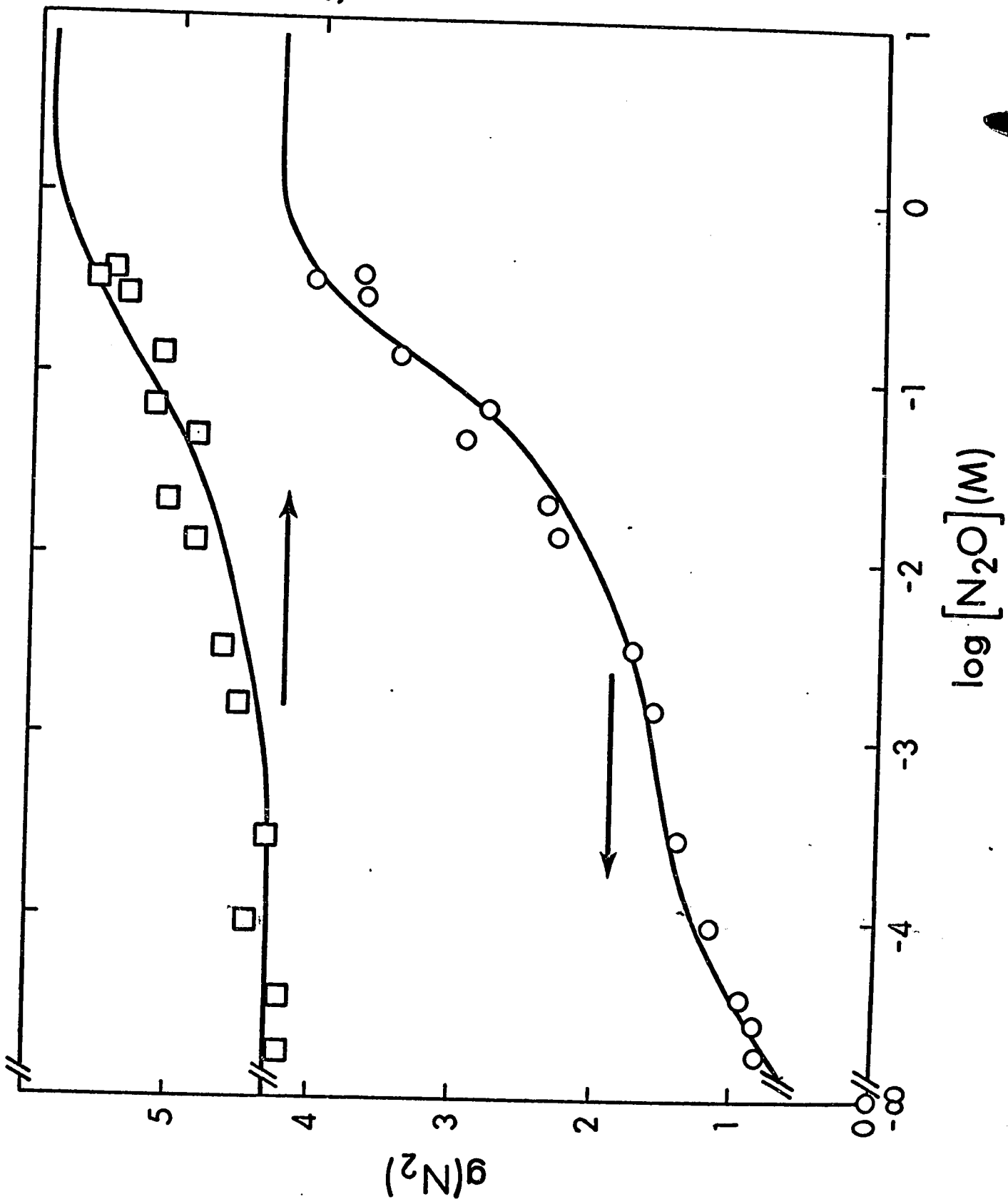


FIGURE IV-9

The effect of nitrous oxide concentration  
at 90° in ethanol.

O, N<sub>2</sub> and □, (H<sub>2</sub> + N<sub>2</sub>) from nitrous oxide  
solutions, corrected for direct radiolysis  
of nitrous oxide. The line through the  
nitrogen yields was calculated by the LAP  
treatment (see Table IV-12). The line through  
the (H<sub>2</sub> + N<sub>2</sub>) points is the sum of the N<sub>2</sub> and H<sub>2</sub>  
(Fig. IV-16) calculated curves.

$g(\text{H}_2 + \text{N}_2)$

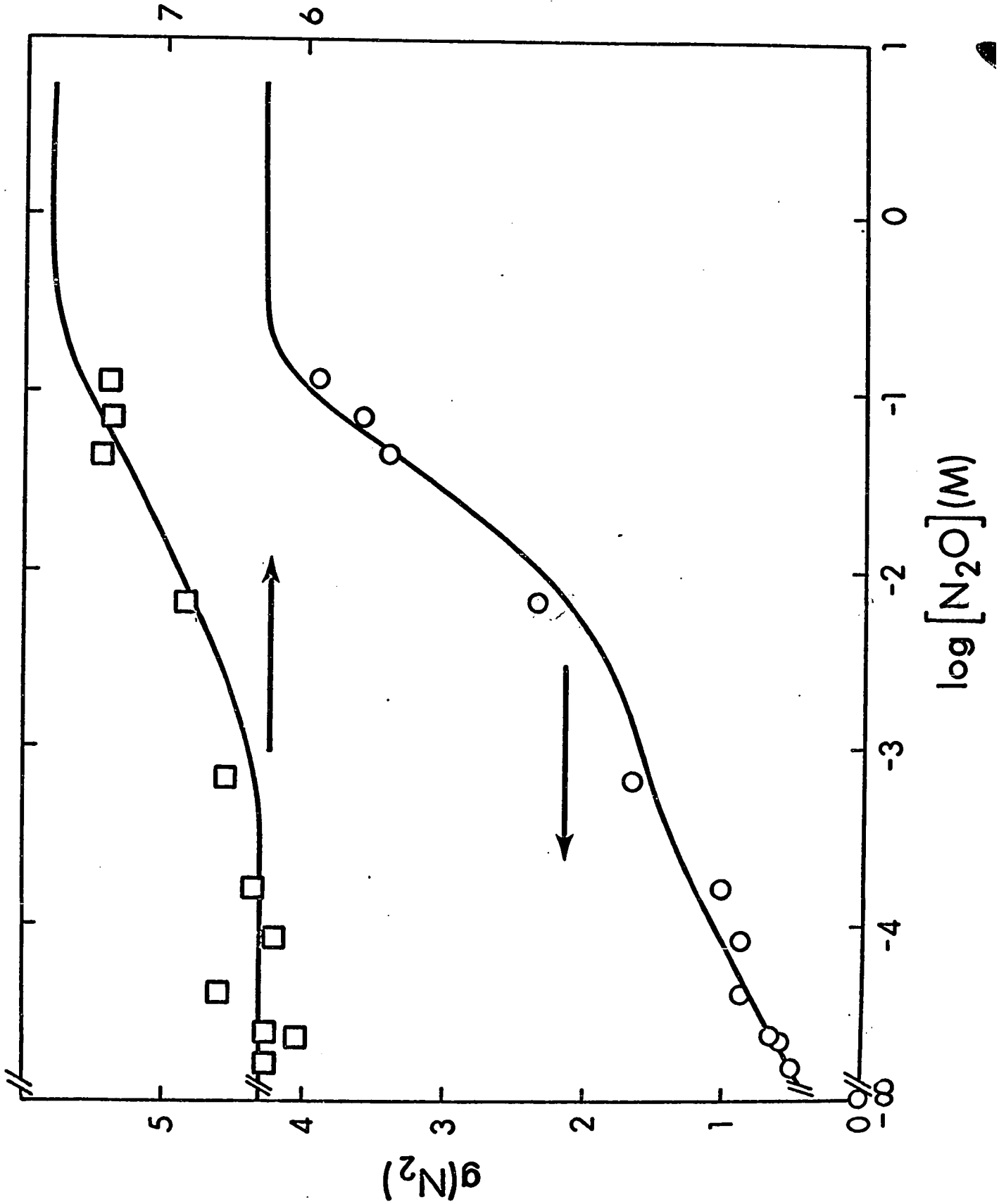


FIGURE IV-10

The effect of nitrous oxide concentration  
at 145° in ethanol.

O, N<sub>2</sub> and □, (H<sub>2</sub> + N<sub>2</sub>) from nitrous oxide  
solutions, corrected for direct radiolysis  
of nitrous oxide. The line through the  
nitrogen yields was calculated by the LAP  
treatment (see Table IV-12). The line through  
the (H<sub>2</sub> + N<sub>2</sub>) points is the sum of the N<sub>2</sub> and  
H<sub>2</sub> (Fig. IV-16) calculated curves.

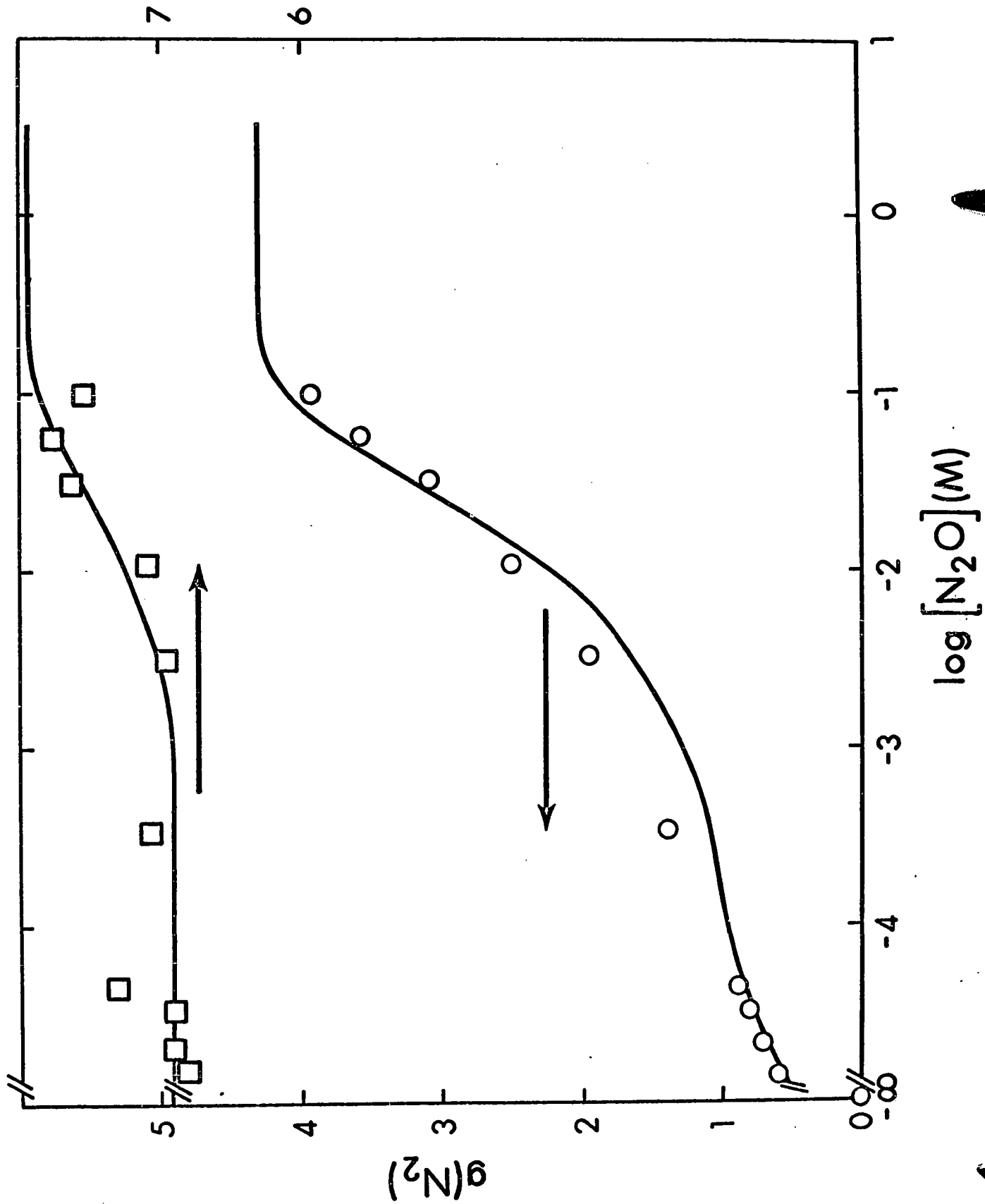


FIGURE IV-11

The effect of acid or nitrous oxide concentration at  $-85^{\circ}$  in iso-propanol.

O,  $N_2$  and  $\square$ ,  $(H_2 + N_2)$  from nitrous oxide solutions, corrected for direct radiolysis of nitrous oxide;  $\Delta$ ,  $H_2$  in the presence of HCl, corrected for the direct radiolysis of the acid. S is  $N_2O$  or  $i\text{-PrOH}_2^+$ . The solid and broken lines through the nitrogen yields were calculated by the 1AP and 2AP treatments, respectively (see Table IV-13). The line through the  $(H_2 + N_2)$  points is the sum of the  $N_2$  and  $H_2$  (Fig. IV-17) calculated curves.

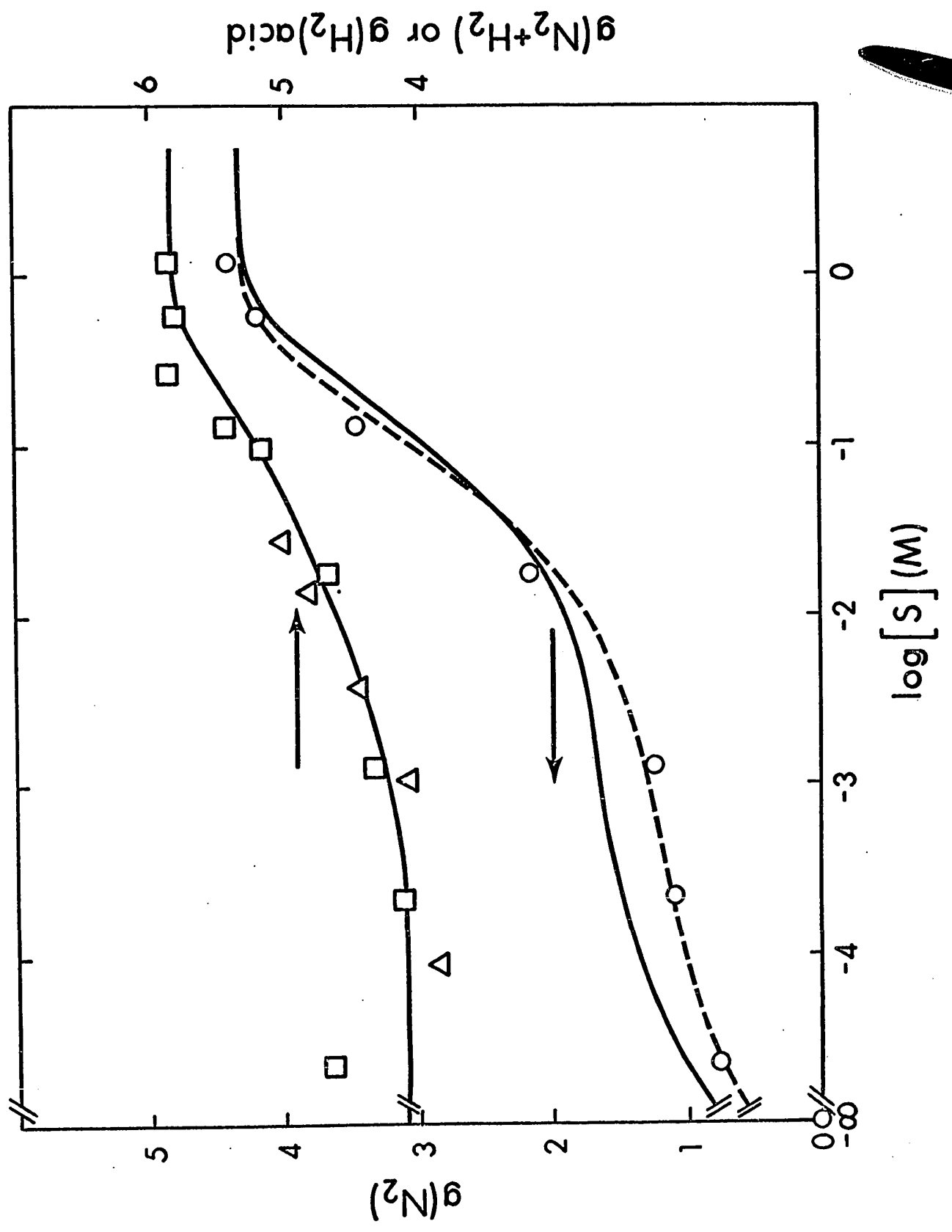


FIGURE IV-12

The effect of acid or nitrous oxide concentration at 25° in iso-propanol.

O, N<sub>2</sub> and □, (H<sub>2</sub> + N<sub>2</sub>) from nitrous oxide solutions, corrected for direct radiolysis of nitrous oxide; Δ, H<sub>2</sub> in the presence of HCl, corrected for the direct radiolysis of the acid. S is N<sub>2</sub>O or i-PrOH<sub>2</sub><sup>+</sup>. The line through the nitrogen yields was calculated by the LAP treatment (see Table IV-13). The line through the (H<sub>2</sub> + N<sub>2</sub>) points is the sum of the N<sub>2</sub> and H<sub>2</sub> (Fig. IV-17) calculated curves.

$g(N_2+H_2)$  or  $g(H_2)$  acid

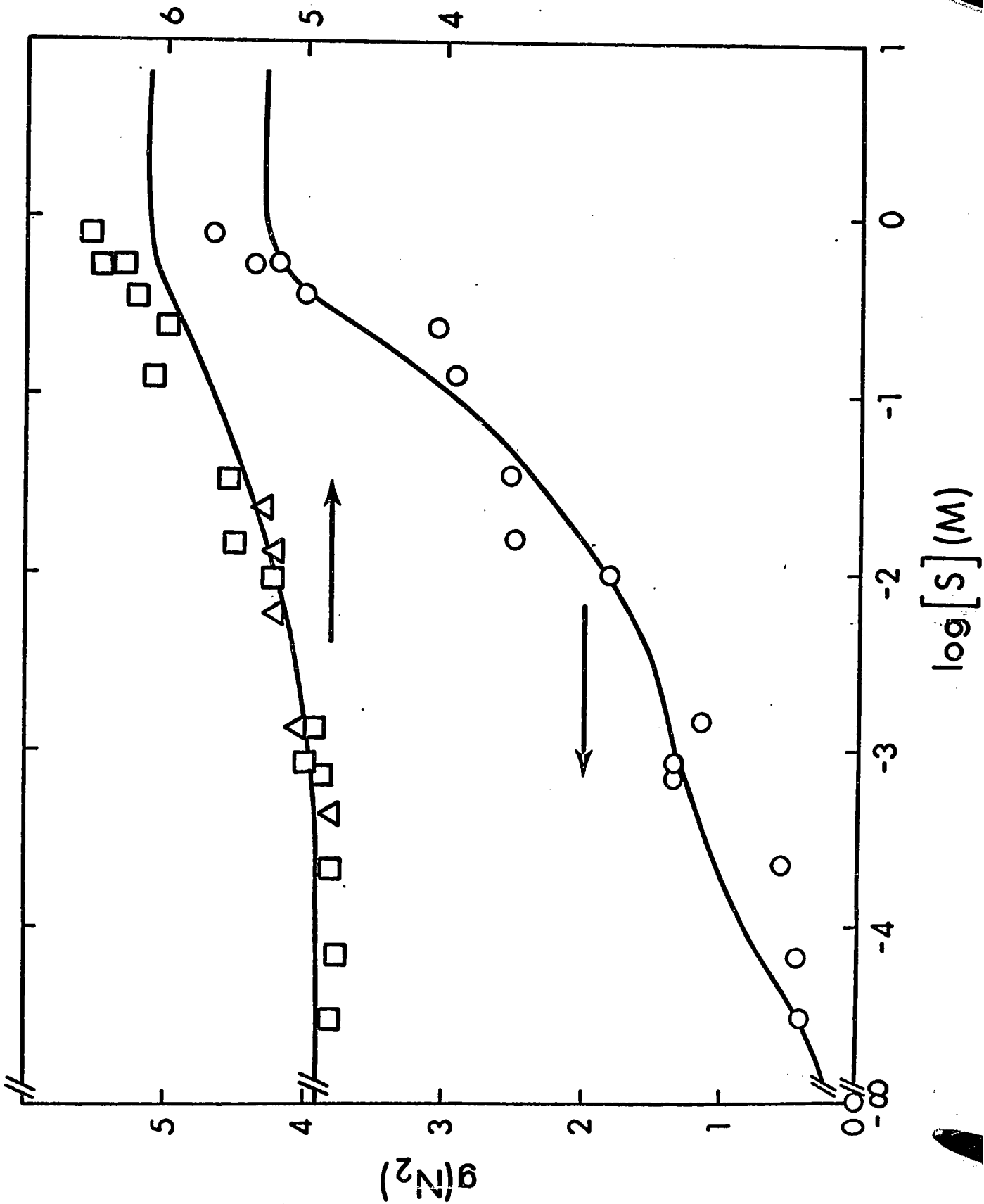
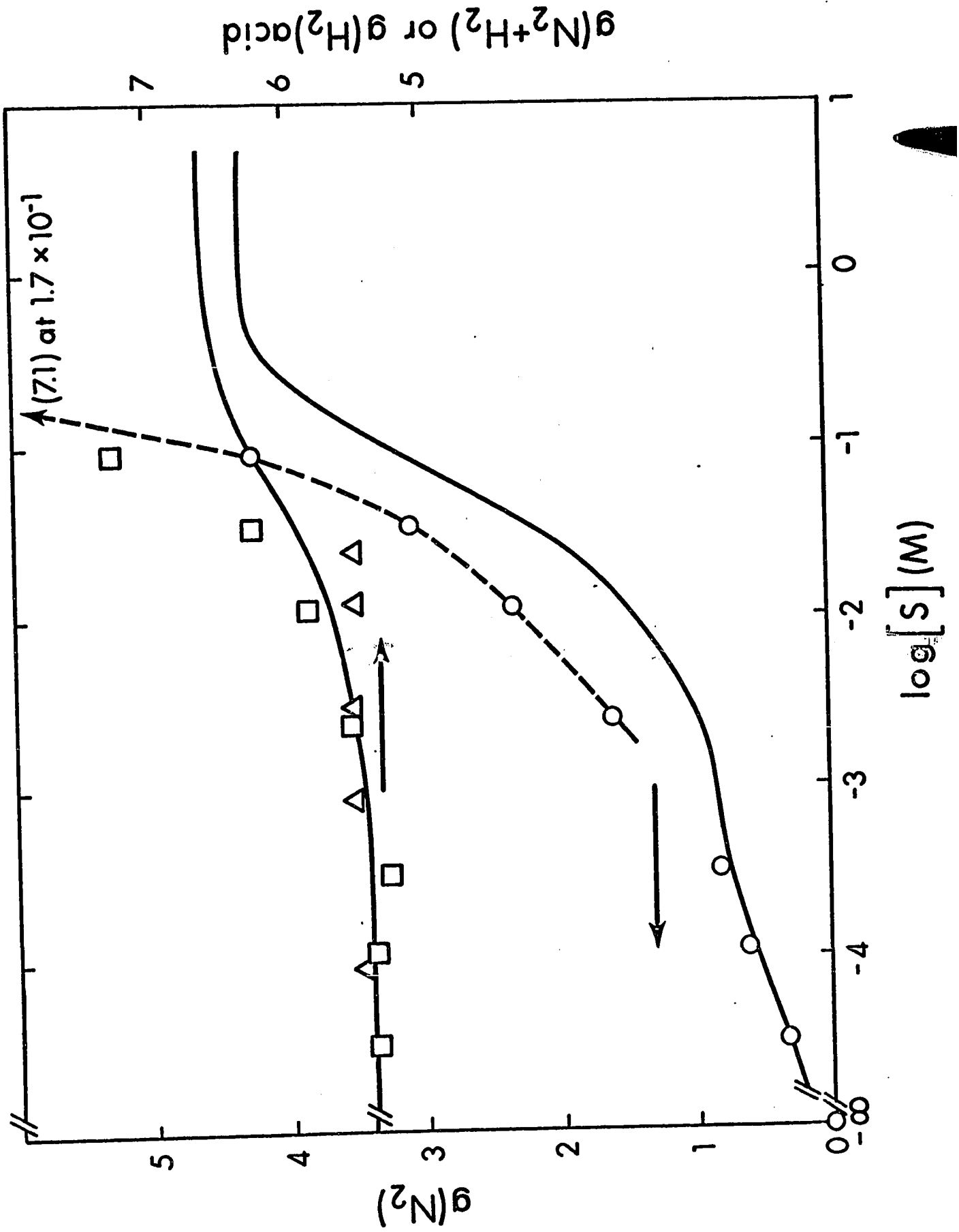


FIGURE IV-13

The effect of acid or nitrous oxide concentration at 140° in iso-propanol.

O, N<sub>2</sub> and □, (H<sub>2</sub> + N<sub>2</sub>) from nitrous oxide solutions, corrected for direct radiolysis of nitrous oxide; Δ, H<sub>2</sub> in the presence of HCl, corrected for the direct radiolysis of the acid. S is N<sub>2</sub>O or i-PrOH<sub>2</sub><sup>+</sup>. The line through the nitrogen yields was calculated by the LAP treatment (see Table IV-13). The line through the (H<sub>2</sub> + N<sub>2</sub>) (Fig. IV-17) calculated curves.



calculation and experiment, a second adjustable parameter is needed and, as in methanol and n-propanol, the complex dielectric constant is used.

The activation energy  $E_T$ , 4.4 kcal/mole, for dielectric relaxation in ethanol, has been estimated from the Arrhenius plot in Fig. IV-14A. The activation energy for viscous flow in ethanol is 3.3 kcal/mole (123) and that for self diffusion is 4.6 kcal/mole (123). These values along with others are reported in Table IV-14. The activation energy for the migration of the radiolytic ions probably equals the activation energy for self diffusion, 4.6 kcal/mole. Since the activation energy for the dielectric relaxation time approximately equals that for the migration of the radiolytic ions, the effect of temperature on  $\tau$  and  $t_{gn}$  will be about the same. Thus the effect of decreasing temperature is expected to be very small, if at all, on the calculated value of  $G(e^-_{solv})_{fi}$ . This is substantiated by the fact that the calculated and experimental values of  $G(e^-_{solv})_{fi}$  differ only by 10% at  $-112^\circ$ .

On the same basis as in ethanol, considering the activation energies for different processes in iso-propanol (see Table IV-15), it appears that the value of  $\tau$  increases more rapidly with decreasing temperature than does that of  $t_{gn}$ . So, the lack of complex dielectric relaxation could be the cause of the crudely calculated value of  $G(e^-_{solv})_{fi}$  being 25% too high at  $-85^\circ$ .

FIGURE IV-14

- A. Arrhenius plots for dielectric relaxation  
in ethanol and iso-propanol.  
O, ethanol;  $\square$ , iso-propanol.
- B. Arrhenius plot of  $[G(H_2)_{t^\circ} - G(H_2)_{-85^\circ}]$   
in iso-propanol.

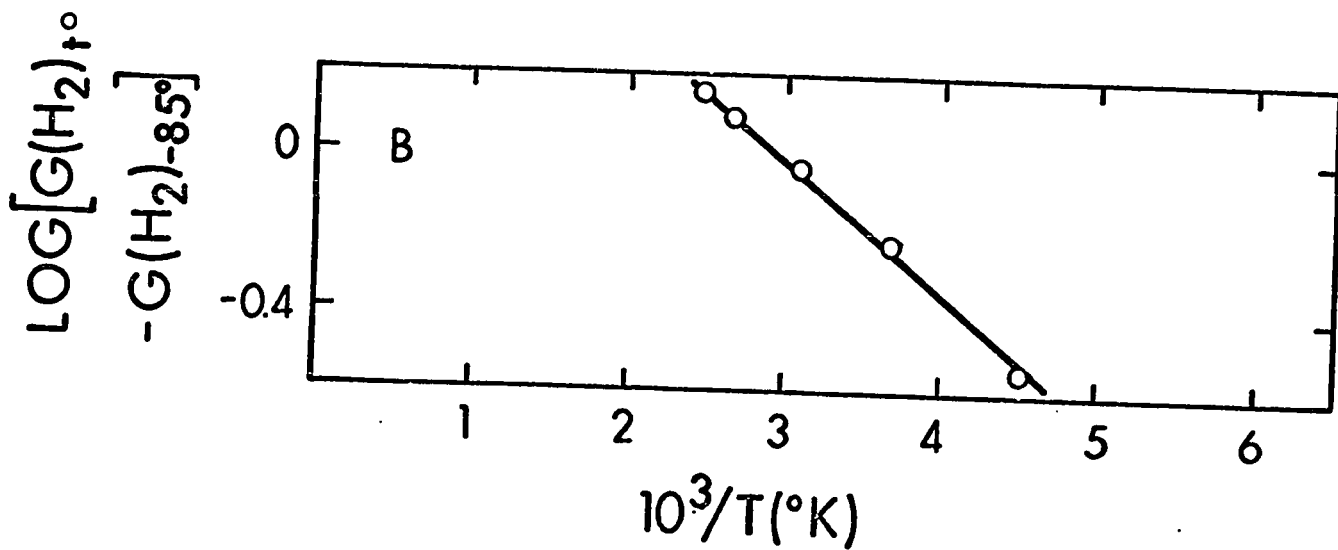
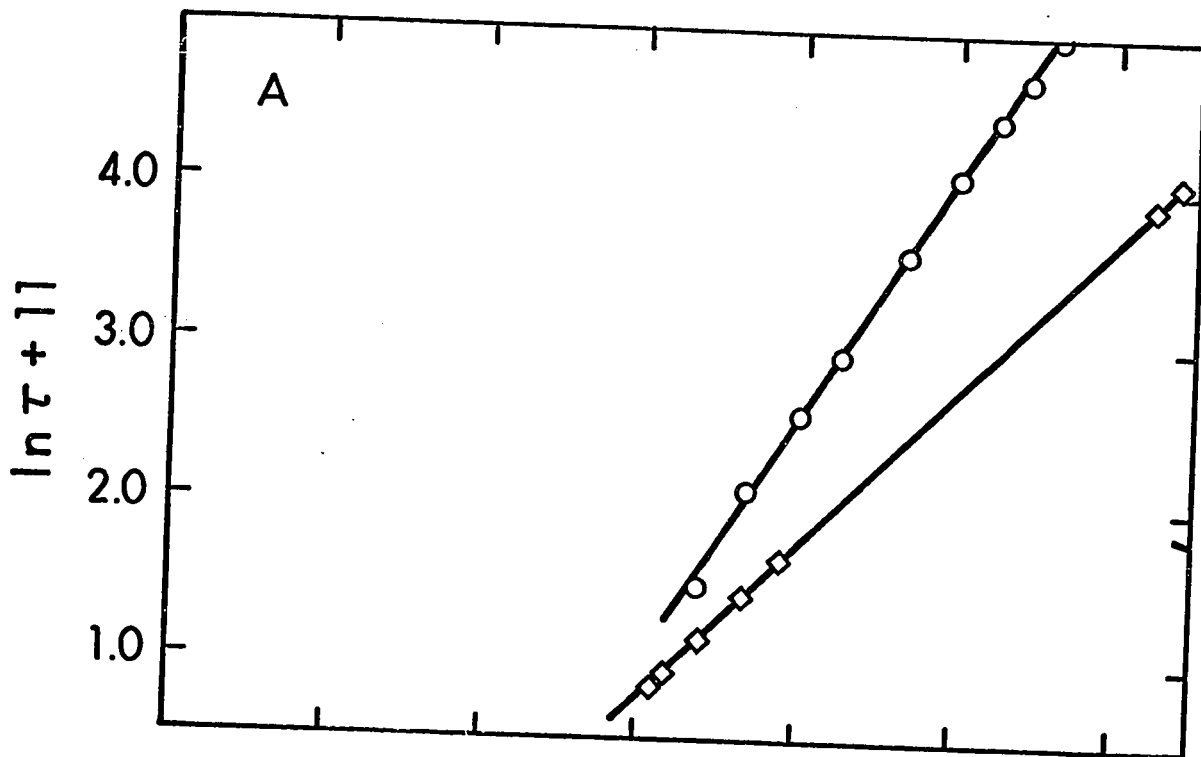


TABLE IV-14

Some Relevant Data for Ethanol

t(°C)	$\tau_{\text{sec}}$ <sup>a</sup>	$E_T$ <sup>b</sup> kcal/mole	E <sub>self</sub> diffusion kcal/mole	E <sub>viscous</sub> flow kcal/mole	E <sub>75</sub> <sup>-</sup> E <sub>85</sub> kcal/mole	E <sub>self</sub> diff <sup>+</sup> (E <sub>75</sub> <sup>-</sup> E <sub>85</sub> )
-112	$7.5 \times 10^{-8}$	4.4	4.6	3.3	0.0	4.6
+25	$1.3 \times 10^{-10}$					
90	$3.4 \times 10^{-11}$					
145	$1.6 \times 10^{-11}$					

a. Calculated from data in Ref. (122).

b. Estimated from the Arrhenius plot in Fig. IV-14A.

TABLE IV-15

Some Relevant Data for iso-Propanol

t(°C)	$\tau$ sec	$E_t^a$ kcal/mole	$E_t^b$ kcal/mole	Self diffusion kcal/mole	Viscous flow k/cal mole	$E_{75}^{E_{85}}$ kcal/mole	$E_{self\ diff}^+(E_{75}^{E_{85}})$
-85	$2.9 \times 10^{-7}$	6.9	5.3	5.3	0.0	5.3	5.3
+25	$2.5 \times 10^{-10}$						
140	$2.1 \times 10^{-11}$						

a. Calculated from data in Ref. (122).

b. Estimated from the Arrhenius plot in Fig. IV-14A.

\_\_\_\_\_ 18

(b) Two-Adjustable-Parameters Treatment

This treatment was applied in the same way as discussed in sections A and B for methanol and n-propanol respectively.

The time averaged values of the complex dielectric constants were calculated by using equation (IV-iv). It will suffice here to indicate the magnitude of the effect required to reduce the calculated values of  $G(e^-_{\text{solv}})_{fi}$  from 1.9 to 1.7 at  $-112^\circ$  in ethanol and from 1.6 to 1.2 at  $-85^\circ$  in iso-propanol. In ethanol, for ion pairs with  $y = 15 \text{ \AA}$ ,  $\tau/t_{gn} = 0.13$ ; for  $y = 17 \text{ \AA}$ ,  $\tau/t_{gn} = 0.10$ ; and for  $y = 20 \text{ \AA}$ ,  $\tau/t_{gn} = 0.05$ . In iso-propanol, for ion pairs with  $y = 15 \text{ \AA}$ ,  $\tau/t_{gn} = 0.32$ ; for  $y = 18 \text{ \AA}$ ,  $\tau/t_{gn} = 0.17$ ; and for  $y = 21 \text{ \AA}$ ,  $\tau/t_{gn} = 0.10$ .

The values of  $\epsilon_{\text{ave}}$  obtained from equation (IV-iv), and which gave the correct values of  $G(e^-_{\text{solv}})_{fi}$  when used in model calculations, were then used to calculate the nitrogen yields. The  $N(y)$  spectra and values of  $\epsilon_{\text{ave}}$  are listed in Tables IV-16 and IV-17 for ethanol and iso-propanol respectively.

The above refinement of the kinetics model led to the dashed curves in Figs. IV-7 and IV-11. The appropriate values of  $\beta_-$  are reported under the heading 2AP in Tables IV-12 and IV-13.

As in n-propanol, the two-adjustable-parameters treatment was not applied to the high temperature systems

TABLE IV-16

N(y) Spectra and Values of  $\epsilon_{ave}$  in Ethanol at  
Different Temperatures

N(y)	<u>-112°</u>		<u>25°</u>		<u>90°</u>		<u>145°</u>	
	<u>y(Å)</u>	<u><math>\epsilon_{ave}</math></u>	<u>y(Å)</u>	<u><math>\epsilon_{ave}</math></u>	<u>y(Å)</u>	<u><math>\epsilon_{ave}</math></u>	<u>y(Å)</u>	<u><math>\epsilon_{ave}</math></u>
2150	15	50	17	24.6	19	16	20	10.2
1100	17	52	20	24.6	21	16	22	10.2
600	20	56	23	24.6	25	16	26	10.2
476	28	60	32	24.6	35	16	36	10.2
270	48	60	54	ditto	58	ditto	62	ditto
116	78	60	88		95		100	
64	113	60	127		138		146	
41	152	60	171		186		196	
28	196	60	221		240		253	
155	>200	60	>250		>300		>300	

$\Sigma N(y) = 5000$

TABLE IV-17

N(y) Spectra and Values of  $\epsilon_{ave}$  in iso-Propanol  
at Different Temperatures

N(y)	<u>-85°</u>		<u>25°</u>		<u>140°</u>	
	<u>y(Å)</u>	<u><math>\epsilon_{ave}</math></u>	<u>y(Å)</u>	<u><math>\epsilon_{ave}</math></u>	<u>y(Å)</u>	<u><math>\epsilon_{ave}</math></u>
2150	15	26.0	17	19.4	20	7.0
1100	18	32.5	20	19.4	23	7.0
600	21	36.0	23	19.4	28	7.0
476	29	41.5	32	19.4	38	7.0
270	48	41.5	54	19.4	64	7.0
116	79	41.5	89	ditto	105	ditto
64	114	41.5	128		152	
41	154	41.5	172		204	
28	199	41.5	223		264	
155	>250	41.5	>300		>300	

$\Sigma N(y) = 5000$

because satisfactory results were obtained with one-adjustable-parameter.

It is observed that in the case of iso-propanol the agreement between calculated and experimental values of  $g(N_2)$  is not satisfactory at  $140^\circ$  (Fig. IV-13). This may be because of two reasons. Firstly, the value of  $G(e^-_{\text{solv}})_{fi}$  at  $140^\circ$  from the homogeneous kinetics plot is 1.0, while the value from the model calculation is 0.8. The latter value was used in the kinetics calculations. Secondly nitrogen is formed by a secondary reaction (reaction [57] to [62], see Introduction p. 33 ). The values of  $g(N_2)$  are so scattered that an attempt to correct the secondary reaction of nitrous oxide was not made.

It is worth commenting on the way Russell and Freeman applied a correction to the experimental nitrogen yields in iso-propanol (25). This was done by subtracting from  $g(N_2)$  the difference between  $g(H_2 + N_2)$  from nitrous oxide solutions and  $g(H_2)$  from hydrochloric acid solutions at the same concentrations. They assumed that at the lower temperature in the presence of hydrochloric acid,  $g(H_2)$  did not exceed 5.5, as it did not at  $140^\circ$ . This assumption appears to be erroneous because of the fact that a high concentration of hydrochloric acid at high temperatures has been found to lower the hydrogen yield (25,132). It is expected that in the concentrated sulfuric acid solutions the hydrogen yield,  $g(H_2)$ , will be greater than 5.5.

## 2. Hydrogen Yields.

Evidently a small amount of electron scavenger remained in the purified ethanol and iso-propanol used by Russell and Freeman (24,25). Apparently this is the reason for their difference in  $G(H_2)$  from pure alcohols and  $g(H_2 + N_2)$  from nitrous oxide solutions below  $10^{-3}$  M, where the scavenging of free ion solvated electrons is complete and scavenging in the spurs is negligible. The values of  $G(H_2)$  in absolutely pure alcohols were estimated in the same way as in methanol and n-propanol in sections A and B respectively. In ethanol these values are  $G(H_2)_0 = 5.3$  at  $-112^\circ$  and  $25^\circ$ ,  $6.3$  at  $90^\circ$  and  $6.9$  at  $145^\circ$  (see Figs. IV-7 to IV-10 and Table IV-18). In iso-propanol these values are  $G(H_2)_0 = 4.1$  at  $-85^\circ$ ,  $4.9$  at  $25^\circ$  and  $5.4$  at  $140^\circ$  (see Figs IV-11 to IV-13 and Table IV-19). The estimated yields as a function of temperature are represented by the dashed curves in Figs. IV-15A and IV-15B for ethanol and iso-propanol respectively.

The reaction of the electron scavenging impurity in ethanol appears to become slightly more efficient as the temperature increases while the reverse seems to be true in the case of iso-propanol. Kinetic analysis of the results in Fig. IV-15A and B indicates that  $(E_{79} - E_{75})$  is about  $+1$  kcal/mole in ethanol and  $-1$  kcal/mole in iso-propanol. The value was  $-1$  kcal/mole in methanol and  $+1$  kcal/mole in n-propanol. The positive values in ethanol and n-propanol might be erroneous because the results might be affected by the apparent existence of a species X in these alcohols;

TABLE IV-18

Relevant Data for the Calculation of the Hydrogen Yields in Ethanol

t(°C)	G(H <sub>2</sub> ) <sub>o</sub>	g(H <sub>2</sub> ) <sub>min</sub> <sup>c</sup>	<sup>a</sup> IAP		<sup>b</sup> 2AP			
			G(H <sub>2</sub> ) <sub>fi</sub> <sup>d</sup>	G(H <sub>2</sub> ) <sub>73</sub> <sup>c</sup>	k <sub>73</sub> /k <sub>74</sub> <sup>c</sup>	G(H <sub>2</sub> ) <sub>fi</sub> <sup>d</sup>	G(H <sub>2</sub> ) <sub>73</sub> <sup>c</sup>	k <sub>73</sub> /k <sub>74</sub> <sup>c</sup>
-112	5.3	2.4	1.9	1.0	0.7	1.7	1.2	0.9
+25	5.3	2.6	1.6	1.1	0.7	---	---	---
90	6.3	3.5	1.4	1.4	0.9	---	---	---
145	6.9	3.6	1.1	2.2	2.2	---	---	---

- a. One-adjustable-parameter treatment.
- b. Two-adjustable-parameters treatment.
- c. Estimated by the same method as illustrated in Appendix B.
- d. G(H<sub>2</sub>)<sub>fi</sub> = G(e<sup>-</sup><sub>solv</sub>)<sub>fi</sub>. Values taken from Table IV-12.

TABLE IV-19

Relevant Data for the Calculation of the Hydrogen Yields in iso-Propanol

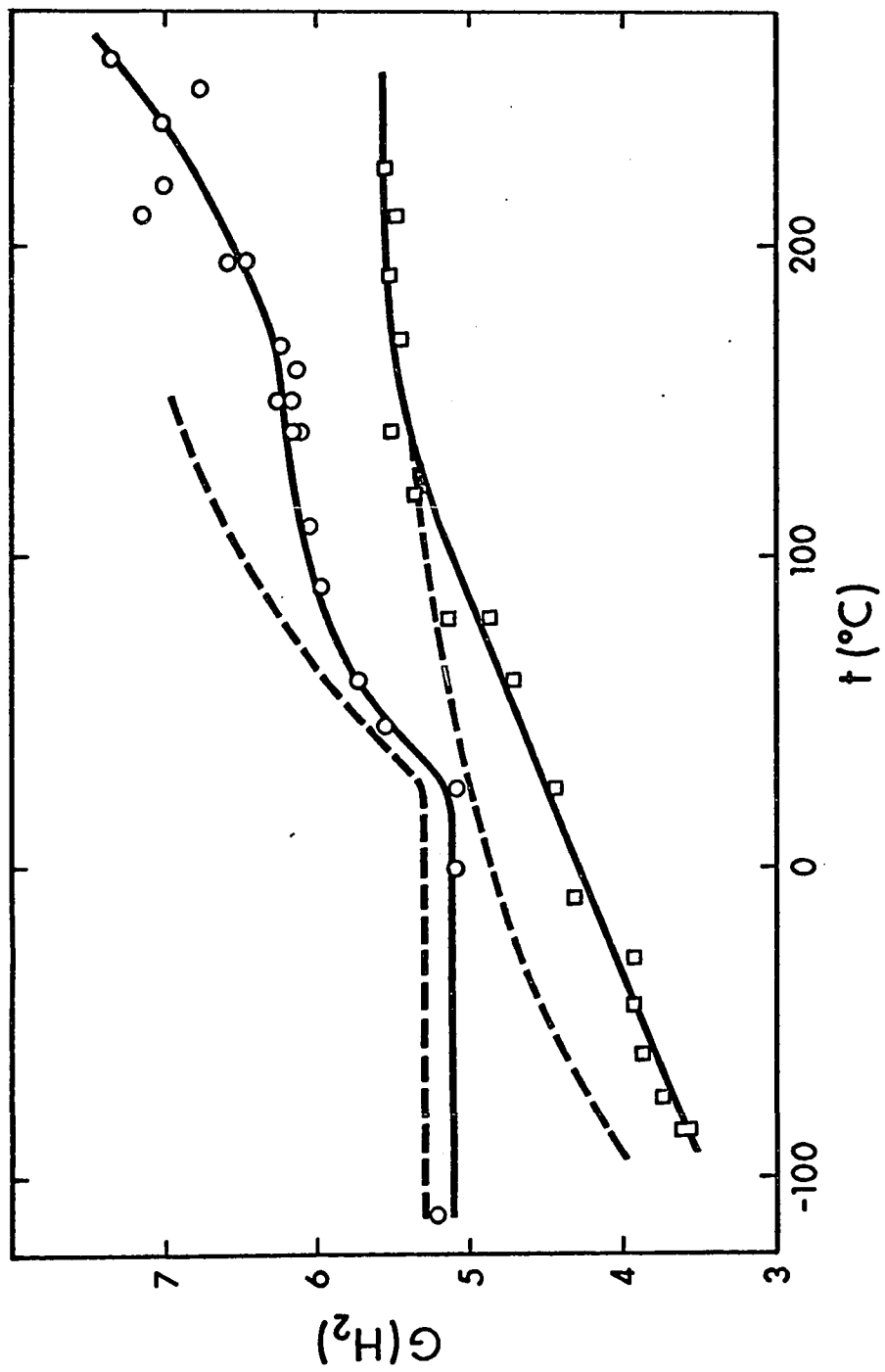
t(°C)	a		b					
	LAP	2AP	C					
	$G(H_2)_o$	$g(H_2)_{min}$	$G(H_2)_{73}$	$G(H_2)_{73}$	$k_{73}/k_{74}$	$k_{73}/k_{74}$		
-85	4.1	1.5	1.6	1.0	0.6	1.2	1.4	0.8
+25	4.9	1.8	1.3	1.8	1.5	---	---	---
140	5.4	2.3	0.8	2.3	1.9	1.0	2.1	1.8

- a. One-adjustable-parameter treatment
- b. Two-adjustable-parameters treatment
- c. Estimated by the same method as illustrated in Appendix B.
- d.  $G(H_2)_{fi} = G(e^-_{solv})_{fi}$ . Values taken from Table IV-13.

FIGURE IV-15

The yield of hydrogen as a function of temperature in ethanol and iso-propanol.

- A. O, purified ethanol; -----, estimated values for absolutely pure ethanol.
- B. □, purified iso-propanol; ----, estimated values for absolutely pure iso-propanol.



there is no species X in methanol or iso-propanol.

The ratio  $k_{85}/k_{75}$  seems to be independent of temperature in ethanol and iso-propanol (see Tables IV-12 and IV-13), so  $E_{85} = E_{75}$ .

To further check the model, the hydrogen yields from the nitrous oxide solutions were calculated as a function of nitrous oxide concentration. The calculations for both ethanol and iso-propanol are similar to those for methanol and n-propanol discussed in sections A and B respectively. According to the proposed mechanism, all free ion solvated electrons ultimately form hydrogen, but only a fraction equal to  $k_{73}/k_{74}$  of the electrons that undergo geminate neutralization lead to hydrogen formation. The values of  $k_{73}/k_{74}$  are reported in Tables IV-18 and IV-19 along with other relevant data for ethanol and iso-propanol respectively.

The hydrogen yields calculated from the one-adjustable-parameter treatment are represented by the full curves in Figs. IV-16 (ethanol) and IV-17 (iso-propanol). The results of the two-adjustable-parameters calculations are represented by the dashed curves in Figs. IV-16 (ethanol at  $-112^{\circ}$ ) and IV-17 (iso-propanol at  $-85^{\circ}$ ).

### 3. Effect of Temperature on the Hydrogen Forming Reactions

The yields of free ions in ethanol and iso-propanol vary slightly with temperature. This variation may be

FIGURE IV-16

The yield of hydrogen as a function of nitrous oxide concentration in ethanol.

□ , 145°; X, 90°; O, 25° and Δ, -112°.

The solid and broken lines were calculated by the 1AP and 2AP treatments, respectively (see Tables IV-12 and IV-18).

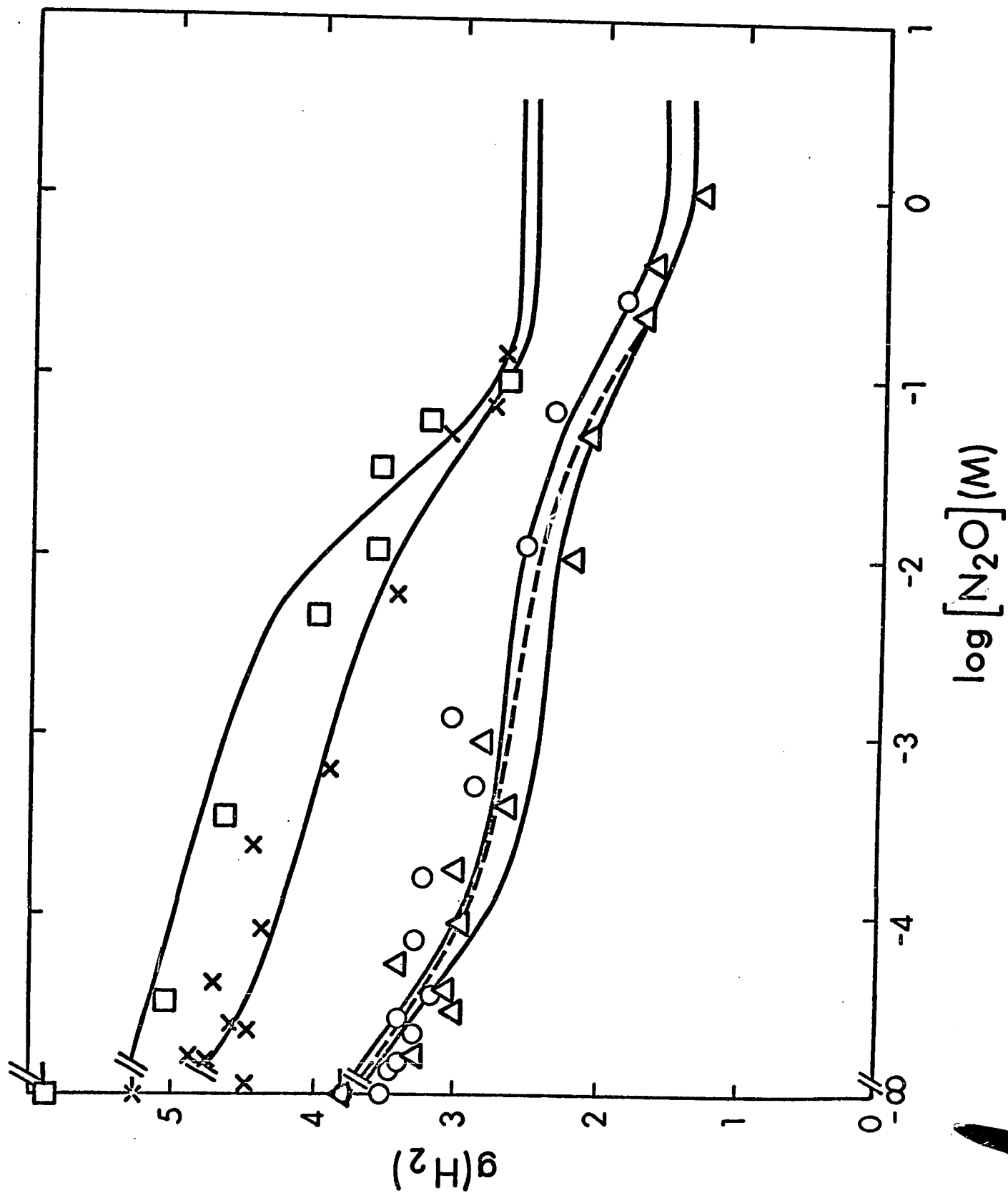
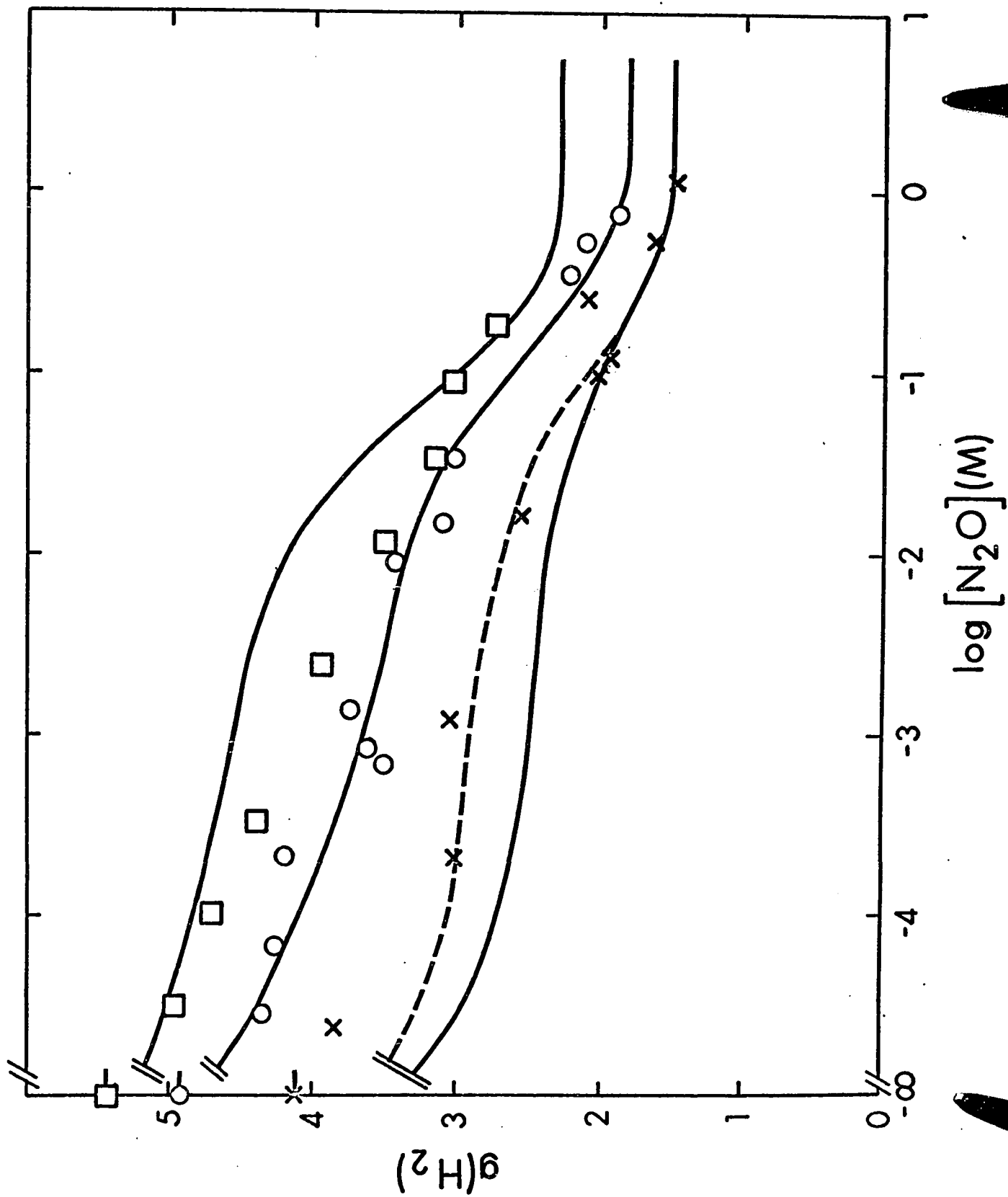


FIGURE IV-17

The yield of hydrogen as a function of nitrous oxide concentration in iso-propanol.  $\square$  , 140°; O, 25°; X, -85°. The solid and broken lines were calculated by the 1AP and 2AP treatments, respectively (see Tables IV-13 and IV-19).



understood in terms of the variation of the values of the quantities in equations (Aii) and (Aiii) in Appendix A.

The value of the ratio  $k_{73}/k_{74}$  increases from about 0.7 at 25° to 2.2 at 145° in ethanol (see Table IV-18). In the case of iso-propanol this ratio increases from 0.8 at -85° to 1.9 at 140° (see Table IV-19). Thus, over these temperature ranges the average difference between the activation energies of reactions [73] and [74] are  $(E_{73} - E_{74}) = 2.4$  kcal/mole and 0.6 kcal/mole in ethanol and iso-propanol respectively.

The yield of  $g(H_2)_{\min}$  has been attributed to reactions [68] and [78] and its temperature variation corresponds to 3.4 kcal/mole in ethanol between 25° and 90° and 0.3 kcal/mole for iso-propanol between -85° and 140°.

The presence of species Y in ethanol between 25° and 90°, as suggested by Russell and Freeman (24,132), is due to reactions [68] and [78].

The relatively small temperature dependence of the hydrogen yield, that has been attributed to reactions [68], [73] and [78] in iso-propanol as in other alcohols, seems to imply that they are caused by secondary effects, such as solvent rearrangements and "cage" effects, rather than by primary decomposition reactions of molecules or radicals. This suggestion is supported by the fact that the maximum experimentally allowed value of the activation energy of such reactions is only 1.5 kcal/mole, calculated from an

Arrhenius plot of  $[G(H_2)_{t^0} - G(H_2)_{-85^0}]$  (see Fig. IV-14B).

Reaction [85] is nearly diffusion controlled in water (18) and in methanol (72). It is assumed to be the same in ethanol and iso-propanol. Thus the activation energy of reaction [85] probably equals that of diffusion, i.e.,  $E_{85} \approx 4.6$  kcal/mole in ethanol and 5.3 kcal/mole in iso-propanol. It was pointed out earlier that  $E_{75} \approx E_{85}$  in both ethanol and iso-propanol and hence  $E_{75} \approx 4.6$  kcal/mole in ethanol and 5.3 kcal/mole in iso-propanol, which means that the activation energy for the decomposition of solvated electrons in ethanol and iso-propanol is approximately the same as that for diffusion.

The value of  $k_{75}$  at 25° in ethanol and iso-propanol can be estimated from the ratio of  $k_{85}/k_{75}$ . Using the value  $k_{85} = 5.2 \times 10^9$  l/mole sec (see Discussion Section B-7) and from the ratio  $k_{85}/k_{75}$  at 25° from Tables IV-12 ( $4.2 \times 10^4$  l/mole in ethanol) and IV-13 ( $1.7 \times 10^4$  l/mole in iso-propanol) we obtain  $k_{75} = 1.2 \times 10^5 \text{ sec}^{-1}$  in ethanol and  $k_{75} = 3.1 \times 10^5 \text{ sec}^{-1}$  in iso-propanol at 25° which correspond to half-lives of 6 and 2  $\mu$  sec at 25° in ethanol and iso-propanol respectively. It is important to mention that the viscosity of iso-propanol is double that of water and if there is any viscosity effect on  $k_{85}$ , then our estimated value of the half-life of reaction [75] will be too low.

From the values of  $k_{75}$  and  $E_{75}$ , the entropy of acti-

vation  $\Delta S_{75}^\ddagger$  can be estimated by the use of equation (IV-xi). This is found to be -21 cal/deg mole and -17 cal/deg mole in ethanol and iso-propanol respectively. These large negative values are similar to those in water, methanol and n-propanol (see Table IV-6).

In each of the liquids methanol, ethanol, n-propanol and iso-propanol, the large negative entropies seem to indicate that the transition state for the decomposition of solvated electrons in these alcohols has a relatively specific structure. This suggests that the ions  $RO^-$  are stronger solvent-structure-makers than is  $e^-_{solv}$  (23).

The degree of success of the model needs a comment. It is concluded from the present study that the model works encouragingly well over a wide range of conditions and is worthy of further development.

R E F E R E N C E S

1. G. R. Freeman, Radiation Res. Rev., 1, 1 (1968).
2. G. R. Freeman, Radiation Research, ed. G. Silini North-Holland Publishing Company, Amsterdam (1967) p.113.
3. F. W. Lampe, J. L. Franklin and F. H. Field, Progress in Reaction Kinetics, G. Porter (ed.) Pergamon Press, London, Vol. 1 p.68 (1961).
4. L. I. Bone, L. W. Sieck and J. H. Futrell, J. Chem. Phys., 44, 3367 (1966).
5. R. H. Lawrence and R. F. Firestone, J. Am. Chem. Soc., 87, 2288 (1965).
6. J. J. J. Myron and G. R. Freeman, Can. J. Chem., 43, 1484 (1965).
7. P. Ausloos and S. G. Lias, J. Chem. Phys., 43, 127 (1965).
8. F. B. Abramson and J. H. Futrell, J. Phys. Chem., 71, 1233 (1967).
9. P. Ausloos, S. G. Lias and A.A . Scala, Adv. Chem. Ser., 58, 264 (1966).
10. W. H. T. Davison, S. H. Pinner and R. Worrall, Proc. Roy. Soc., London A252, 187 (1959).
11. E. Hayon and J. J. Weiss, J. Chem. Soc., 3962 (1961).
12. F. Williams, Nature 194, 348 (1962).
13. P. Wilmenius and E. Lindholm, Arkiv. Fysik 21, 97 (1962).

14. E. Lindholm and P. Wilmenius, *Arkiw. Kemi.*, 20, 255 (1963).
15. K. Ryan, W. Sieck and J. Futrell, *J. Chem. Phys.*, 41, 111 (1964).
16. Solvated Electron, *Advances in Chemistry Series 50*, American Chemical Society Publications, 1965.
17. E. J. Hart, *Actions Chimiques et Biologiques des Radiations -X*, Masson et Co., Paris (1966).
18. L. M. Dorfman and M. S. Matheson, *Progress in Reaction Kinetics*, G. Porter (ed.) Pergamon Press, London Vol. 3, ch.6 (1965).
19. J. H. Baxendale and F. W. Mellows, *J. Am. Chem. Soc.*, 83, 4720 (1961).
20. J. A. Taub, D. A. Harter, M. C. Sauer, Jr., and L. M. Dorfman, *J. Chem. Phys.*, 41, 979 (1964).
21. G. R. Freeman and J. M. Fayadh, *J. Chem. Phys.*, 43, 86 (1965).
22. G. R. Freeman, *J. Chem. Phys.*, 46, 2822 (1967).
23. K. N. Jha and G. R. Freeman, *J. Chem. Phys.*, 48, 5480 (1968).
24. J. C. Russell and G. R. Freeman, *J. Phys. Chem.*, 72, 816 (1968).
25. J. C. Russell and G. R. Freeman, *J. Phys. Chem.*, 72, 808 (1968).
26. J. J. J. Myron and G. R. Freeman, *Can. J. Chem.*, 43, 381 (1965).

27. M. R. Ronayne, J. P. Buanino and W. H. Hamill, J. Am. Chem. Soc., 84, 4230 (1962).
28. D. Skelly and W. H. Hamill, J. Chem. Phys., 44, 2891 (1961).
29. C. F. Luck and W. Gordy, J. Am. Chem. Soc., 78, 3240 (1956).
30. B. R. Loy, J. Polymer, Sci., 44, 341 (1960).
31. H. Szwarc, J. Chim. Phys., 59, 1067 (1962).
32. S. Ohnishi and I. Nitta, J. Chem. Phys., 39, 2848 (1963).
33. R. W. Fessenden and R. H. Schuler, J. Chem. Phys., 33, 935 (1960).
34. R. W. Fessenden and R. H. Schuler, J. Chem. Phys., 39, 2147 (1963).
35. C. Chachaty and E. Hayon, J. Chim. Phys., 61, 1115 (1964).
36. J. A. Leone and W. Koski, J. Am. Chem. Soc., 88, 224 (1966).
37. J. Kroh and J. Mayer, Bull. Acad. Polon. Sci. Ser. Sci. Chim., 14, 51 (1966).
38. I. A. Taub and L. M. Dorfman, J. Am. Chem. Soc., 84, 4053 (1962).
39. M. Imamura, S. U. Choi and N. Lichtin, J. Am. Chem. Soc., 85, 3565 (1963).
40. J. Teplý, A. Habbergerová and K. Vacek, Coll. Czech. Chem. Comm., 30, 793 (1965).

41. L. M. Theard and M. Burton, *J. Phys. Chem.*, 67, 59 (1963).
42. R. A. Basson and H. J. van der Linde, *J. Chem. Soc.*, A, 1182 (1967).
43. J. M. Flournoy, L. H. Baum and S. Siegel, *J. Chem. Phys.*, 36, 2229 (1962).
44. J. N. Pitts Jr., F. Wilkinson and G. S. Hammond, *Adv. Photochem.*, W. A. Noyes Jr., G. S. Hammond and J. N. Pitts Jr., (eds.), Interscience Publishers Inc., New York, 1963, Vol. 1, p.1.
45. B. Brocklehurst, G. Porter and J. M. Yates, *J. Phys. Chem.*, 68, 203 (1964).
46. W. M. McClain and A. C. Albrecht, *J. Chem. Phys.*, 43, 465 (1965).
47. D. W. Skelly and W. H. Hamill, *J. Chem. Phys.*, 43, 3497 (1965).
48. J. L. Kropp and M. Burton, *J. Chem. Phys.*, 37, 1742 (1962).
49. J. Yguenabide, N. A. Dillon and M. Burton, *J. Chem. Phys.*, 40, 3040 (1964).
50. A. Singh and G. R. Freeman, *J. Phys. Chem.*, 69, 666 (1965).
51. D. L. Dugle and G. R. Freeman, *Trans. Faraday Soc.*, 61, 1 (1965).
52. S. Arai and L. M. Dorfman, *J. Phys. Chem.*, 69, 2239 (1965).

53. L. M. Dorfman, N. E. Shank and S. Arai, *Adv. Chem. Series*, 82 58 (1968).
54. F. S. Dainton, T. J. Kemp, G. A. Salmon and J. P. Keene, *Nature*, 203, 1050 (1964).
55. J. D. McCollum and W. A. Wilson, U. S. Tech. Report ASD-61-170 (1961).
56. J. W. T. Spinks and R. J. Woods, *An Introduction to Radiation Chemistry*, J. Wiley and Sons, New York (1963).
57. W. Sieck, F. Abramson and J. H. Futrell, *J. Chem. Phys.*, 45, 2859 (1966).
58. P. Kebarle and A. M. Hogg, *J. Chem. Phys.*, 42, 798 (1965).
59. P. Kebarle, S. K. Searles, A. Zolla, J. Scarborough and M. Arshadi, *J. Am. Chem. Soc.*, 89, 6393 (1967).
60. S. D. Hamann, *Physico-Chemical Effects of Pressure*, Butterworth, London (1957).
61. H. A. Bethe, *Handbuch Physik*, 24, 273 (1933).
62. A. H. Samuel and J. L. Magee, *J. Chem. Phys.*, 21, 1080 (1953).
63. R. L. Platzman, *Basic Mechanism in Radiobiology*, National Academy of Sciences, Washington (1953).
64. D. E. Lea, *Actions of Radiation in Living Cells*, Cambridge University Press, Cambridge (1955).
65. D. C. Walker, *Quart. Rev.*, 21, 79 (1967).
66. M. C. R. Symons, *Quart. Rev.*, 13, 99 (1959).

67. M. C. R. Symons and W. T. Doyle, *Quart. Rev.*, 14, 62 (1960).
68. G. Stein, *Disc. Faraday Soc.*, 12, 227 (1952).
69. R. L. Platzman, *Physical and Chemical Aspects of Basic Mechanisms in Radiobiology*, Publ. No. 305, 22 (1953).
70. G. Czapski and H. A. Schwarz, *J. Phys. Chem.*, 66, 471 (1962).
71. F. S. Dainton, E. Collinson, D.R. Smith and S. Tazuké, *Proc. Chem. Soc.*, 140 (1962).
72. G. V. Buxton, F. S. Dainton and M. Hammerli, *Trans. Faraday Soc.*, 63, 1191 (1967).
73. J. W. Boag and E. J. Hart, *Nature*, 197, 45 (1963).
74. J. P. Keene, *Nature*, 197, 47 (1963).
75. M. S. Matheson, W. A. Mulac and J. Rabani, *J. Phys. Chem.*, 67, 2613 (1963).
76. E. A. Shaede and D. C. Walker, *Chem. Soc.*, Special Publication 22, 277 (1967).
77. J. H. Baxendale and G. Hughes, *Z. Phys. Chem.*, (Frankfurt), 14, 306 (1958).
78. E. Hayon and J. J. Weiss, 2nd Proc. Intern. Conf. Peaceful Uses of Atomic Energy, Geneva, 29, 80 (1958).
79. N. F. Barr and A. O. Allen, *J. Phys. Chem.*, 63, 928 (1959).
80. G. Scatchard, *J. Am. Chem. Soc.*, 52, 52 (1930).
81. J. Jortner, *Radiation Res.*, 4, 24 (1964).
82. J. H. Baxendale, *Radiation Res.*, 4, 139 (1964).

83. W. L. Jolly, C. J. Hallada and M. Gold, Metal-Ammonia Solutions, G. Lepoutre and M. J. Sienko (eds.), (1964).
84. S. Gordon, E. J. Hart, M. S. Matheson, J. Rabani and J. K. Thomas, J. Am. Chem. Soc., 85, 1375 (1963).
85. M. C. Sauer Jr., S. Arai and L. M. Dorfman, J. Chem. Phys., 42, 708 (1965).
86. M. Anbar and E. J. Hart, J. Am. Chem. Soc., 86, 5633 (1964).
87. J. Jortner, S. A. Rice and E. G. Wilson, Ref. 83, p.222.
88. M. Anbar and E. J. Hart, J. Am. Chem. Soc., 87, 1244 (1965).
89. U. Schindewolf, Adv. Chem. Series, 81, 598 (1968).
90. W. C. Grottschall and E. J. Hart, J. Phys. Chem., 71, 2102 (1967).
91. S. Arai and M. C. Saur, Jr., J. Chem. Phys., 44, 2297 (1966).
92. J. Jortner and R. M. Noyes, J. Phys. Chem., 70, 770 (1966).
93. K. B. Harvey and G. B. Porter, Introduction to Physical Inorganic Chemistry, Addison-Wesley, (1963).
94. G. E. Adams and R. D. Sedgwick, Trans. Faraday Soc., 60, 865 (1964).
95. W. V. Sherman, J. Phys. Chem., 70, 667 (1966).
96. E. Hayon and M. Moreau, J. Phys. Chem., 69, 4053 (1965).
97. J. Teplý and A. Habersbergerová, Coll. Czech. Chem.

- Commun., 30, 785 (1965).
98. J. Teplý and A. Habersbergerová, Coll. Czech, Chem. Commun., 32, 1350 (1967).
99. W. V. Sherman, J. Phys. Chem., 71, 4245 (1967).
100. J. W. Fletcher and G. R. Freeman, Can. J. Chem., 45, 635 (1967).
101. W. V. Sherman, J. Phys. Chem., 71, 1695 (1967).
102. J. C. Russell and G. R. Freeman, J. Chem. Phys., 48, 90 (1968).
103. L. G. Walker, Ph.D. Thesis, Dept. of Chemistry, University of Alberta.
104. M. G. Robinson and G. R. Freeman, J. Chem. Phys., 48 983 (1968).
105. E. D. Stover and G. R. Freeman, J. Chem. Phys., 48, 3902 (1968).
106. G. R. Freeman, Adv. Chem. Series, 82, 339 (1968).
107. H. Seki and M. Imamura, J. Phys. Chem., 71, 870 (1967).
108. E. Hayon and J. J. Weiss, J. Chem. Soc., 3962 (1961).
109. G. Meshitsuka and M. Burton, Radiation Res., 8, 285 (1958).
110. M. G. Robinson and G. R. Freeman, J. Phys. Chem., 72, 1394 (1968).
111. J. W. Boyle, Radiation Res., 17, 427 (1962).
112. International Critical Tables, E. W. Washburn, Ed. (McGraw-Hill Book Co., New York, 1926), Vol. 3 p.264.

113. E. W. Kanning, E. G. Bobalek and J. B. Bryne, J. Am. Chem. Soc., 65, 1111 (1943).
114. I. M. Kolthoff and S. Bruckenstein in Treatise on Analytical Chemistry, I.M. Kolthoff, P. J. Elving and E. B. Sandell, Eds. (Interscience Encyclopedia, Inc., New York 1959), Part I, Vol 1, p.488.
115. I. I. Bezmann and F. H. Nerhock, J. Am. Chem. Soc., 67, 1330 (1945).
116. H. S. Harned and B. B. Owen, The Physical Chemistry of Electrolytic Solutions, (Reinhold Publishing Corp., New York 1958), 3rd ed. pp.755-757.
117. C. R. Noller, Textbook of Organic Chemistry (W. B. Saunders Co., Philadelphia, Pa., 1966) 3rd ed., pp.128-140.
118. Handbook of Chemistry and Physics (Chemical Rubber Publ. Co., Cleveland, Ohio, 1967), 48th ed., pp. 90-91.
119. R. H. Johnsen, J. Phys. Chem., 65, 2144 (1961).
120. F. S. Dainton, G. A. Salmon and J. Teplý, Proc. Royal Soc., London A286, 27 (1965)
121. R. M. Leblanc and J. A. Herman, J. Chim. Phys., 63, 1055 (1966).
122. Calculated from data in "Tables of Dielectric Dispersion Data for Pure Liquids and Dilute Solutions" NBS Circular 589, 1958.
123. J. R. Partington, R. F. Hudson and K. W. Bagnall, J. Chim. Phys., 55, 77 (1958).

113. E. W. Kanning, E. G. Bobalek and J. B. Bryne, J. Am. Chem. Soc., 65, 1111 (1943).
114. I. M. Kolthoff and S. Bruckenstein in Treatise on Analytical Chemistry, I.M. Kolthoff, P. J. Elving and E. B. Sandell, Eds. (Interscience Encyclopedia, Inc., New York 1959), Part I, Vol 1, p.488.
115. I. I. Bezmann and F. H. Nerhock, J. Am. Chem. Soc., 67, 1330 (1945).
116. H. S. Harned and B. B. Owen, The Physical Chemistry of Electrolytic Solutions, (Reinhold Publishing Corp., New York 1958), 3rd ed. pp.755-757.
117. C. R. Noller, Textbook of Organic Chemistry (W. B. Saunders Co., Philadelphia, Pa., 1966) 3rd ed., pp.128-140.
118. Handbook of Chemistry and Physics (Chemical Rubber PUBL. Co., Cleveland, Ohio, 1967), 48th ed., pp. 90-91.
119. R. H. Johnsen, J. Phys. Chem., 65, 2144 (1961).
120. F. S. Dainton, G. A. Salmon and J. Teplý, Proc. Royal Soc., London A286, 27 (1965)
121. R. M. Leblanc and J. A. Herman, J. Chim. Phys., 63, 1055 (1966).
122. Calculated from data in "Tables of Dielectric Dispersion Data for Pure Liquids and Dilute Solutions" NBS Circular 589, 1958.
123. J. R. Partington, R. F. Hudson and K. W. Bagnall, J. Chim. Phys., 55, 77 (1958).

124. R. M. Barrer, *Trans. Faraday Soc.*, 35, 644 (1939).
125. F. S. Dainton, J. P. Keene, J. T. Kemp, G. A. Salmon and J. Teply, *Proc. Chem. Soc.*, 265 (1964).
126. R. A. Basson and H. J. Van der Linde, *J. Chem. Soc.*, (A), 28 (1967).
127. A. A. Frost and R. G. Pearson, *Kinetics and Mechanism*, John Wiley and Sons, New York, p.98 (1953).
128. E. M. Fielden and E. J. Hart, *Trans. Faraday Soc.*, 63, 2975 (1967).
129. W. H. Holtslander and G. R. Freeman, *Can. J. Chem.*, 45, 1661 (1967).
130. P. Alder and H. K. Bothe, *Z. Naturforschg*, 20a, 1700 (1965).
131. G. G. Meisels, *J. Chem. Phys.*, 41, 51 (1964).
132. J. C. Russell and G. R. Freeman, *J. Phys., Chem.*, 71, 755 (1967).

A P P E N D I X A

Relevant Equations for Nonhomogeneous Kinetics Calculations

The yield of free ions is given by (22)

$$G(e^-_{\text{solv}})_{\text{fi}} = \frac{\Sigma N(y) \phi_{\text{fi}}}{\Sigma N(y)} \cdot G(\text{total ionization}) \quad (\text{Ai})$$

where  $N(y)$  is the relative number of thermalized electron-ion pairs that have an initial separation distance  $y$  and

$$\phi_{\text{fi}} = e^{-r/y} \quad (\text{Aii})$$

where

$$r = \xi^2 / \epsilon k T \quad (\text{Aiii})$$

where  $\xi$  is the charge on an electron,  $\epsilon$  is the static dielectric constant of the liquid,  $k$  is Boltzmann's constant and  $T$  is the absolute temperature.

The yield of nitrogen at a given mole fraction  $N_s$  of nitrous oxide is given by

$$g(N_2) = \frac{\Sigma N(y) \phi_-}{\Sigma N(y)} \cdot g(\text{total ionization}) \quad (\text{Aiv})$$

where  $\phi_- = \phi_{\text{fi}} + \phi_-(1 - \phi_{\text{fi}}) \quad (\text{Av})$

where  $\phi_- = 1 - (1 - f_{-N_s})^{\beta_- \nu} \quad (\text{Avi})$

where  $0 \leq f_- \leq 1$  is the encounter efficiency of reaction (16) and will be assumed to be unity, and  $\beta_-$  and  $\nu$  are parameters described by equations (Avii) and (Aviii), respectively.

$$\beta_- = \frac{1}{(u_+ + u_-)} \left( \frac{b_- D_-}{\lambda_-^2} + \frac{b_s D_s}{\lambda_s^2} \right) \quad (\text{Avii})$$

where  $(u_+ + u_-)$  is the sum of the mobilities of the positive ion and solvated electron,  $b_-$ ,  $D_-$  and  $\lambda_-^2$  are respectively the average number of new neighbors a solvated electron encounters per diffusive jump, the diffusion coefficient and mean square jump distance of the electrons, and  $b_s$ ,  $D_s$  and  $\lambda_s^2$  are the corresponding quantities for the  $N_2O$  molecules.

$$v = 6\epsilon(y^3 - r_o^3)/4.32 \times 10^{-7}d \quad (\text{Aviii})$$

where  $r_o$  is the center to center distance between the solvated electron and the positive ion at the instant the solvated electron makes its final jump in the absence of nitrous oxide, and  $d$  is a constant taken as unity.

Also the time  $t_{gn}$ , required for geminate neutralization to occur is given by (22)

$$t_{gn} = \epsilon(y^3 - r_o^3)/4.32 \times 10^{-7}(u_+ + u_-) \text{ sec} \quad (\text{Aix})$$

The calculation of the nitrogen yields for all systems studied in the present work is similar. As a sample calculation, the nitrogen yields in n-propanol are presented in Table A-I.

TABLE A-1

Calculation of  $g(N_2)$  in n-Propanol

$\frac{N_s}{4.0 \times 10^{-4}}$	$y(10^{-8} \text{ cm})$	$N(y)$	$\phi_{fi}$	$\beta_v$	$\phi_-$	$N(y)\phi_-$	$g(N_2)$
	17	2150	0.1977	71	0.2211	475	
	19	1100	0.2345	106	0.2677	294	
	22	600	0.2858	175	0.3360	202	
	31	476	0.411	522	0.5264	251	
	52	270	0.5886	2530	0.8570	231	
	85	116	0.7231	11136	0.9973	116	
	123	64	0.7993	33728	1.00	64	
	165	41	0.8462	81408	1.00	41	
	>200	<u>183</u>	>0.90	>90000	1.00	<u>183</u>	
<b>Total</b>		<b>5000</b>				<b>1857</b>	<b>1.60</b>
$1.6 \times 10^{-3}$	17	2150	0.1977	71	0.2874	618	
	19	1100	0.2345	106	0.3590	395	
	22	600	0.2858	175	0.4668	280	
	31	476	0.4111	522	0.7538	359	
	52	270	0.5886	2530	0.9940	268	
	85	116	0.7231	11136	1.00	116	
	>100	<u>288</u>	>0.80	>20000	1.00	<u>288</u>	
	<b>Total</b>		<b>5000</b>				<b>2324</b>
$6.4 \times 10^{-3}$	17	2150	0.1977	71	0.5012	1078	
	19	1100	0.2345	106	0.6243	687	
	22	600	0.2858	175	0.7787	467	
	31	476	0.4111	522	0.9822	468	
	52	270	0.5886	2530	1.00	270	
	>60	<u>404</u>	>0.70	>9000	1.00	<u>404</u>	
	<b>Total</b>		<b>5000</b>				<b>3374</b>

TABLE A-1 continued

$\underline{N_s}$	$\underline{y(10^{-8} \text{cm})}$	$\underline{N(y)}$	$\underline{\phi_{fi}}$	$\underline{\beta_v}$	$\underline{\phi_-}$	$\underline{N(y)\phi_-}$	$\underline{g(N_2)}$
$2.56 \times 10^{-2}$	17	2150	0.1977	69	0.8824	1897	
	19	1100	0.2345	104	0.9568	1052	
	22	600	0.2858	171	0.9937	596	
	31	476	0.4111	510	1.00	476	
	>50	<u>674</u>	>0.50	>2000	1.00	<u>674</u>	
Total		5000				4695	4.04
<hr/>							
$1.024 \times 10^{-1}$	17	2150	0.1977	64	0.9997	2149	
	>20	<u>2850</u>	>0.20	>90	1.00	<u>2850</u>	
Total		5000				4999	4.30
<hr/>							

A P P E N D I X B

Estimation of Values of  $g(H_2)_{\min}$ ,  $G(H_2)_{53}$  and  $k_{53}/k_{54}$  in  
Methanol

The methods of evaluating  $G(H_2)_{53}$  and  $k_{53}/k_{54}$  will be illustrated by an example. At  $-97^\circ$ , the hydrogen yield in pure methanol would be  $G(H_2)_0 = 4.9_5$ . The minimum value obtained by the addition of nitrous oxide was  $g(H_2)_{\min} \approx 1.5$  (Fig. III-6, p.65). The yield of hydrogen from free ions in pure methanol was  $G(H_2)_{fi} = 2.4$ , calculated from the crude model. Thus the yield from reaction (53) was  $G(H_2)_{53} \approx 4.9_5 - 1.5 - 2.4 = 1.1$ ; hence  $G_{54} \approx 4.6 - 2.4 - 1.1 = 1.1$  and  $k_{53}/k_{54} \approx 1.0$ .

The similar procedure can be used to calculate these quantities in ethanol, n-propanol and iso-propanol after substituting proper reaction numbers and values of  $G(H_2)_0$ ,  $g(H_2)_{\min}$ ,  $G(H_2)_{fi}$  and  $g(\text{total ionization})$ . These values are recorded in Tables IV-5, IV-11, IV-18 and IV-19 for these alcohols.